Spring 2019

Computational fluid dynamics modeling and comparison of advanced techniques for heat transfer augmentation for nuclear applications

Salman Mohammed Alzahrani

Department: Nuclear Engineering and Radiation Science

COMPUTATIONAL FLUID DYNAMICS MODELING AND COMPARISON OF ADVANCED TECHNIQUES FOR HEAT TRANSFER AUGMENTATION FOR NUCLEAR APPLICATIONS

by

SALMAN MOHAMMED ALZAHRANI

A DISSERTATION

Presented to the Faculty of the Graduate School of the

MISSOURI UNIVERSITY OF SCIENCE AND TECHNOLOGY

In Partial Fulfillment of the Requirements for the Degree

DOCTOR OF PHILOSOPHY

in

NUCLEAR ENGINEERING

2019

Approved by:

Shoaib Usman, Advisor
Carlos Castano
Ayodeji Alajo
Lana Alagha
Safwan Jaradat

ABSTRACT

Passive safety is the most important feature of NuScale's reactor designs. Twist tape is one passive heat enhance heat technique. The present research investigated thermo-hydraulic characteristics of natural and forced convection of water under different configurations of twisted tape inserted in tube as well as NuScale rod bundles for uniform wall heat flux using computational fluid dynamics (CFD) using ANSYS Fluent 18.1. Results for twist tape inserted in tube under natural circulation showed that heat transfer enhanced and pressure drop increased to 28% and 102.8% over the plain tube respectively. Regularly spaced tapes, and different widths of the twisted tapes also played a significant role in both heat transfer and pressure drop. Moreover, the results revealed a strong effect of twist ratios on the inner wall temperature. The impact of twisted tapes along sub-channel for the water flow through NuScale SMR's 2X2 RB at the normal operating conditions showed that the Nusselt number (Nu) and secondary flow were enhanced by 101% and 0.16 as compared to the case of plain sub-channel, respectively. On the other hand, the pressure drop for a sub-channel with twisted tape is always higher than the plain sub-channel. The flow in rod bundle sub-channels under natural convection with twist along the sub-channel showed that heat transfer and pressure drop are increased by 39.5% and 112.5% as compared to the case of plain sub-channel respectively. In addition, all results showed that Nu and pressure drop are influenced by changing the twist ratio, and tape geometry. Finally, twisted tapes were effective in enhancing the Nu in sub-channels under both natural and forced convection conditions. The smallest twist ratio in all cases resulted in the high pressure drop and Nu.

ACKNOWLEDGMENTS

First and foremost, I would like to express my deepest gratitude my advisor, Dr. Shoaib Usman, for the successful completion of this work. His constant encouragement, valuable guidance, meticulous supervision, motivation, keen interest, constructive criticisms, and input have been invaluable during the course of this research.

Also, I wish to express my sincere gratitude to my advisory committee, Dr. Carlos Castano, Dr. Ayodeji Alajo, Dr. Lana Alagha, and Dr. Safwan Jaradat, for their valuable suggestions throughout this research, and for taking an interest in my work and examining my dissertation.

The financial sponsorship provided for me by King Abdulaziz City for Science and Technology, is tenaciously appreciated.

I would like to thank all my friends in Missouri University of Science and Technology, Rolla, for providing help and support me.

Finally, from the bottom of my heart, I would like to acknowledge and thank my parents and my family for their support and encouragement throughout the years. Without them, none of this would be possible.

TABLE OF CONTENTS

Page

LIST OF ILLUSTRATIONS

LIST OF TABLES

NOMENCLATURE

Symbol	Description
p/d	Twist Ratios
D	Diameter (mm)
v	Tangential speed
r	Angular frequency
w	Frequency of Rotation
r'	Center of Mass
L	Length (mm)
p	Twist Pitch
S	Free Space Twisted Tape
W	Width (mm)
K	Thermal conductivity (W/m K)
M	Dynamic Viscosity (Kg/m-s)
C_p	Specific Heat (j/kg-k)
Q	Heat Flux (W/m^2)
Tw	Temperature Of Pipe Wall (K)
Tb	Bulk Temperature (K)
H	Heat Transfer Coefficient ($W/m^2 K$)
ΔP	Pressure Drop (Pa)
y/L	Dimensionless Axial Position
Nu	Nusselt number

D_h	Hydraulic Diameter
P_w	Wetted Perimeter of the Channel
Re	Reynolds number
SF	Secondary Flow
Uxi	Velocity in Xi direction
Uzi	Velocity in Zi direction
ρ	The Density of the fluid
v	The velocity
l	The characteristic length
Ra	Rayleigh number
Gr	Grashof number
Pr	Prandtl number.

1. INTRODUCTION

1.1. OVERVIEW

The demand for clean energy is growing and, according to a recent International Energy Outlook report, is estimated to increase by 49% from 2007 to 2035, (Figure 1.1). As the world seeks to minimize the detrimental effects of fossil-based energy on the environment. The nuclear power industry looks to fill new orders by developing nuclear reactors with higher thermal efficiency. Operating temperatures in the current fleet of nuclear power plants are relatively low, but development of the next generation of nuclear reactor plants will further increase thermal efficiency, resulting in increased production of safe electricity [1, 2, and 3].

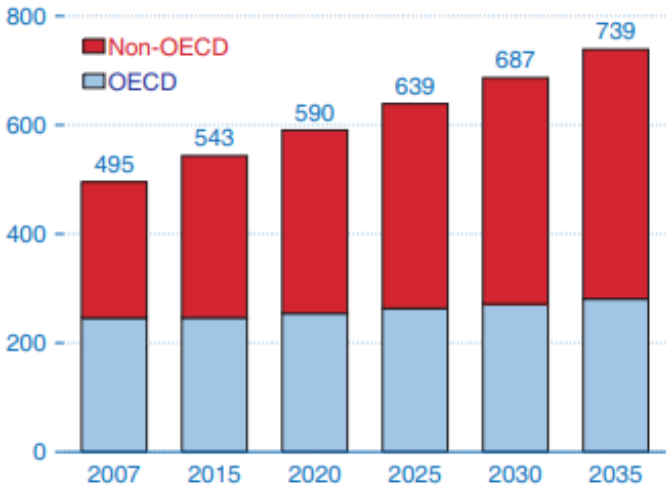

Figure 1.1. World marketed energy consump tion, 2007-2035 (quadrillion Btu) [1]

Safe operation of nuclear power plants, while managing the heat and pressure build-up that results from energy production and conversion process is critically

important. Extensive research is being conducted around the world to keep nuclear energy production process safe and predict the performance of the system and any anticipate accidents. One approach to this safety enhancement is use of natural forces and phenomena to ensure safety with human intervention.

Most types of reactors use the energy released from continuous fission of fuel atoms to heat water or gas to produce steam, which drives the turbine attached to the generators producing electricity. General types of nuclear reactors are [4]:

- Pressurized Water Reactor (PWR)
- Boiling Water Reactor (BWR)
- Pressurized Heavy Water Reactors (PHWR)
- Gas Cooled Reactor (GCR)
- Fast Breeder Reactors (FBR)

PWRs, are the most commonly utilized reactors, account for approximately 60% of nuclear power reactors in the world [5]. Among the several new PWR designs developed in the U.S. is the NuScale small modular reactor (SMR). This innovative design is an integral PWR that utilizes natural convection for cooling the reactor core. The design is driven by the demand for reactors with the ability to maintain safety standards in emergency situations without damaging the core [6]. In fact, NuScale features an unparalleled level of an advanced passive nuclear power, as the design does not utilize external sources of power, like electric pumps or coolant. NuScale power plants are designed for 1 to 12 NuScale Power Modules (NPM), which are complete systems of components - including primary and secondary systems - that produce power [7]. The scaling of the facility is based on addition NPM to match the need.

A NuScale module contains two separate independent passive safety systems for decay heat removal. The first system is an emergency core cooling system (ECCS) that provides a passive means of decay heat removal in the event of a loss-of-coolant accident (LOCA). The second system is decay heat removal system (DHRS), providing decay heat removal when normal feed water is not available. NPMs are submerged in water pool housed in a reactor building designed to support modules residing underground [7]. The large pool provides 30 days of core and containment cooling, eliminating the need for additional water. After 30 days, water boil-off and passive air cooling of the containment vessel provide adequate conditions to remove core decay heat for an indefinite period of time.

Each NPM contains a reactor core, two steam generators (SGs) inserted within a reactor pressure vessel (RPV), and a pressurizer, all housed in a containment vessel (CNV), shown in Figure 1.2. Each NPM has core thermal output of 160 MWt and can generate up to 50 MWe with yield total 600 MWe for 12 NPMs.

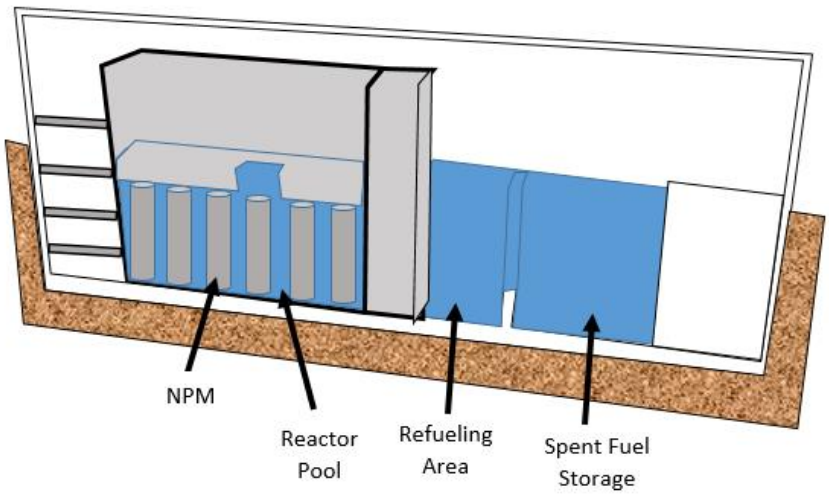

Figure 1.2. Example of a NuScale Power Module (NPM) [6]

The nuclear core contains 37 fuel assemblies and 16 control rod assemblies (CRA). The NuScale fuel assembly length is approximately one half the length of a typical PWR fuel assembly. The fuel assembly length including springs is 2.4 m. Each fuel assembly contains fuel rods in a 17x17 square lattice configuration. There are 264 fuel rods inside the fuel assembly with 24 guide tubes, and a top and bottom nozzle. The fuel rods are approximately 2 m in length. The fuel is uranium dioxide (UO2) with gadolinium oxide (Gd2O3); the fuel rod cladding is comprised of M5. The assembly is supported by five spacer grids, providing support for the rods and to reduce vibration from flow. Spacer grids are used also to induce a swirling flow that will enhance heat transfer, shown in Figure 1.3 [8]. Four of the spacer grids are used to produce swirling flow around the fuel rods that are HTP, while the HMP spacer grid at the bottom of the assembly does not produce swirling flow.

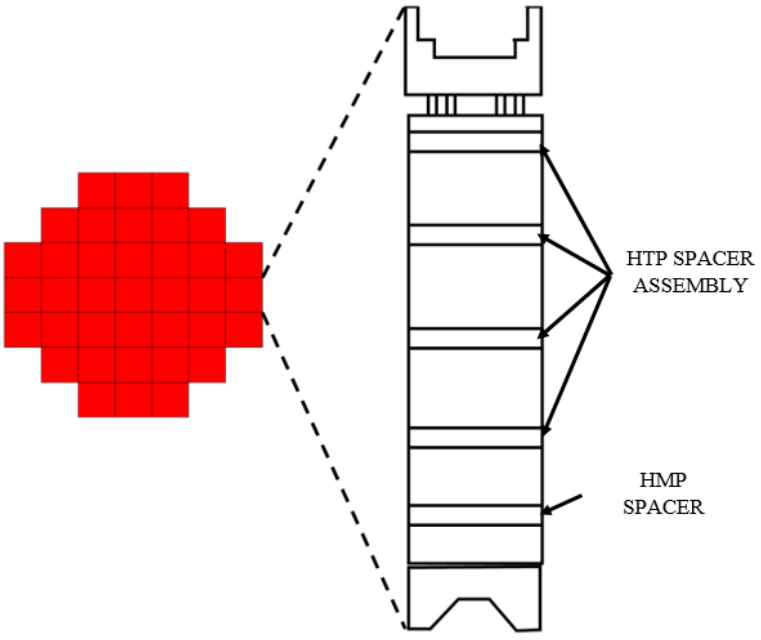

Figure 1.3. Fuel assembly with five spacer grids [8, 9]

1.2. HEAT TRANSFER ENHANCEMENT TECHNIQUES

Because of the high power density of a nuclear reactor heat transfer enhancement techniques are highly desirable. This need is valid for normal operation, accident mitigation as well as post shutdown decay heat removal. Swirl flow induce enhancement is proposed by many researchers. Swirling flow can be generated by many techniques in reactors. The study of these techniques and approaches is key to developing the effectiveness of heat transfer by increasing boundary layer turbulence in the fluid flowing inside the device, or by generating strong secondary flows and increasing the effective surface area. In general, three different methods can be employed for heat transfer enhancement:

1.2.1. Active Method. The active method requires an external power supply to preserve the enhancement of mechanisms. The following list includes eight different active method that can be employed to enhance heat transfer [10]:

1.2.1.1. Electrohydrodynamics (EDH). Electrohydrodynamics utilizes the interaction of the electric field with the flow field to enhance to heat transfer. This technique converts electrical energy into kinetic energy by conjugation of high voltage and current electricity with the flow field in a dielectric fluid medium. The technique is successful through fluid displacement by volumetric electric forces.

1.2.1.2. Jets. Jets force the motion of a single-phase fluid normally or obliquely to the surface. Jets depend on increasing projection of fluid at high velocity, thus increasing the heat transfer coefficient.

1.2.1.3. Surface vibration. Surface vibration at high or low frequency is used to enhance single-phase heat transfer. A piezoelectric device vibrates the surface to foster.

1.2.1.4. Mechanical aids. This technique depends on mechanical means of rotating the surface to stir the fluid.

1.2.1.5. Spray. A spray generated by a pressure-assisted atomizer or air is another active method for heat transfer enhancement. Spray droplet accumulate on the heated surface and improve heat transfer.

1.2.1.6. Fluid vibration. Fluid vibration is used to increase single-phase heat transfer in certain applications. In this technique, vibrations range from pulsations of about 1Hz to ultrasound.

1.2.1.7. Injection. In this approach, the main bulk fluid is injected with more fluid, either different fluid or the same. The injection method is used only in a single-phase flow.

1.2.1.8. Suction. The suction method involves vapor removal, film boiling, or fluid withdrawal in a single-phase flow.

1.2.2. Passive Techniques. Passive techniques, where the system can be safely cooled with no dependence on an active system or electricity. Generally these methods are advantageous compared with active techniques due to lower cost, easier production, installation and no need for surveillance or maintenance. In general, passive approaches utilize surface or geometric modification, or incorporate the use of an insert to enhance the system. Listed below are nine possible approaches for passive heat transfer enhancement [11]:

1.2.2.1. Treated surfaces. This approach employs a fine-scale modification of surfaces such as cavities, pits or other heat transfer surfaces shown in Figure 1.4. These treated surfaces are usually used for boiling and condensation enhancements.

Figure 1.4. Examples of treated surfaces [12]

1.2.2.2. Rough surfaces. This approach is used to modify the surface to disturb the viscous sublayer and is directed primarily toward single-phase flow.

1.2.2.3. Displaced enhancement devices. These inserts, that enhance energy transport at the heated or cooled surface of the tube with bulk fluid from the core flow, are used primarily with forced flow. Examples include wire matrix inserts, metallic mesh, rings, balls, or discs, among others. Recently use of nanofluids are reported to enhance heat transfer.

1.2.2.4. Extended surfaces. This approach increases heat transfer coefficients by disturbing the flow field. The extended surface technique is routinely employed in applications by shaping or perforating the surfaces.

1.2.2.5. Swirl flow devices. A swirl flow devices, used to create whirl in the main flow or produce secondary flow in the fluid. These swirl flow inducing devices include; a tube insert, altered tube flow arrangements, and duct geometry modifications. This technique is used for single-phase flows as well as two-phase flows. Twisted tape, helical strips, dimples, ribs, and cored screw-type tube inserts are examples of duct

geometry modifications, shown in Figure 1.5. Advantages of the use of swirl flow devices include; improved thermal hydraulic performance, boiling and condensation.

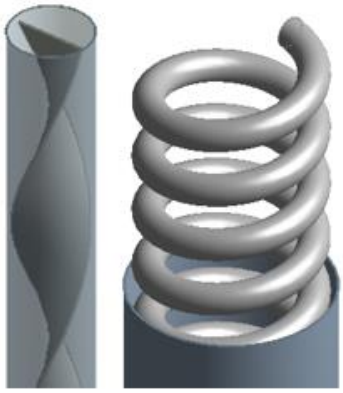

Figure 1.5. Examples of swirl flow devices

1.2.2.6. Surface tension devices. Surface tension devices are utilized to direct the flow of liquid in boiling and condensing. For example, wicking or grooved surfaces work well as surface tension devices.

1.2.2.7. Coiled tubes. The use of coiled tubes creates strong secondary flows or dean vortices. Coiled tubes are relatively more compact devices, but still promote high heat transfer coefficients.

1.2.2.8. Additives for liquids. This technique depends on adding solid particles, gas bubbles, and soluble trace additives to reduce drag resistance. In the case of boiling systems, trace additives are added to reduce the surface tension of liquids. Use of surfactant, nanoparticles etc. have been reported to produce good results.

1.2.3. Compound Method. Compound augmentation techniques – that is, the use of more than one of the listed approaches - typically perform better than individual

techniques operating separately. However, this approach involves complex design and can potentially produce better improvement of thermohydraulic performance. Compound method examples include utilizing an internally finned tube with a twisted tape insert; use of an electrical field with gas-solid suspension; and pulsations of air with a fluidized bed. Thermal performance factor (TPF) is used to evaluate the effectiveness of a heat transfer enhancement technique with Equation 1.1 [12]:

$$TPF = \frac{Nu/Nu_0}{(f/f_0)^{1/3}} \tag{1.1}$$

where $Nu, Nuo, f, and\ f_0$ are the Nusselt number and friction factor for a duct configuration, with and without inserts, respectively.

1.3. TWISTED TAPE

In most PWR designs, mixing vanes on spacer grids play a distinct role in crossflow mixing in rod bundles to improve heat transfer performance while the fuel rods remain in fixed positions [13]. Due to this important hydrodynamic feature, research is often focused on enhancing coolant mixing. Optimization is often the issue when the increase of heat transfer is required while maintaining the pressure drop at an acceptable level. As twisted tape insertion is a passive heat transfer augmentation technique that has yielded significant results in past studies, this work focuses on its application for heat transfer enhancement in nuclear reactors, specifically NuScale SMR core. With its distinct geometric features, the enhancement characteristics of twisted tape depend on the twist ratio – that is, the ratio of pitch to the inside diameter (y=p/d), while “pitch” is the distance between two points on the tape that are on the same plane (a full 360o twist) [14], as shown in Figure 1.6.

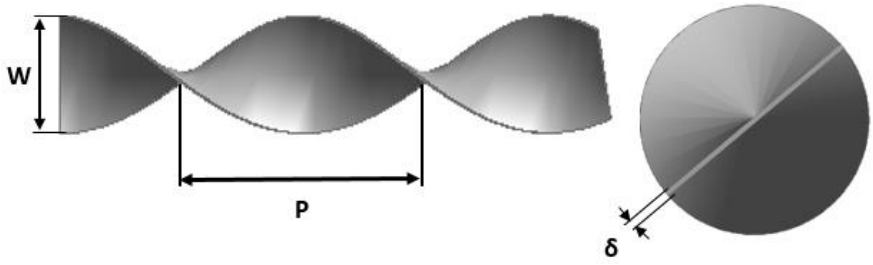

Figure 1.6. Characteristic geometric features of twisted tape

Insertion of twisted tape inside a pipe changes the flow field in several ways, including reduced axial velocity, increased flow length, and induced secondary fluid circulation or swirl. Each of these effects aid in the enhancement of heat transfer within the pipe. More detailed support for the insertion of twisted tape is listed as follows:

- Streamlines of flow field and velocity induced by twisted tape affect more than the plain tube. They influence the heat transfer coefficient by raising the turbulence of heat convection and increasing the tangential velocity near the tube walls.

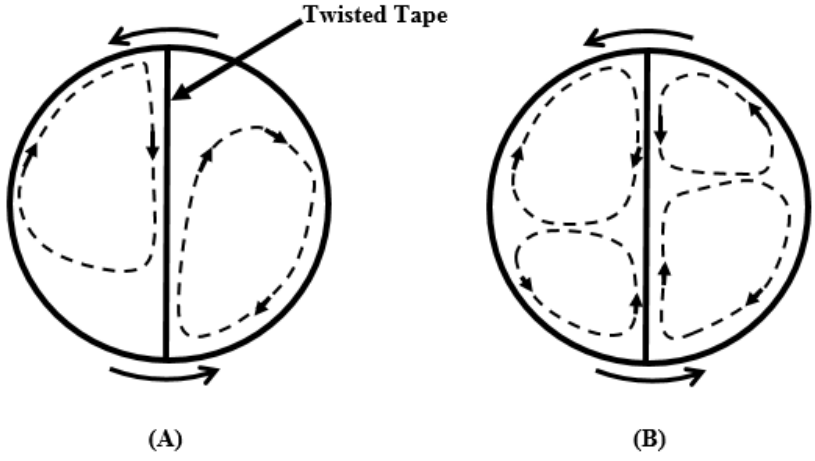

Figure 1.7. (A) The simple swirling flow at a low Reynolds number (Re) or at a high twisted ratio (y). (B) The swirling flow at a high Reynolds number (Re) or at a low twisted ratio (y)

- Increased wetted perimeter occurs as a result of dividing flow into two hydrodynamically independent flows with smaller hydraulic diameters.
- The fin effect of twisted tape can alter the heat transfer area. If the contact between the tape and the pipe surface is tight, heat transfer by conduction over the tape and to the fluid is possible as, shown in Figure 1.8 [15].

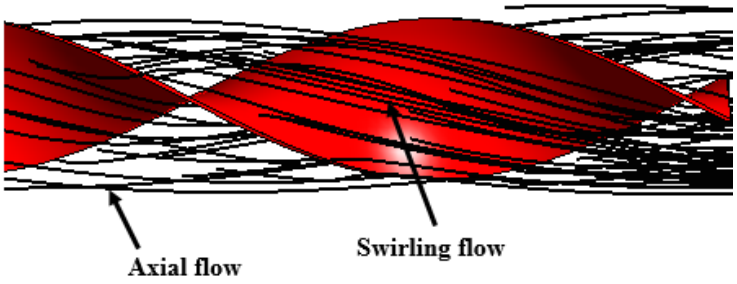

Figure 1.8. Swirling flow around the twisted tape

- The secondary flow induced by twisted tape increases the stream mixing due of the swirling flow. The centrifugal force induced by insertion of twisted tape generates the swirl flow at both sides of the tape. The force moves in the direction of bulk flow as shown in Figure 1.7.

1.4. OBJECTIVES OF WORK

The flow along the rods and spacer grids plays a major role in maintaining safe reactor operations by removing the heat from the core. Multiple studies focus on the development of numerical simulations that study the behavior of fluid flow between fuel rods and spacer grids. This research aims to evaluate the impact of several different configurations of twisted tape on the enhancement of heat transfer and pressure drop under natural circulation. The research will determine the ideal configuration for

development of the lateral flow field in several subchannels by applying twisted tape in a rod bundle geometry representative of a NuScale SMR fuel assembly under natural and forced convection. The purpose and motivation for this research are listed as follows:

- The focus of this research is on natural circulation flow with twisted tape under the same heat flux boundary conditions for all cases.
- Heat transfer enhancement, pressure drop, and inner surface temperature are studied using the variant twisted tape geometries:
    - Full Length Twisted Tape (FLTT).
    - Regularly Spaced Twisted Tape (RSTT).
    - Different Widths Twisted Tape (DWTT).
- As there is currently no published research on the relationship of two or more configurations of twisted tape under identical conditions and under natural circulation, this research represents the first investigation of natural circulation with twisted tape in a pipe by computational fluid dynamics (CFD).
- The comparisons based on thermal enhancement have been made between the variant twisted tape used in the present research and the best one to use into NuScale SMR.
- The research aims to numerically evaluate the impact of twisted tape on water flow through a 2x2 PWR rod bundle by using CFD under normal operating conditions for the NuScale SMR.

- Open literature contains limited phenomenological models or empirical correlations on the use of twisted tape for enhancing heat transfer in nuclear reactors.
- This work intends to improve thermo-fluid dynamic parameters for the gap between two channels by using twisted tape through a 4x4 PWR rod bundle numerically.
- The CFD simulations carried out is used to compare the numerical results of the presence of twisted tape inside spacer grid only, as well as the presence of twisted tape along the entire sub channel at the normal operating conditions.
- The research aims for numerical analysis of the effects of twisted tape on a PWR subchannel domain under natural convection for the NuScale SMR.
- The research aims to evaluate the impact of a variation of twist ratios on flow field into subchannel under natural convection.
- To the best of author's knowledge, this work is the first investigation of its kind on the use of twisted tape with natural convection for the water flow through PWR rod bundles.

1.5. DISSERTATION OUTLINE

This dissertation used CFD modeling and comparison of twisted tape enhancement techniques for heat transfer augmentation in NuScale SMR. Section 2 contains a detailed literature survey of research works in the past relating to the use of twisted tape for heat transfer enhancement. Section 3 includes a numerical investigation

of the effect of twisted tape on the natural circulation for tubes. In Section 4, the ideal configuration of twisted tape for fuel rod bundles using the results from Section 3. The analysis also includes evaluation of commercial code software ANSYS Fluent 18.1, its application for solving flow through a 2x2 PWR rod bundle under normal operating conditions for the NuScale SMR. Finally, the main objective of Section 5 is to numerically evaluate the impact of the insertion of twisted tape on a 2x2 PWR rod bundle of a PWR under natural convection for the NuScale SMR, with a variation of twisted tape ratios under the same heat flux boundary conditions for all cases. Section 6 includes the conclusions of this study.

2. LITERATURE SURVEY

2.1. OVERVIEW

The use of passive techniques to enhance heat transfer is a beneficial topic for study by scientists and engineers. Passive techniques do not require any external power source for heat transfer enhancement and are, therefore, preferred for multiple engineering applications. Fortunately, numerous studies focused on passive methods of heat transfer have contributed to the progress of those applications in several industries, including air-conditioning, refrigeration, and commercial heat pump industries, as well as in the petroleum, solar collector, chemical engineering, and, of course, nuclear industries. This section discusses several experimental and numerical studies focused on passive enhancement techniques. Specifically, insertion of twisted tape is one heat transfer augmentation technique that has provided significant results in past studies. Section 2.2 covers studies in heat transfer enhancement that focus on the use of different types of inserts, under both laminar and turbulent flow regions. Experimental and numerical studies of tubes fitted with twisted tape inserts under both laminar and turbulent flow are reviewed in Section 2.3. Finally, Section 2.4 discusses studies that concentrate on the flow in rod bundle subchannels under natural and forced convection conditions, which is more pertinent for nuclear engineering.

2.2. HEAT TRANSFER ENHANCEMENT USING DIFFERENT PASSIVE TECHNIQUES

Sanvicente et al. [16] experimentally investigated natural convection in an open channel with differential heating. Their study focused on the case when one wall is

uniformly heated and the other is not heated at all. Under the conditions of their experiments, they reported spatial variation of heat transfer coefficients, temperature variation, and spatial-temporal evolution of the flow field. Their results showed that reversed flow and heat induces flow oscillation, which would directly impact the mean Nusselt number (Nu). These results are significant to our work in that twisted tape also induces flow oscillation; hence, twisted tape is expected to produce similar results. Mohammed et al. [17] investigated laminar natural convection heat transfer from the inner surface of a uniformly heated vertical circular pipe. Their results show that Nu increased with increased heat flux. They proposed a general correlation for their data relating log of Nu with the log of Ra. Lee [18] studied natural convection for vertical pipes to investigate heat and mass transfer under the boundary conditions of uniform wall temperature, uniform wall concentration, uniform heat flux, and uniform mass flux. Tsuji and Nagano [19] also studied turbulent natural convection for a vertically suspended heated plate. Velocity in the laminar boundary layer showed a near wall peaking, while the temperature seemed to reduce exponentially as it moved away from the wall. A transition from laminar to turbulent heat transfer was also clearly observed. Shigeo and Adrian [20] used different end temperatures with the ratio of diameter/length = 0.112 to experimentally study the phenomena of natural convection in a vertical pipe. Most of these studies were limited to simple geometries without any heat transfer enhancing devices, such as twisted tape.

Eiamsa-ard et al. [21] studied the heat transfer and friction factor characteristics, employing louvered strips inserted in a concentric tube heat exchanger. The Reynolds number (Re) range in this study was $6000<Re<42,000$, with two turbulent flow devices:

the louvered strips with forward or backward arrangements, and the louvered strip with various inclined angles (θ=15°, 25°, and 30°) (Figure 2.1).

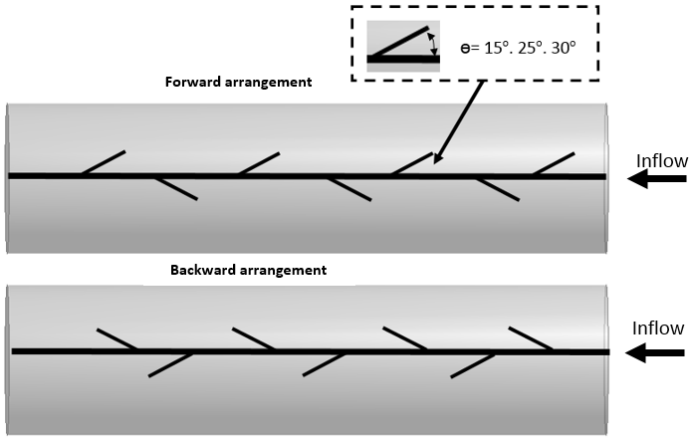

Figure 2.1. Louvered strips with forward and backward arrangements

Authors [21] found that the use of louvered strips led to a higher heat transfer rate over the plain tube. Increases in average Nu and friction loss using forward louvered strips were 284% and 413%, while for the backward louvered strip were 263% and 233%. On the other hand, they found a better overall enhancement ratio for the louvered strip with backward arrangement compared to that of the forward arrangement. Ibrahim [22] experimentally investigated the heat transfer characteristics and friction factor in horizontal double pipes of flat tubes with full length helical screw elements. This investigation involved different twist ratios and helical screw inserts with different spacer lengths. Re ranged between 570<Re<1310. Cold and hot water was used in the tube side and shell side, respectively. The author found a decrease in Nu and friction factor with increasing spacer length or twist ratio for the flat tube. In addition, they compared their data on plain circular tube with previously reported plain circular tube data from other

sources. Their data showed an increase in heat transfer and pressure drop as compared to the previously reported results. Therefore the exact extent of the enhancement due to helical screw is difficult to evaluate (Figure 2.2).

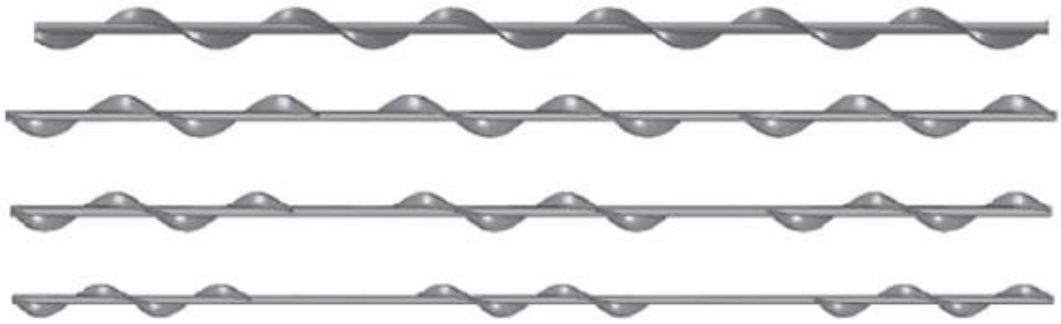

Figure 2.2. Helical screw with various spacer length [22]

Bhuiya et al. [23] studied turbulent flow heat transfer for a tube fitted with double helical tape inserts with different helix angles at 9°,15°, 21°, and 28°. They observed that Nu, friction factor, and thermal enhancement efficiency increased as helix angles decreased, under identical conditions. Nu and friction factor increased up to 305% and 170%, respectively, compared with the plain tube. The experimental work of Gul and Evin [24] studied heat transfer and flow friction characteristics by placing short helical tape at the entrance of a uniformly heated tube. Total mass flux, momentum ratio, and flow rates were 160-1628 kg/m-2, 0-8.6, and 5000-30,000 Kg s^{-1}, respectively. Different helical tapes with helical angles of 30^{o}, 45^{o}, and 60^{o} were used. Their results showed that helical tape inserted into the tube led to higher heat transfer rate - up to 20% depending on Mh/MT and Re at constant pumping power - than the non-swirling flow. Also, enhancement efficiency increased with an increasing momentum ratio and

decreased with an increasing Re. Tijing et al. [25] experimentally studied the heat transfer and pressure drop characteristics of an internal aluminum star-shaped fin cross-section of straight and twisted types (Figure 2.3), with water as the working fluid. They found that the straight fin configuration was best to produce heat transfer, as the heat transfer rate increased by 18%–48% with a mean increase of 35%. The average increase in pressure drop from that of the plain tube was 286%. They recommended that the twisted fin configuration may be effective in a cross-flow heat exchanger, where the twisted fin forced hot fluid to move circumferentially, while moving along the axial direction.

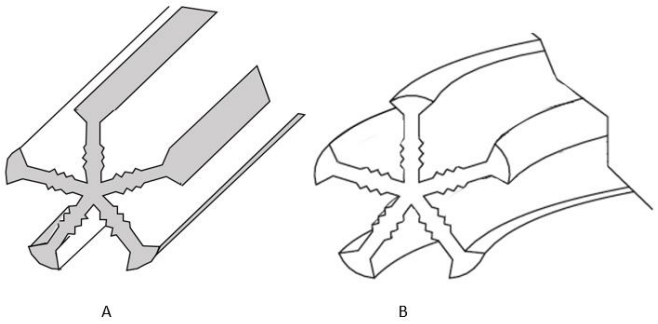

Figure 2.3. (A) Straight fin. (B) Twisted fin [25]

The work of Chandrasekar et al. [26] studied laminar flow convective heat transfer and friction factor characteristics by using Al_2O_3 water nanofluid with a uniformly heated horizontal tube with and without wire coil inserts. The results showed that Nu number in the fully developed region increased by 12.24% at Re=2275 for the plain tube with nanofluid compared to distilled water. Nu number increased by 15.91%

and 21.53% with pitch ratios 3 and 2 (Figure 2.4), respectively, at Re=2275 compared to distilled water, while no significant increase in pressure drop was found using nanofluid.

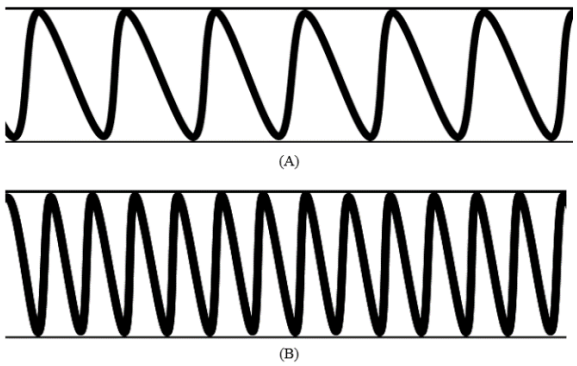

Figure 2.4. Wire coil inserts into tube with pitch ratios 3 and 2

Wang and Sunden [27] carried out a comprehensive comparison of thermal and hydraulic performance of tube inserts, including twisted tape and wire coil inserts under both laminar and turbulent flows. According to them twisted tape was more effective than those with wire coil inserts, without considering a pressure drop penalty. In addition, the shape of the insert was important for the enhancement of thermal and hydraulic performance, regardless of insert thickness. Sideman and Levin [28] enhanced the heat transfer rate by using square-edged, triangular, and circular grooves under laminar flow with a range of $300<Re<1000$. They observed that the square-edged groove was the most efficient shape to enhance the heat transfer rate. Rainieri et al. [29] studied the impact of an internal helical ridge on the heat transfer coefficient and friction factor characteristics with uniform wall heat flux. Figure 2.5 shows a cross-section of a helix tube. Five different geometries were used in their study under laminar flow forced convection for a Newtonian fluid. The results showed an agreement with the results obtained by previous

investigations for those formed with spirally fluted inner tubes. Results also showed an increase in heat transfer enhancement and friction factor.

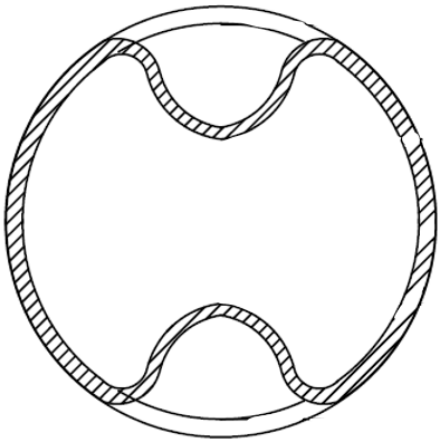

Figure 2.5. A cross-section of helix tube

Barba et al. [30] conducted an experiment to study the heat transfer and pressure drop characteristics in a corrugated tube with moderate Re number in the range, 100< Re<800. It was observed that friction factor increased by a factor of 1.83-2.45 as compared to the plain tube. There was also an increase in Nu compared to the smooth wall. Kareem et al. [31] carried out a numerical investigation of the laminar flow heat transfer enhancement in a smooth corrugation tube (Figure 2.6). Computational fluid dynamics (CFD) were employed for water flowing at a low Re number, 100<Re<700. The authors found the heat transfer enhancement range was 21%–60% with a friction factor increase of 19%–36%. Saha [32] conducted an experimental investigation of the heat transfer and pressure drop characteristics of a laminar flow of oil through rectangular and square ducts, with internal transverse rib turbulators inserted on two opposite surfaces of the ducts, and with wire coils. Saha found a 50% increase in heat transfer and

pressure drop when ribs and wire coil were both inserted, as compared to the insertion of individual ribs or individual wire coils, when utilizing constant pumping power. Therefore, the study recommended the rib-coil combination for laminar flow heat transfer over the rib inserts or coil inserts alone.

Figure 2.6. A spirally-corrugated tube configuration [31]

Bilen et al. [33] studied the surface heat transfer and friction characteristics of a fully developed turbulent air flow through grooved tubes with different geometric groove shapes. The results showed considerable enhancement with circular, trapezoidal, and rectangular grooves by 63%, 58%, and 47%, respectively, in comparison with that of the smooth tube at a higher Re number. This enhancement was due to improved flow mixing and disturbances than that of a smooth tube. In addition, the study found that by avoiding the sharp vertical corner or providing little radius on the corner of the groove may produce beneficial flow disturbances and decrease the recirculation region effect. Kathait and Patil [34] studied the effect of discrete corrugated rib-roughened tube (Figure 2.7) on heat transfer characteristics and frictional losses under different fluid flow rates and under a wide Re number range, $7000<Re<50,000$. They reported increases in Nu and friction factor by 2.73 and 2.78, corresponding to P/e (pitch to rib height ratio) of 10, e/D (height

ratio to tube diameter) of 0.044 for the corrugated tube with five gaps. At Re=7343, results show that the type-3 corrugated tube with (P/e) of 10 is thermo-hydraulically superior to that of other configurations.

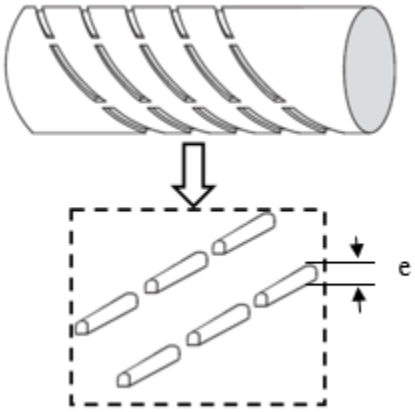

Figure 2.7. A circular tube with discrete corrugated ribs [34]

García et al. [35] compared the performance of tube inserts including corrugated tubes, dimpled tubes (Figure 2.8), and wire coils under laminar, transition, and turbulent regimes. The experimental results showed that the artificial roughness effect on the pressure drop and heat transfer were more obvious. Moreover, this shape strongly affects the advance of the transition to turbulence. Wire coils were more advantageous at a Re value range of 200<Re<2000. For Re values higher than 2000, the use of corrugated and dimpled tubes were favored over wire coils due to a lower pressure drop encountered for similar heat transfer coefficient levels.

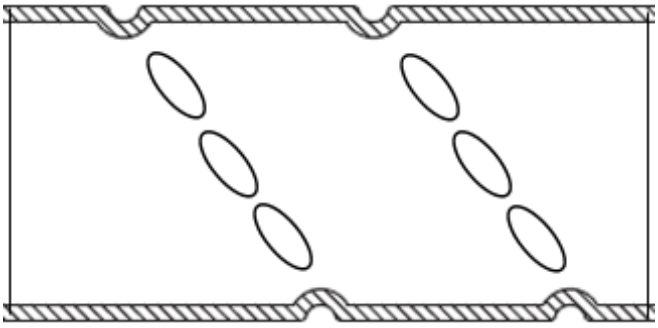

Figure 2.8. Dimpled tubes

2.3. HEAT TRANSFER ENHANCEMENT USING TWISTED TAPE

In laminar flow, there are several configurations of twisted tape, including full-length twisted tape (FLTT), short-length twisted tape (SLTT), regularly spaced twisted tape (RSTT), and different widths of twisted tape (DWTT). Manglik and Bergles [36] experimentally studied the effect of twisted tape in laminar flow under free convection for water and ethylene with uniform wall temperature. Their experiments were in the range of $300 \leq Re \leq 3000$ for horizontal pipes. The results revealed that hydraulic diameter, partitioning of tube flow, helically twisting fluid motion,
and secondary fluid motion were responsible for heat transfer enhancement. Moreover, they proposed a new swirl parameter to describe the effects of tape-induced effects under laminar conditions. Their new model predictions fit well with the experimental data for both Nu and the friction factor, with most data within ± 10% to 15%. Naphon [37] carried out an experimental investigation on the heat transfer coefficient and pressure drop in a double pipe with twisted tape inserts. Their results also concluded that the heat transfer coefficients were higher for tubes with twisted tape inserts, but that the pressure drop also increased. Date et. al. [38] investigated the heat transfer enhancement in viscous laminar

flows in a tube. Their study was conducted under uniform heat flux boundary condition. Hong and Bergles [39] carried out an experimental investigation of laminar flow heat transfer and friction factor characteristics into an electrically heated metal tube with two twisted-tape inserts. In their study, water and Ethylene glycol were used as fluid. They found that Nu for fully developed flow was affected by twisted ratio. Nu numbers were as much as nine times the plain tube. They also found the friction factor was affected by tape twist only at a higher Re. Saha and Dutta [40] studied the laminar flow heat transfer and friction factor characteristics for the tube fitted with short-length twisted tape, regularly spaced twisted tape, and smoothly decreasing pitch full length. The Prandtl number range was $205<Pr<518$ with a constant wall heat flux (UHF) boundary condition. They found that SLTT (~up to 33% length of the tube) performed better than FLTT. For thermos-hydraulic performance, there was not much difference between various twist ratio results, while Nu and friction factor are approximately 15% lower for twisted tape as compared to smooth pipe. The performance analysis showed twisted tape with smoothly varying was worse than the twisted tape that was with uniform pitch. Agarwal and Rao [41] experimentally investigated the heat transfer and friction factor characteristics in a circular tube with uniform wall temperature under laminar flow conditions ($70<Re<4000$) with twisted tape inserts ($y=2.41- 4.84$). Nu was found to be 2.28 - 5.35 (for $y=2.41$) and 1.21 - 3.70 times (for $y= 4.84$) as compared to plain tube respectively. Friction factors were found to be 3.13 - 9.71 times the plain tube. Lianshan et al. [42] investigated another interesting problem of converging and diverging tubes (CD) with RSTT under natural convection for a sucrose solution. The results of their experimental and numerical studies found that Nu enhancement occurred with RSTT.

They also tried to find the optimal geometry and concluded that the enhancement of heat transfer was due to the increase in tangential velocity. Du Plessis and Kroger [43] presented a correlation to take out the friction factor characteristics for laminar flow. They suggested that friction factor enhancement is related to heat transfer enhancement in plain tube fitted with twisted tape. Al-Fahed and Chakroun [44] carried out experimental work on heat transfer and pressure drop for a tube fitted with DWTT and a constant wall temperature boundary condition under laminar flow. They observed that the twisted tape width showed no effect on heat transfer and friction factor at a low range Re. However, there was a more pronounced effect on heat transfer in the high range Re number. They proposed a new correlations which fits well with the experimental data for both heat transfer and the friction factor, with a deviation of 10% and 15%, respectively. They recommended using baggy-fit twisted tape for low Re number flows. Bhattacharyya et al. [45, 46] carried out two experimental studies on heat transfer and pressure drop for laminar flow through a circular duct having integral helical rib roughness, integral transverse rib roughness, and fitted with center-cleared twisted tape. In the first investigation, they found that the integral helical rib roughness in combination with the center-cleared twisted tape performed significantly better than each enhancement technique individually. In the second investigation, they found that the transverse rib roughness in combination with the center cleared-twisted tape performed significantly better. Al-Fahed et al. [47] experimentally investigated the heat transfer coefficient and pressure drop characteristics for a plain tube, microfin tube, and twisted tape (Figure 2.9) under laminar flow condition with three different twist ratios and two different widths, and with oil as the working fluid.. The results indicated that twist ratio and width of the

tape have a significant effect on the performance of the twisted tape insert. As the twist ratio decreased, the heat transfer increased. The microfin tube was not recommended for use in laminar flow conditions, as it showed an insignificant increase in heat transfer and pressure drop. Additionally, results were favorable toward loose-fitting twisted tape with low twist ratios under high pressure conditions.

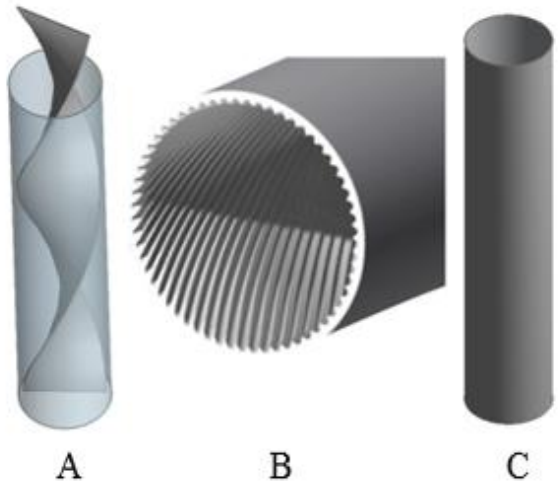

Figure 2.9. (A) Tube with twisted tape. (B) Microfin tube. (C) Plain tube

Liao and Xin [48] carried out experimental work on heat transfer and friction characteristics inside four tubes with three-dimensional internal extended surfaces (Figure 2.10) and copper continuous or segmented twisted tape inserts. They used water, ethylene glycol, and ISO VG46 turbine oil as the working fluid. Prandtl number range was 5.5<Pr<590; Re number range was 80<Re<50,000. It was observed that the Stanton number (the ratio of heat transfer rate to the enthalpy difference) could be enhanced up to 5.8 times inside a tube with three-dimensional extended surfaces and twisted tape inserts, compared to an empty smooth tube under high viscous fluid. Also, results showed an

increase in the friction factor by nearly 6.5 times. They observed that replacement of twisted tape inserts with the segmented twisted tape inserts induced a high decrease in the friction factor and a small decrease in the Stanton number. Promvonge and Eiamsa-ard [49] experimentally studied the heat transfer enhancement efficiency characteristics and friction factor in a circular tube fitted with conical ring turbulators and twisted tape with twist ratios of y=3.75 and 7.5. Their results showed a higher heat transfer rate and enhancement efficiency with a tube fitted with the conical ring and twisted tape than that of the conical ring alone. In addition, they proposed a new correlations between Nu, friction factor, and enhancement efficiency.

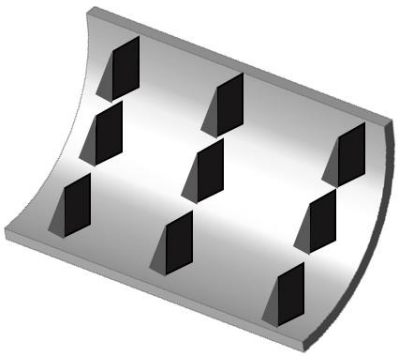

Figure 2.10. Three-dimensional internal extended surfaces

Ferroni et al. [50] studied physically separated, multiple SLTT. They observed that pressure drops for a spaced twisted tape configuration were at least 50% lower than pressure drops for continuous FLTT. They also proposed a correlation for the friction factor that incorporated the Re number, twist ratio, and spacing, that seems to be in agreement with their experimental results. Patil [51] conducted the experiment to study the heat transfer and friction factor characteristics in a circular tube fitted with various

lengths twisted tape from 11.0 mm to 23.8 mm. It was observed that the friction factor decreased by 18%-56% with reduced-width twisted tape inserts, as compared to the full-width tape. A slight decrease in Nu of 5%-25% was observed also with the tape widths 19.7 mm and 11.0 mm, respectively. Ray and Date [52] numerically investigated the heat transfer characteristics of laminar flow and heat transfer through a square duct with twisted tape inserts under axially and peripherally constant wall heat flux conditions. They found significant enhancement in heat transfer rate with square duct at high Prandtl and Re number with lower twist ratios. Saha et al. [53] conducted an experiment to study the heat transfer and pressure drop characteristics in a circular tube fitted with RSTT elements. In their study, Re number ($45<Re<1150$), Prandtl number ($205<Pr<518$), twist ratios ($2.50\leq y\leq 5$), space ratio ($0\leq s\leq 5$), tape width (0.461-0.923), rod diameter (0.115-0.231), and phase angle (0^{o}, 90^{o}, and 180^{o}) governed the thermo-hydraulic characteristics. It was observed that reducing tape widths yielded poor results, and the pinching of tapes in place was a better choice for thermo-hydraulic performance, compared to connecting the tape elements by rods. Sarada et al. [54] investigated turbulent flow heat transfer in a horizontal tube with twisted tape of varying twist ratios. Their experiment for the horizontal channel used air as a working fluid. They found that the enhancement of heat transfer varied between 36% to 48% for full-width (26 mm) and 33% to 39% for reduced-width (22 mm) inserts. They also reported that the friction factor depended on the twist tape width. Ujhidy et al. [55] carried out the experimental work to study tubes containing twisted tape and helical static elements for laminar flow of water. The experimental results showed that secondary flow was induced in the channel between the tube wall and the surface of a helical element. They reported good agreement between

the measured data and those of numerical calculations. They proposed a modified Dean number (ratio of geometric average of inertial and centrifugal forces to the viscous force) to compare the flow types that induced secondary flow in coils with the flow type in tubes fitted with twisted tape and helical static elements. Saha's [56] experimental investigation presented the effect of the rectangular and square ducts with combined internal axial corrugations on all duct surfaces, with twisted tape inserts with and without oblique teeth (Figure 2.11) on heat transfer and the pressure drop characteristics under the laminar flow of viscous oil (175<Pr<538). The results showed that duct aspect ratio, corrugation angle, corrugation pitch, twist ratio, space ratio, length, tooth horizontal length and tooth angle of the twisted tape, Re number, and Prandtl number all affected the flow friction and thermal characteristics. Results also showed that the axial corrugations combined with twisted tape with and without oblique teeth performed better than either axial corrugations or twisted tape alone.

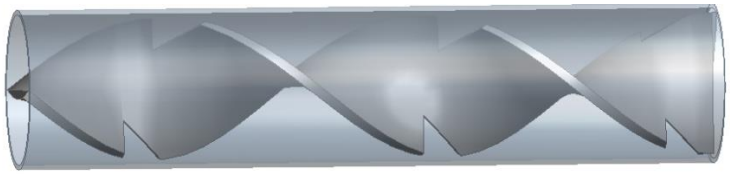

Figure 2.11. Diagram of full length twisted tape with oblique teeth

In turbulent flow, colburn and King [57] experimentally studied the heat transfer enhancement and friction coefficient in a tube fitted with several types of inserts to induce a swirl in the flow. In this study, air and water were used as the working fluid under turbulent flow. Results showed that the heat transfer coefficient depended on the degree of swirl and on the density or temperature difference. Results

also showed that the heat transfer coefficients for air were smaller than the coefficients for water. Authors suggested the observed phenomena were primarily the result of centrifugal force aiding convection when the fluid was heated up. Smithberg and Landis [58] carried out an experimental and numerical investigation of turbulent flow heat transfer, velocity distributions, and friction losses in a tube with twisted tape inserts under isothermal and forced convection heating conditions. The results recommended using twisted tape to generate swirl flow as a cheap and efficient equipment modification for tubular heat exchangers operating under critical local conditions. Additionally, Nu increased markedly with tightly-wound tapes, and results suggested there would be an even greater increase in the friction factor due to the flow mixing effects. Thorsen and Landis [59] conducted the experiment and analysis for twisted tape fitted in a circular tube using both cold and hot air as the working fluid under turbulent flow, with a Re range $0<Re<100,000$ and a with twist ratio of y=3.15-8. They found that centrifugal force aided the convection when the fluid was heated up and inhibited convection when the fluid was cooled. There was a clear enhancement with low twist ratio, and decrease in heat transfer was observed with an increased Re number. Lopina and Bergles [60] investigated the heat transfer and pressure drop characteristics for swirl flow generated by a continuous twisted tape. Authors observed that the difference between the isothermal and the heated flow friction factors for the swirl flow of liquids were less than the corresponding difference for a plain tube (without twisted tape). Their results showed an improvement of about 20% with a swirl flow of water, compared to straight flow at constant pumping. Brevi et al. [61] studied the heat transfer characteristics of heat exchangers at high pressures (about 50 bar) with exchangers of larger dimensions fitted

with twisted tape inserts. Their results showed a much higher increase in heat transfer coefficient ranging from 100% to 150% at specific mass flow rates of 70 to 100 g/ (cm2 sec). They also observed an increase in burnout thermal power ranging from 30% to 50%, with a drastic reduction of the post-burnout length and a complete vanishing of dangerous, post-burnout temperature oscillations. Date [62] formulated terms of partial differential equations of momentum and heat transfer to predict the friction and heat transfer characteristics. The study was mainly focused on the problem of fully developed, laminar and turbulent, flow in a tube containing a twisted tape. In laminar flow, the predictions were to demonstrate the influence of Re number, twist ratio, Prandtl number, and the fin parameter on the flow characteristics. In turbulent flow, differential equations were calculated to predict the turbulent viscosity. Rao and Sastri [63] experimentally studied the friction factor and heat transfer coefficient in decaying turbulent swirl flow generated by a twisted tape. Results obtained were compared with existing data for a stationary tube containing a twisted tape. They found that the enhancement in heat transfer with high twist ratios, higher than 5, can be used without much increase in friction factor under laminar flow. In general, the enhancement in heat transfer offsets the rise in friction factor due to rotation of flow. The heat transfer characteristics in an isothermal tube with twisted tape inserts at three different pitch (y=3.6, 5.4, and 7.1) and different widths were studied by Al-Fahed and Chakroun [64]. They found enhancement in heat transfer with increased twisted tape width. Interestingly, small twist ratio (y=3.6) and tape width (W=10.8 mm) increased heat transfer nearly as much as the tight-fit tape for the same twist ratio. Neshumayev et al. [65] experimentally studied the heat transfer augmentation in the gas-heated tubes of a fire tube boiler fitted with twisted tape, straight

tape, and combined turbulator (as showing in Figure 2.12). The twist ratio was y=4.12 for twisted tape. For the combined turbulator, twist ratio was y=2.16 in the internal twisted tape, external tape $H360^{o}$= 110 mm, and the relative height of a tape (rib) e/D0 = 0.098; 0.2. The results showed the heat transfer coefficient for twisted tape was higher than straight tape, while the mean heat transfer of twisted tape was lower than the mean heat transfer for the combined turbulator.

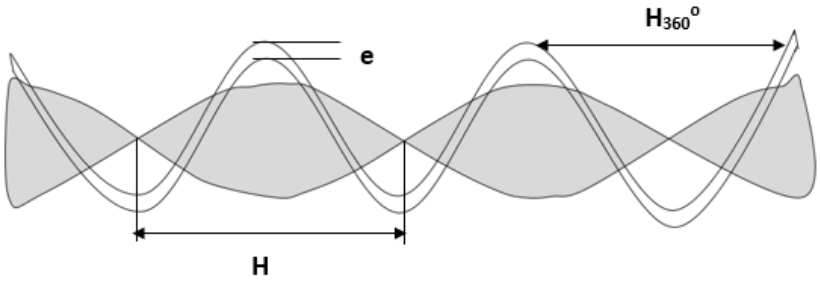

Figure 2.12. Combined turbulators insert

Eiamsa-ard et al. [66] conducted an experiment on heat transfer and friction factor characteristics for the uniform heat flux tube fitted with FLTT in a double pipe heat exchanger, with cold and hot water used as working fluids in the shell side and tube side, respectively. There were two different cases: (1) FLTT at different twisted ratios (y=6.0 and 8.0); and (2) twisted tape with different free space ratios (S=1.0, 2.0, and 3.0). Their experimental results showed that the heat transfer coefficient increased with a decrease in twist ratio for FLTT, while the decrease in free space ratio would improve both the heat transfer coefficient and friction factor for RSTT elements, when compared to those without twisted tape. Maner and Bergles [67] studied the augmentation of highly viscous laminar heat transfer inside tubes with constant wall temperature for three configurations:

a smooth tube, a tube fitted with twisted tape, and an internally-finned tube. The test fluid was Polybutene 20. Their results showed that the heat transfer coefficient was enhanced 3 to 4 times that of the plain tubes, and friction factors of the internally-finned tube and twisted tape were 1.69 and 3.38 times, respectively, those of the plain tube. The heat transfer characteristics under turbulent flow was presented by Krishna et al. [68] for the double pipe heat exchanger employed with straight full twist inserts (Figure 2.13) in single direction and left-right direction with a twist ratio of y=4.0 with varying spacer distances of 2, 3, and 4 inches. The experimental results confirmed that Nu increased with an increase in Re number and decrease of spacer distance for both laminar and turbulent flows.

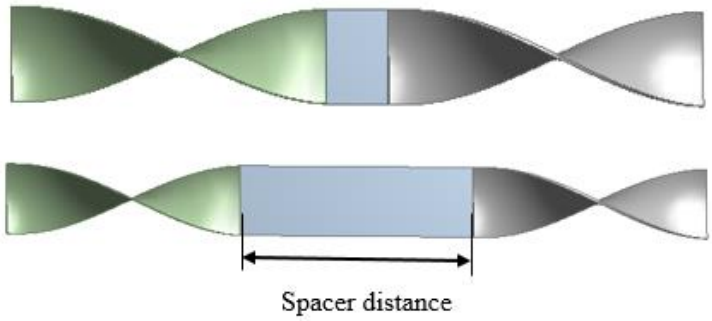

Figure 2.13. Diagram of straight full twist inserts

Thianpong et al. [69] evaluated the friction factor and compound heat transfer behaviors for a dimpled tube (Figure 2.14) fitted with twisted tape inserts (y=3, 5, and 7) compared to that of a plain tube, with a Re range of 12,000<Re<44,000, using air as the working fluid. The dimpled surfaces were arranged in a staggered line for two pitch ratios

of p/D=0.7 and 1.0. The results showed significant enhancement with the dimpled tube fitted with twisted tape compared to the dimpled tube alone and the plain tube.

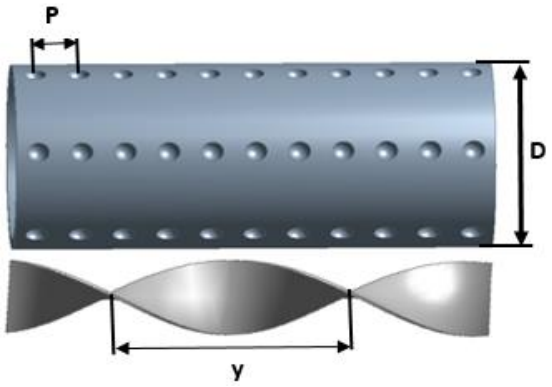

Figure 2.14. Diagram dimpled tube and twisted tape

Saha et al. [70] experimentally investigated the heat transfer, friction factor, and enhancement efficiency characteristics in a circular tube fitted with SLTT with several tape length ratios 0.29, 0.43, 0.57 and 1.0 (full-length tape) and at a single twist ratio of y=4.0. Re values were in a turbulent region, air was the test fluid, and the study took place under uniform wall heat flux boundary conditions. Their results showed that the SLTT of LR=0.29, 0.43, and 0.57 produced lower heat transfer and friction factor values compared to the full length tape - about 14%, 9.5% and 6.7% against 21%, 15.3%, and 10.5%, respectively - while at the same Re range. The enhancement efficiency of the tube containing FLTT was found to be higher than tube containing SLTT. Bhuiya et al. [71] experimentally determined the pressure drop, thermal performance factor, and heat transfer characteristics of flow of air in a circular tube equipped with perforated twisted tape inserts (Figure 2.15) with four different porosities, RP=1.6%, 4.5%, 8.9%, and

14.7%. This study was conducted in a turbulent flow regime with a Re range of 7200< Re<49,800, and under uniform wall heat flux boundary conditions. The results showed that the heat transfer rate, friction factor, and thermal performance factor of the tube fitted with perforated twisted tape were higher than those of the smooth tube, about 110%–340% and 110%–360% and 28%–59% higher, respectively.

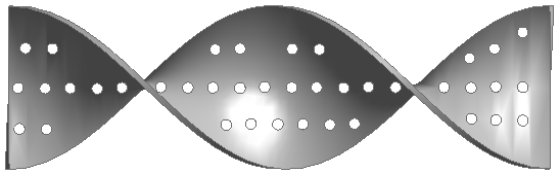

Figure 2.15. Diagram of p erforated twisted tape

Eiamsa-Ard and Promvonge [72] experimentally investigated the heat transfer and flow friction characteristics in a circular tube fitted with two types of twisted tape: (1) typical twisted tape and (2) alternate clockwise and counter-clockwise twisted tape (Figure 2.16) under turbulent flow (3000<Re<27000), uniform heat flux conditions, using water as working fluid.

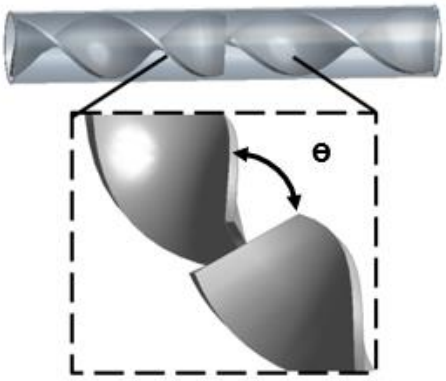

Figure 2.16. Diagram of clockwise twisted tape with angle

Twist ratios were y=3.0, 4.0 and 5.0, each with three twist angles, h=30^{o}, 60^{o} and 90^{o}. They reported that the clockwise and counter-clockwise twisted tape produced a higher heat transfer rate, friction factor, and heat transfer enhancement index than the plain twisted tape at identical conditions. Additionally, heat transfer rate increased with the decreasing of twist ratio and the increasing of twist angle values. Murugesan et al. [73] studied the heat transfer, friction factor, and enhancement efficiency characteristics in a double pipe heat exchanger fitted with square-cut twisted tape (Figure 2.17) and plain twisted tape, with twist ratios of y=2.0, 4.4, and 6 under turbulent flow range 2000<Re< 12,000. The experimental results revealed that the heat transfer rate, friction factor, and thermal enhancement factor in the tube equipped with square-cut twisted tape were significantly higher than those fitted with plain twisted tape.

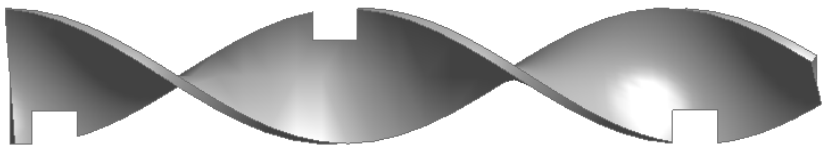

Figure 2.17. Diagram of square-cut twisted tape

Experimental work carried out by Jaisankar et al. [74] studied the heat transfer and flow friction characteristics for FLTT, twisted tape with rod and spacer at the trailing edges at lengths of 100 mm, 200 mm, and 300 mm, with twist ratios y=3 and 5, under turbulent flow (Figure 2.18). Results showed a slight decrease in Nu by 11% and 19% using twisted tape with rod and spacer, respectively, when compared with FLTT. Likewise, friction factor decreased by 18% and 29% for twisted tape fitted with rod and spacer, respectively, as compared with FLTT.

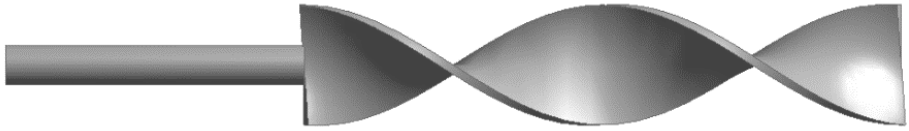

Figure 2.18. Diagram of twisted tape with various rod length

Seemawute and Eiamsa-ard [75] evaluated the fluid flow and heat transfer enhancement characteristics for peripherally-cut twisted tape (Figure 2.19) with an alternate axis uniform heat flux circular tube. In this experiment, Re number was 5000<Re<20,000 and the study was conducted using water as the testing fluid in a turbulent flow. They reported higher increase in heat transfer rate, friction factor, and thermal performance with peripherally-cut twisted tape with an alternate axis than those in the tube equipped with peripherally-cut twisted tape and typical twisted tape.

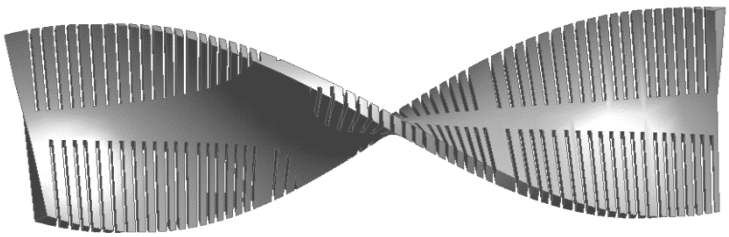

Figure 2.19. Diagram of peripherally-cut twisted tape

2.4. PREVIOUS RELATED WORK ON ROD BUNDLE SUBCHANNELS UNDER NATURAL AND FORCED CONVECTION CONDITIONS

Malen et al. [76] investigated PWR core design that utilized U (45%, w/o) ZrH1.6 fuel with and without twisted tape inserted, with an inverted core (fuel and coolant channel interchanged). An inverted PWR core design was compared to a typical rod bundle utilizing U–ZrH1.6 fuel. Their results showed that using twisted tape would

enhance the heat transfer and for the optimal power of 6869MWt; the enhancement was 135% as compared to the standard rod bundle. Twisted tape have been known to enhance CHF [77, 78], power, burnup, and heavy metal loading of an inverted design. Malen's [76] work was subsequently extended by Todreas and Ferroni [79, 80]. Likewise, Akiba et al. [81] studied the effect of twisted tape on liquid film flow rate on the fuel rod under air-water conditions in a boiling water reactor (BWR). Their results show an increase in the film flow rate in the annular dispersed flow regime caused by twisted tape. Weisman et al. [77] proposed a phenomenological model for CHF enhancement under twisted tape conditions. Arment et al. [82] proposed a correlation between critical heat flux and pressure drop at operating conditions applicable to PWRs for tubes containing multiple SSLT. Bieder et al. [83] used CFD to simulate the experiments of the OECD/NEA-KAERI rod bundle at the MATiS-H facility. Their study showed the effects of split-type and swirl-type spacer grid geometries. The results showed a good fit with the experimental data. Liu and Ferng [84] investigated thermo-hydraulic characteristics for different types of grid designs by CFD. Their results showed the secondary flow could be reasonably captured by using a CFD model with the RSM turbulence model. Moreover, the split-vane pair grid enhanced flow mixing and heat transfer were compared to the standard grid. In et al. [85] utilized CFD to simulate the heat transfer experiments in rod bundles with a split vane at a PWR's operating conditions. Their results showed a decrease in heat transfer enhancement close to the spacer grid at 28,000<Re<42,000, but good agreement between the decay rate at 6 D_h (hydraulic diameter) downstream of the grid and the fully heated experimental data. In addition, there was a good enhancement of heat transfer at 6 to 7 D_h due to multiple vortices predicted near the spacer. Lee and Choi

[86] also studied the RSM (Reynolds averaged Navier-Stokes) turbulence model by comparing two mixing vanes, small-scale vortex flow (SSVF) and large-scale vortex flow (LSVF), to enhance the performance of the spacer grid. Their results showed that the LSVF mixing vane increased in the safety and thermal efficiency of the rod bundle. Holloway et al. [87] utilized a thin heated film sensor to measure azimuthal variations in heat transfer in a split-vane pair grid, disc grid, and standard grid. Results showed that for a split-vane pair grid, there were variations in azimuthal heat transfer at 2.2 D_h downstream from the grid. In all axial locations, the disc grid had the most uniform azimuthal heat transfer distribution. Hata et al. [88] carried out a numerical investigation for vertical 5x5 rod bundles in liquid sodium for two types of bundle geometry - equilateral square array (ESA) and equilateral triangle array (ETA) - under the natural convection. The authors used heat fluxes for each cylinder, equally given at a Rayleigh number from $3.08x10^4$ to $4.19x10^7$, with liquid temperature TL= 673.15 K. The values of S/D (ratios of the diameter of flow channel to the rod diameter) were from 1.8 to 6 on each bundle geometry. The authors found that the average Nu values for the vertical single cylinder with ESA at Nx=1-5 for Ny=1-5 were 25.94%–69.04% lower than that of a vertical single cylinder alone. Results also showed Nu values of the vertical single cylinder with ETA were 16.35%-60.36% lower than the vertical single cylinder alone. Additionally, in the case of the fixed cross-section with ESA and ETA, the average Nu value for the vertical 5x5 rod bundle with various S/D=2 with ESA increased to 4/3 times higher than with ETA. On the other hand, Nu of ETA bundles increased by 24.97% compared to those with ESA at the fixed heating element number. Tandian et al. [89] studied the heat transfer in vertical triangular subchannel under natural convection that

was in the APWR and the PHWR nuclear reactors by zirconia-water nanofluid. In their study, the heat flux values were within 9.1 to 30.9 kW/m^2 range and ZrO2 concentrations of 0 (pure water), 0.27, and 3 volume-% of ZrO_2. Their results showed that the ZrO_2 concentration had no significant influence to heat transfer at those concentration levels used under the natural convection. Choi al. [90] carried out an investigation to improve understanding of natural circulation phenomena for nuclear power plants that use water for cooling. They identified phenomena that influence natural circulation such as the effect of non-condensable gases on condensation heat transfer; steam liquid interaction; and natural circulation in a closed loop. Moysés and Santos [91] evaluated a 5x5 PWR rod bundle segment with a split-vane spacer grid by CFX 11.0. Their results were later compared with those found by Karoutas et al. [92] and In et al. [85] in one subchannel computational domains. Their results showed a good agreement between the profiles of the lateral velocities obtained in the experiments. However, there were differences between profiles predicted by CFX 11.0 and the previous CFD simulations observed for distances away from the grids. Additionally, the CFX 11.0 showed a better qualitative agreement with the experiment compared to the previous CFD. Muhammed et al. [93] investigated the flow behavior and pressure drop across the coolant channel in the region of spacer grid by CFX. Their results showed good agreement with the experimental data. Moreover, their results concluded that the single channel can be used to predict pressure drop in spacer grids of nuclear fuel assemblies. Podila et al. [94] simulated a 5x5 rod assembly with a split-type spacer grid by ANSYS Fluent 14 in accordance with the OECD/NEA MATiS-H benchmark. Authors found trends for the three velocity components and a good agreement between the predicted circulations for the subchannel

and data from previous experiments. Du Plessis [95] carried out an experimental and numerical investigation of the laminar swirl flow heat transfer in a smooth tube subjected to axially constant tube wall temperature. Du Plessis used two 3D marching integration finite difference procedures, involving primitive variables as well as vorticity and velocity. They observed good agreement between the experimental and numerical results. Peña-Monferrer [96] carried out an experimental and numerical investigation of the turbulence effects of split-type and swirl-type spacer grid geometries on a single phase in a PWR rod bundle using CFD. Their results agreed with the experiments of the OECD/NEA-KAERI rod bundle on turbulent mixing in a rod bundle with spacers that were in the MATiS-H facility. Authors demonstrated that the described procedure to simulate PWR spacer-grids in rod bundles was valid to obtain realistic fluid mechanic predictions. Moreover, they found that the experimental data fit well with the simulation. Khan et al. [97] carried out a numerical investigation of turbulence to analyze the flow behavior and pressure drop across a single coolant channel along the spacer grid with all geometrical details using CFD Ansys-CFX. In this investigation, the model, average velocity, Re, and the cross-flow velocities were K-e, 2.52 to 7.35 m/s, $40000<Re<117000$, and 0.2 to 0.57 m/s respectively. They observed that the single cell approach was accurate and economical for predicting the pressure drop across the spacer grid. Also, they confirmed the applicability of K-e model with scalable wall function for the prediction of the hydraulic characteristics of spacer grids. Navarro and Santos [98] numerically studied the effect of the vanes arrangement in the spacer grid on four average thermo-fluid dynamic parameters: pressure, secondary flow, Nu, and thermal non-uniformity of turbulent flow through a 5X5 rod bundle, using CFD. The results showed

significant improvement and combination of swirl and cross-flow between subchannels with peripheral vanes, while the grid without peripheral vanes showed a well-defined swirl flow on each of the vaned subchannels. Pressure drop and secondary flow were slightly influenced by the vane arrangement, while there was significant enhancement in heat transfer and mixing downstream the grids by vane arrangement. Chen et al. [99] numerically and experimentally evaluated the heat transfer and secondary flow for a 5x5 rod bundle with a spacer grid, including spring, dimple, and mixing vane. Numerical CFD results were validated by the experimental results. Their findings showed that strong secondary flow induced by the spacer grid gradually decayed along the rod bundle after the mixing vane. Nu and swirl factor were defined to investigate the thermo-hydraulic performance of the rod bundle. Lee [100] conducted experimental work on the augmentation of convection heat transfer of water rod bundle flow for a 4x4 tightly arrayed rod bundle with P/D =1.08 and Re=10400. Lee observed that heat transfer was enhanced by 77% downstream of the twist-vane spacer grid. Podila and Rao [101] evaluated OECD/NEA-KAERI MATiS-H benchmark data to predict the turbulence intensities as well as velocity variation downstream of the split-vane spacer grid in 5x5 rod bundle. CFD tool STAR-CCM+ was used in this evaluation. Results showed that turbulence intensities downstream of the split-vane spacer grid were affected by the upstream length and the mesh density in the spacer region. A good agreement for the location of peaks and valleys between the predicted and measured axial velocities was achieved in this study.

3. EFFECT OF TWISTED TAPES DESIGN ON THE NATURAL CIRCULATION; HEAT TRANSFER AND PRESSURE DROP ENHANCEMENTS

3.1. OVERVIEW

Many nations today have a preference for adding nuclear power to their national energy mix. There are many reasons for this choice, ranging from environmental considerations (global warming), national energy security, and socioeconomic issues [102]. A new generation of nuclear reactors involving different technologies, commonly known as Generation IV, is being developed globally to meet the criteria of enhanced safety [103]. Passive safety is one of the improved features, where natural forces (no pumps, fans etc.) and phenomena (negative temperature coefficient of reactivity by using Hydrides and other advanced fuels) are relied upon to keep the reactor safe under all conditions. Passive techniques are mostly preferred due to their simplicity and the economic advantage of maintenance, installation, and operation [104].

For passive safety, natural circulation is highly desirable to ensure residual heat removal; hence, many newer reactor designs have incorporated natural circulation for normal operation and accident mitigation. For example, AP1000 by Westinghouse uses natural convection [102] for cooling during an accident. Likewise, NuScale's design uses natural circulation for normal operation as well as for passive safety.

Gas cooled reactors are also being investigated for energy production application. Natural circulation is relied for passive heat removal during depressurization natural circulation [105, 106]. Many techniques are employed to enhance heat transfer under forced convection conditions, such as twisted tape, ribs, baffles, plates, helical, wire coils,

etc. [27]. Most of these techniques have been quite comprehensively investigated for forced convection and have been shown to produce improvement for industrial applications, but there are limited data on the effectiveness of these techniques for natural convection/circulation systems.

The velocity profile and fundamental nature hydrodynamics of natural circulation is quite different than forced convection, and the wealth of data and knowledge accumulated on the effects of twisted tapes (as discussed in the previous section) in tubes for forced convection is not readily applicable for natural circulation flow. Heat transfer and pressure drop enhancement due to twisted tapes in natural circulation need to be further investigated. Natural convection is driven by buoyancy force, which is responsible for the fluid motion in natural convection/circulation. The body force momentum equation for natural circulation is represented in Equation 3.1 [107];

$$F = \rho 0\, g\, \beta\, \Delta T \tag{3.1}$$

The main objective of this section is to evaluate the impact of twisted tapes' configurations for the enhancement of heat transfer and pressure drop by investigating three configurations of twisted tapes; (a) full length twisted tape (FLTT), (b) regularly spaced twisted tapes, (RSTT), and (c) different widths for a twisted tape with same heat flux boundary condition for all cases. The focus of this section is on natural circulation flow. Twisted-tape geometry is important for several other special nuclear applications, for example, the application of a prismatic gas cooled reactor. However, we have used water as working fluid for this numerical study. Moreover, natural circulation in this study is established by constant heat flux from the tube walls.

3.2. PHYSICAL MODEL

Twisted tapes are generally metallic tapes that are simple to manufacture and are twisted as per the required application. Twisted tapes are inserted into the flow to increase the heat transfer, but they also cause an increased pressure drop. The enhancement characteristics of using twisted tape depend on the *twist ratio,* which is the ratio of pitch to the inside diameter, while *"pitch"* is the distance between two points on the tape that are on the same plane (a full 360º twist) [108]. Twisted tapes lead to flow field modifications. Rather than a circular channel, the channel is divided into two half circles. Each half will be subjected to rotation motion in addition to the axial motion. The frequency of rotation would be 3.2:

$$\omega = \frac{v}{2ry} \tag{3.2}$$

The center of mass for the half channel would be at the location at r' 3.3:

$$r' = \frac{4r}{3\pi} \tag{3.3}$$

It will rotate with a frequency of ω and exerting a centrifugal force of on the tube wall as shown in Equation 3.4:

$$F_{Cent} = \frac{mv^2}{4y^2 r} \tag{3.4}$$

Due to these forces, hydraulics of the flow is changed, and hence there is a pronounced change in heat transfer. In this study, classic twisted tapes are fitted for the full length of the tube. Free space twisted tapes and different widths of the twisted tapes are used for enhancing heat transfer rate. The geometries that are simulated for twisted tapes are depicted in Figure. 3.1. For the simulations, the twisted tapes thickness that is

fitted in the tube was 0.2 mm. This thickness was used for two reasons: (a) to simulate reactor core dimension (which is a small dimension), and (b) To fit with the basic width of the tube that is used in this study. The diameter (d), length (L), free space between twisted tape (S), and different widths (W) for twisted tape that were used in this work are 9 mm, 100 mm, (S=W, 2W, 3W), and width (W, 9 m m, 8 mm and 7 mm) of copper, respectively. The twist pitch (p) values used in this study were 225, 65, 54, 30, and 25, thus producing twist ratios (p/d) of 25, 7.2, 6, 3.3, and 2.7.

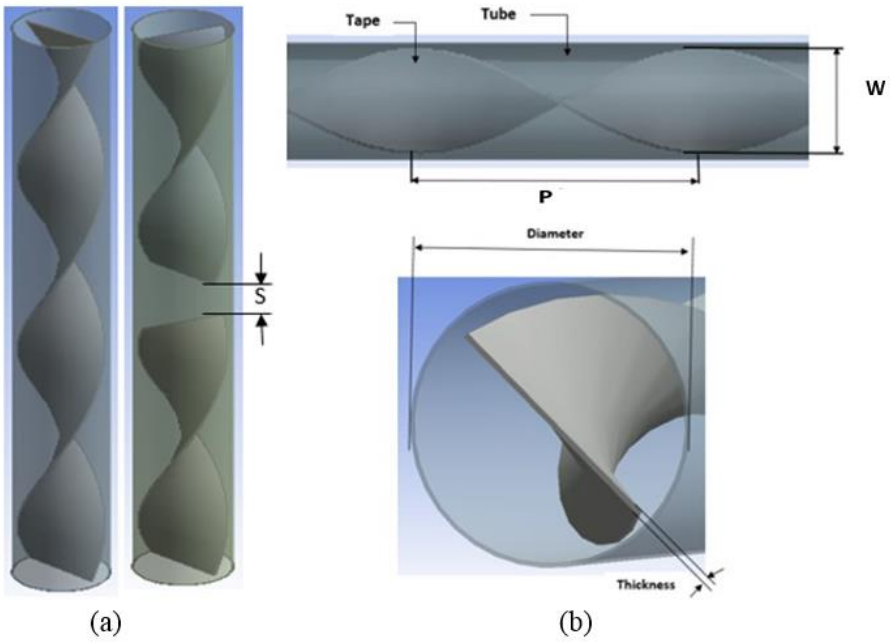

Figure 3.1. (A) Classic twisted tape fitted inside the tube and a free space twisted tapes. (B) Twisted tape terminology

Because of the common use of light-water reactors (LWRs), water is selected as the fluid for this study. The specific heat, thermal conductivity (k), and dynamic viscosity (μ) for H_2O are given as 4182J/kg-K, 0.6 W/m-K, 0.001003 Kg/m-s, respectively. The Boussinesq approximation was used with the density equal to 998 kg/m3 for water to

simulate natural circulation. In other words, density is taken as constant except where it appears as a multiplier to the gravitational acceleration. This approach is well accepted for simulating buoyancy-driven flows.

3.3. NUMERICAL MODEL

ANSYS/FLUENT 18.1 is used to perform CFD simulations of the geometry described Mass conservation, Momentum equation and Energy conservation [109]. For this study laminar solution was used for solving three dimensional, steady-state conditions. This choice is due to the low velocity expected in these natural circulation conditions. For simplicity conduction of heat to the tape was neglected, meaning that no fin effects from the tape were included.

3.3.1. Boundary Conditions. The heat flux on the wall was modeled as constant and uniform. Velocity boundary conditions at the tube wall were assumed to be “no slip”. At the inlet, temperature was 298 K. At the outlet, a pressure-outlet was open to atmospheric pressure and the temperature was set at 298 K. Heat flux at the tube wall was simulated in the range between 1,000 to 10,000 W/m^2.

3.3.2. Numerical Solution. The tubes and twisted tapes that were used in this Study were meshed by using Ansys Meshing. Proper meshing for such simulations are critical to capture the thermal hydraulic behavior. The mesh splits fluid flows into two smaller subdomains to make heat transfer and fluid flow amenable to analytical solutions [110]. Furthermore, presence of twist will induce swirl, which in turn leads to heat-transfer enhancement. In fact, twisted-tape-inserted pipes are in many ways significantly more complicated and difficult to mesh when compared with pipes without twisted tapes,

such as the number of nodes and elements produced. For this project, meshing was performed separately for the pipe with twisted tape and without twisted tape, as shown in Figure 3.2. For simple pipe without tapes to generate fine mesh, vertical length was divided into 200 equal segments (0.5 mm each). Each simulation took about 1 to 6 h of CPU time on a Core2Due CPU E8400 @ 3.00 GHz and memory 4.00 GB memory. Computation speed can be significantly increased with high power computers.

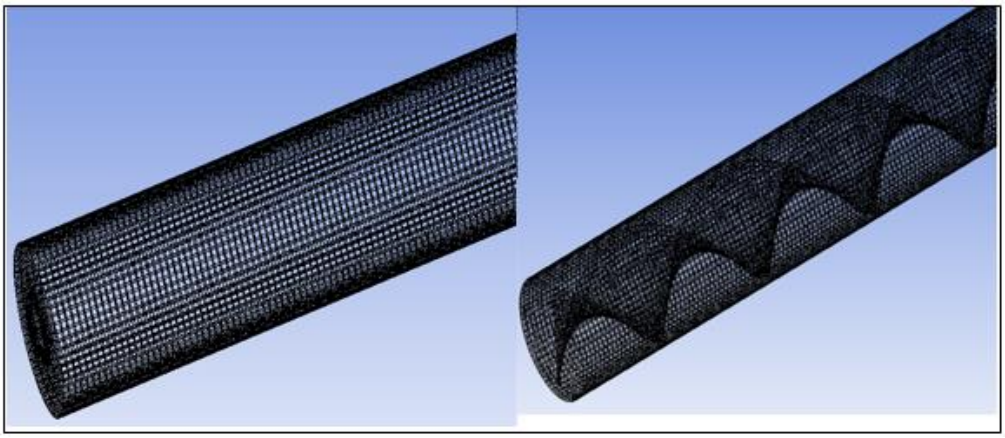

Figure 3.2. Meshing of plain pipe and pipe with twisted tape

To make sure that the results acquired do not vary with the cell size, a grid independence test was performed for plain tube and pipe with twisted tape that had the lowest twisted ratio. For the case of plain tube, eight grid systems were used to calculate the average Nusselt number. The difference between calculated values of ~105 k and ~146 k grid system is very small. For this reason, a grid system with ~96 k cells is used for calculations with plain tube, as shown in Figure 3.3. Any mesh less than 105 k did not provide stable results. Simulation with less than 45 k mesh fineness did not even converge.

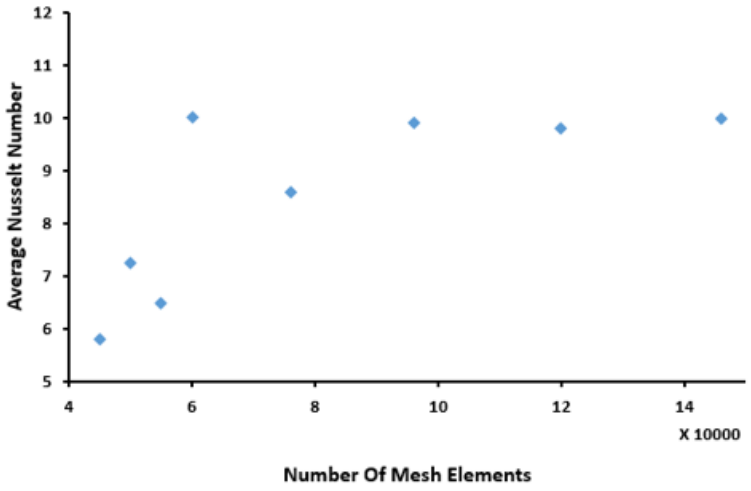

Figure 3.3. Grid independence study for plain tube

On the other hand, seven grid systems were tested to calculate the average pipe wall temperature for tube with twisted tape (p/d= 2.7). The difference between calculated values of ~750 k and ~1 M grid system is very small. For this reason, grid system with ~750 k cells is used for the rest of the simulations. Less mesh fineness showed result fluctuations, as can be seen in Figure 3.4.

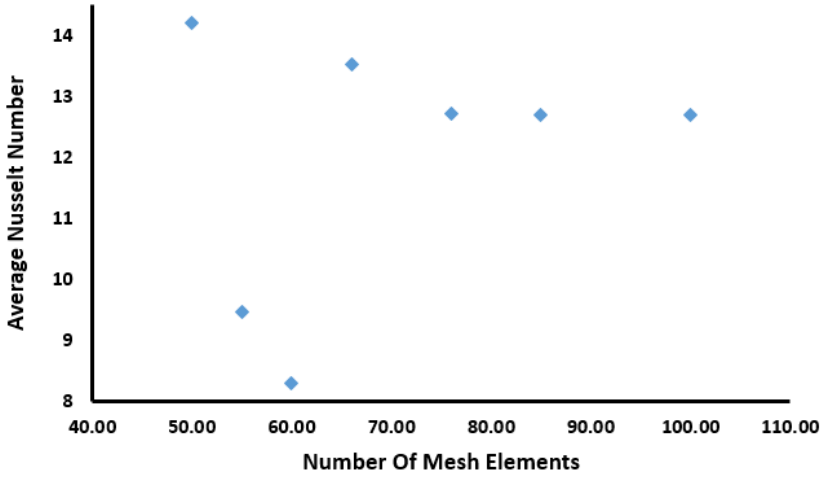

Figure 3.4. Grid independence study for tube with twisted ratio 2.7

For a plain tube to generate fine mesh, vertical length was divided into 100-500 depending on mesh complexity for segments (0.2 mm - 1 mm) multiple methods such as hex dominant and tetrahedrons were used depending on twisted ratio. In general, each case study must be initialized before the FLUENT code begins iterating towards a converged solution. In this work, the inlet zones option was chosen for initialization. The number of iterations ranged between 300 and 1500 depending on each case.

Only steady-state solution was sought for this study. To capture the natural circulation, Boussinesq approximation was used while all other physical properties (specific heat, viscosity etc.) were keep constant. A constant gravity value of -9.8m/s2 was applied. For the solution method, PISO (pressure-implicit with splitting of operators) was found to be most suitable for this application and was thus used. PISO improves the computational efficiency by performing two additional corrections in the algorithm; (a) neighbor cell correction and (b) skewness correction. Second order upwind was applied for numerical solution of the equations for momentum and energy. A body force weighted pressure solver was used for this work.

3.3.3. Data Reduction. As a constant wall heat flux (q") boundary condition was applied, the heat transfer coefficient is calculated by the following Equations [111]:

$$q = h * (\Delta T) \tag{3.5}$$

$$\Delta T = T_s - T_b \tag{3.6}$$

$$h = \frac{q}{(T_w - T_b)} \tag{3.7}$$

$$h_{avg} = \frac{1}{N} . \sum_{i=0}^{i=n} h_i \tag{3.8}$$

$$T_b = \frac{T_0 + T_i}{2} \tag{3.9}$$

3.4. RESULTS AND DISCUSSION

Generally, two variables, heat flux and the flow restriction, can affect the thermal hydraulic behavior of a natural circulation system. Consequently, the wall temperature along the pipe will depend on the applied heat flux and the tape geometry. Figure 3.5 shows the distribution of inner wall temperature for uniform heat flux of 10,000 W/m^2 without any tape. The distribution of inner wall temperature for variation of twisted tape ratios with the dimensionless pipe length (y/L) for full-length tape for q=10,000 W/m^2. The value of the inner wall temperature increases from the inlet until a certain point where it reaches the maximum. For this case, the maximum is at y/L= 0.89. After this point, the wall temperature decreases because at the entrance of the tube the thickness of the boundary layer is almost zero. After that point, the thickness of the boundary layer gradually increases until the point of maximum wall temperature. From the inlet to this point of maximum temperature, the water in the tube is heated by convection from the wall. Beyond the maximum temperature point, we see a drop in the wall temperature due to end effects. This type of behavior was experimentally observed by Said and co-workers [112], who reported a similar drop in gas and wall temperature of their channel.

Some of the changes in physical properties with the increased temperature may also have contributed to the behavior of the end effect. For example, when thermal conductivity increases it causes less resistance to the flow of heat. Moreover, when the viscosity increases, it causes radial flow of the hotter layers of fluid nearer from the wall to the center [113, 114, 115].

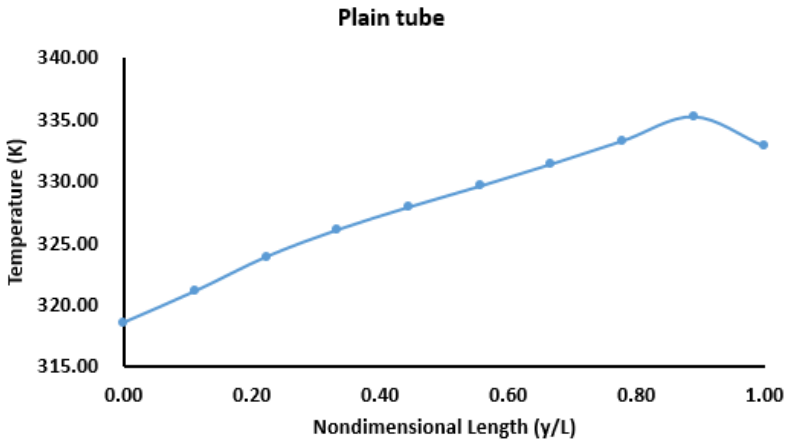

Figure 3.5. Axial distribution of inner wall temperature along the plain pipe

Figures 3.6, 3.7, 3.8, 3.9 and 3.10 show the variation of point of maximum temperature for various values of twisted ratios (p/d =25, 7.2, 6, 3.3 and 2.7) for full-length tape. When a twisted table is inserted, the location of maximum temperature shows strong dependence on the twist ratio. For p/d= 25, 7.2, 6, 3.3, and 2.7, the location of maximum temperature was observed at y/L= 0.530, 0.335, 0.308, 0.227, and 0.202, respectively.

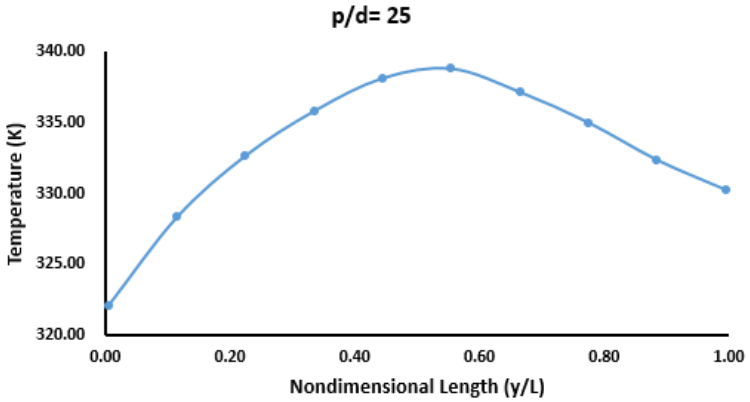

Figure 3.6. Axial distribution of inner wall temperature along the pipe with p/d=25

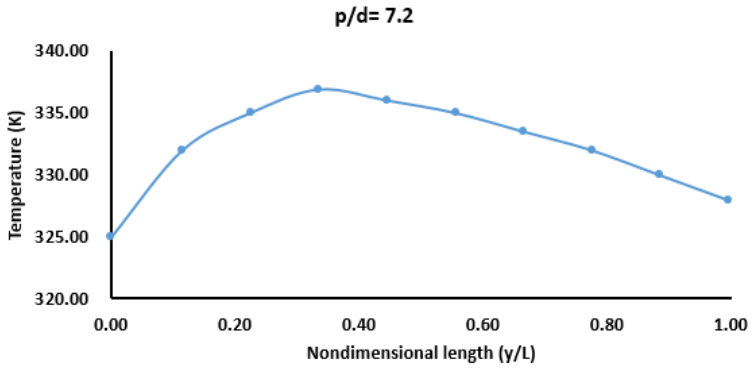

Figure 3.7. Axial distribution of inner wall temperature along the pipe with p/d=7.2

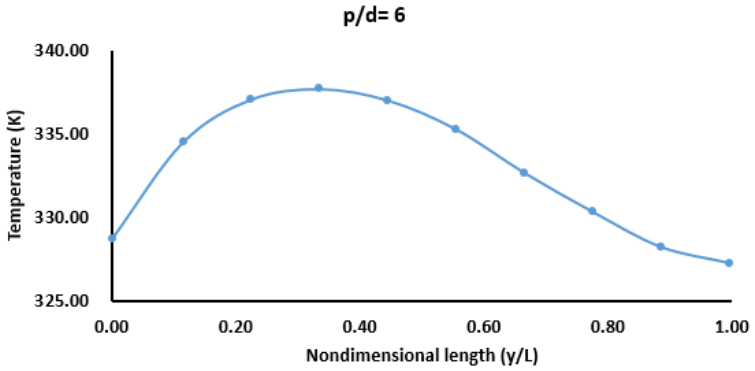

Figure 3.8. Axial distribution of inner wall temperature along the pipe with p/d=6

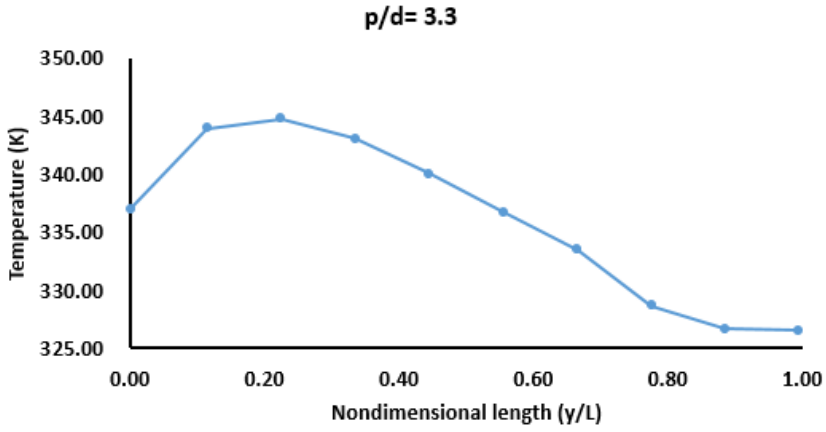

Figure 3.9. Axial distribution of inner wall temperature along the pipe with p/d=3.3

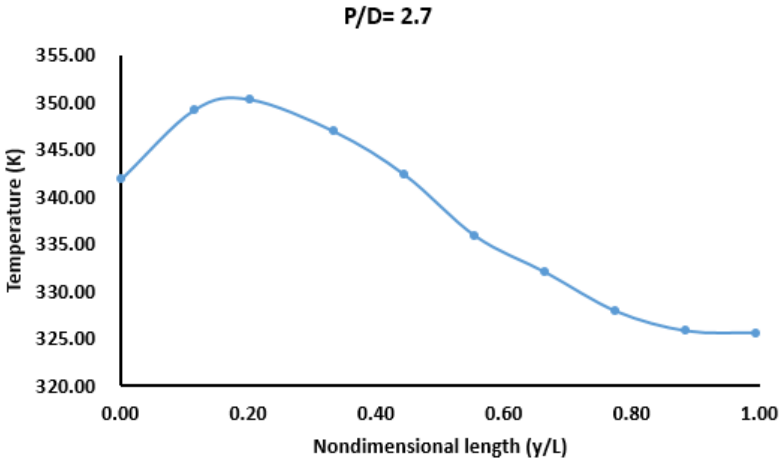

Figure 3.10. Axial distribution of inner wall temperature along the pipe with p/d=2.7

It is interesting to notice that the point of maximum temperature almost reached the inlet (y/L = 0.202) for a twist ratio of 2.7. Figure 3.11 shows the twist ratio relationship with maximum temperature location. An exponential relationship seems to fit well with the data having an R^2 of 95%.

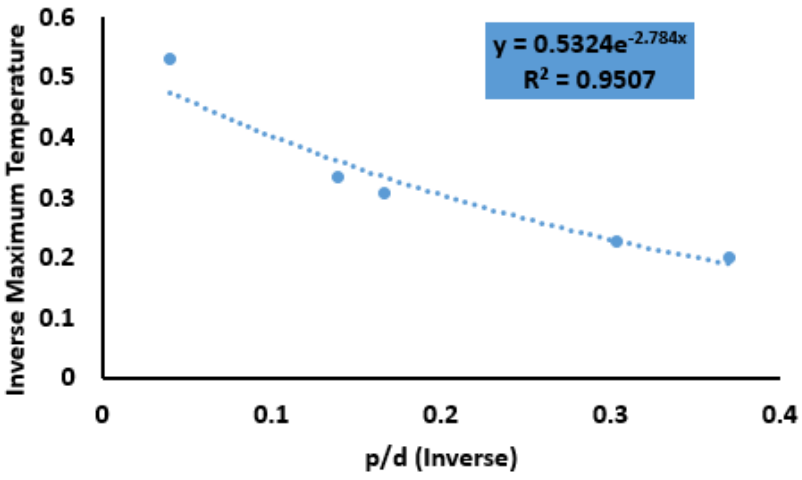

Figure 3.11. Relationship between twist ratio and maximum temperature location

3.4.1. Heat Transfer. Figure 3.12 shows the variation of heat transfer coefficient *h* with twisted ratios (p/d =25, 7.2, 6, 3.3 and 2.7) for different heat fluxes (10000W/m2, 5000W/m^2, 3000W/m^2 and 1000W/m^2) with full-length tape. The highest heat transfer coefficient *h* is achieved for the twisted ratio (p/d =2.7), which is the lowest twist ratio in this study. Moreover, the heat transfer coefficient with lowest twisted ratio (p/d =2.7) is higher than for p/d = 25, 7.2, 6, and 3.3 by about 16%, 11%, 7.2%, and 1.6%, respectively, for q=10,000 W/m^2. On the other hand, the heat transfer coefficient with the twisted ratio (p/d =2.7) is better than the heat transfer coefficient for the smooth tube without twisted tape under similar operating conditions by 28%. These results are plotted in Figure 3.12. The inverse of twist ratio (p/d)-1 is used as the horizontal axis, and the inverse of heat transfer coefficient (1/h) is plotted on the vertical axis. All data sets for various wall boundary conditions fit well to exponential lines with R^2 in the rate of 92% to 98%. It is also interesting to note that the exponent starts with -0.441 for q=1,000 W/m^2 and increases to -0.554 and -0.756 for q=3,000 W/m^2 and 5,000 W/m^2, respectively, but for 10,000 W/m^2 the exponent goes down to -0.458. For the case of regularly spaced twisted tapes (RSTT), there is a fixed amount of gap between the tapes followed by the twisted tape of the same length (see Figure 3.1). This technique is known to have advantages over the continuous tape. Figure 3.13 shows the variation of heat transfer coefficient *h* with RSTT with twist ratios of p/d =25, 7.2, 6, 3.3, and 2.7 for heat flux of 10,000 W/m^2. The effect of spacing is obvious in Figure 3.13, where continuous tape (FLTT) is compared with a spacing of 2W (two times width) and 3W geometries.

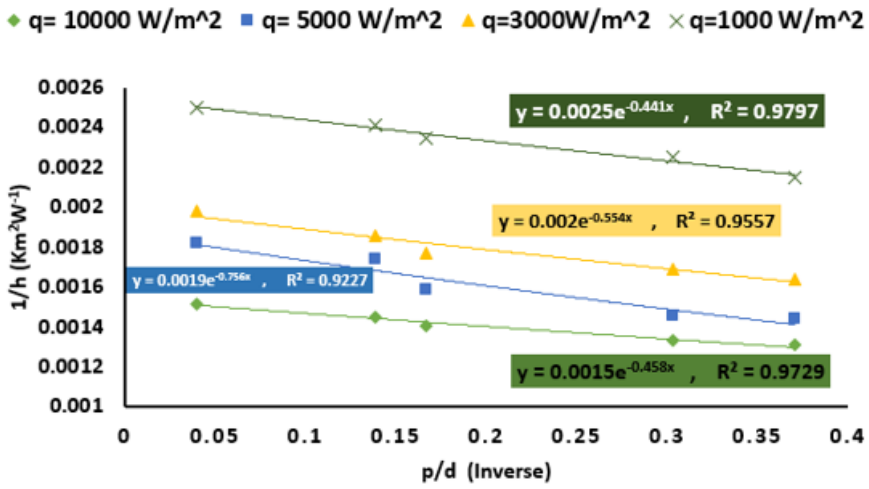

Figure 3.12. Inverse of twisted tape ratios with inverse of heat transfer coefficient for full-length twisted tape

The space effect is more pronounced for p/d ratios of 3.3 to 7.2. Heat transfer enhancement with spacing is reduced for this range and the reduction is related to the spacing length. The twist ratio (p/d = 2.7) produces better heat transfer coefficient than plain tube without twisted tapes for (FLTT, S=2W and S=3W) by about 28%, 27.4%, and 26%, respectively.

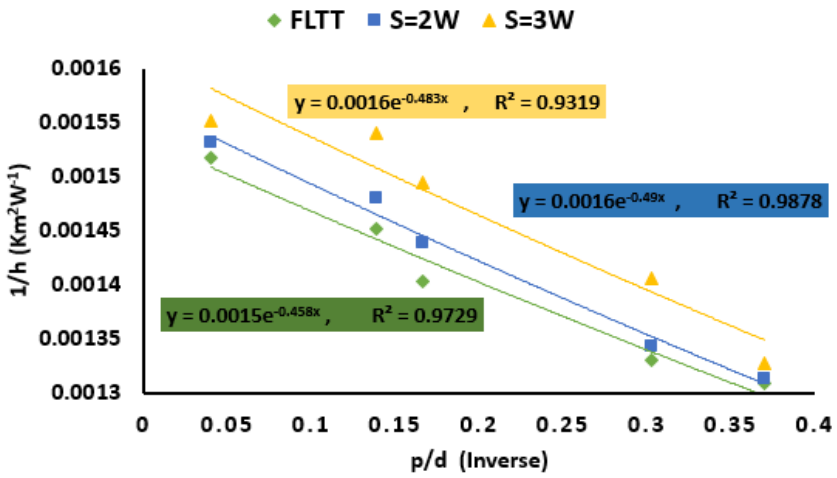

Figure 3.13. Inverse of twisted tapes ratios with heat transfer coefficient for RSTT

Figure 3.14 shows the variation of heat transfer coefficient *h* with twist ratios of p/d = 25, 7.2, 6, 3.3, and 2.7 for different widths of the twisted tapes for heat flux of 10,000 W/m^2. Heat transfer enhancement with reducing widths is reduced for this range. The reduction is related to the widths reduction. However, heat transfer coefficient with the twisted ratio (p/d = 2.7) is better than heat transfer coefficient for the plain tube without twisted tapes for (W = 9 mm, 8 mm and 7 mm) by about 28%, 27% and 25.8% respectively. The real advantage of spacing is in the pressure drop.

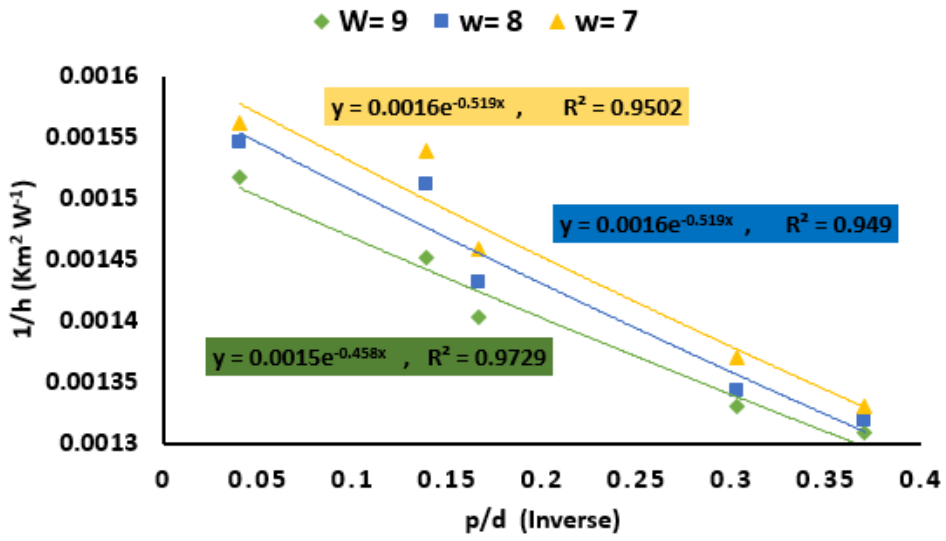

Figure 3.14. Inverse of twisted tape ratios with inverse of heat transfer coefficient for different widths of the twisted tapes

3.4.2. Pressure Drop. The effect of using the twisted tape ratio on the pressure drop is presented in Figure 3.15. The smallest twist ratio p/d =2.7 results in the highest pressure drop for both RSTT and FLTT. The increase in pressure drop for p/d = 2.7 for FLTT is found to be 55.6%, 31.7%, 26.5%, and 7 % higher than those for larger twist ratios (p/d = 25, 7.2, 6, and 3.3), respectively. For RSTT with 2W spacing, the pressure

drop was found to be 57%, 40%, 27.7%, and 6.5% for the smallest for twist ratios, p/d = 25, 7.2, 6, and 3.3, respectively. Thus, the increase in pressure drop is found to be 102.8%, 96.2% and 90% over the plain tube for FLTT, RSTT (2W), and RSTT (3W), respectively.

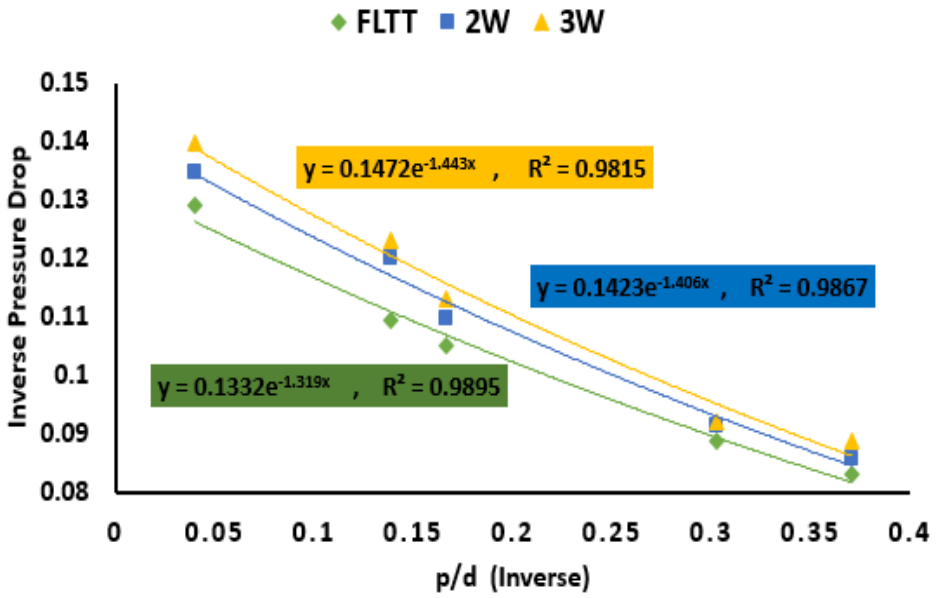

Figure 3.15. Inverse of twisted tape ratios with inverse of pressure drop for FLTT and RSTT

Figure 3.16 shows the variation of the pressure drop with twisted ratios (p/d =25, 7.2, 6, 3.3 and 2.7) for different tape widths. The smallest twist ratio p/d =2.7 is the highest pressure drop for (W = 9 mm, case of FLTT). The increase in pressure drop for p/d = 2.7 for W = 9 mm is found to be 55.6%, 31.7%, 26.5%, and 7% higher than those for larger twist ratios p/d = 25, 7.2, 6, and 3.3, respectively. For W = 8 mm, pressure drop is found to be 55.8%, 32.1%, 26.8%, and 6.3% for larger twist ratios p/d = 25, 7.2, 6, and 3.3, respectively. Moreover, W = 7 mm is found to be 60.9%, 34.7%, 28.8%, and

6.7%, respectively. In fact, the main cause of increased pressure drop is swirl flow and the dissipation of dynamic pressure at high viscosity drop near the tube wall. Thus, the increasing pressure drop is found to be 102.8%, 97.4%, and 93.87% over the plain tube for W = 9 mm, 8 mm and 7 mm. All the results for heat transfer and pressure drop are presented in Table 3.1.

Table 3.1. Variation of heat transfer and pressure drop for various twisted tapes and twisted ratios

d/p		FLTT	RSTT		DWTT		
			2W	3W	W=9 mm	W=8 mm	W=7 mm
$h^{-1} \times 10^{-6}$ (km^2W^{-1})	**0.04**	1518	1532	1551	1518	1547	1562
	0.138	1452	1481	1541	1452	1512	1540
	0.16	1403	1440	1494	1403	1431	1459
	0.030	1330	1343	1406	1330	1343	1370
	0.37	1308	1313	1328	1308	1318	1330
$\Delta P^{-1} \times 100$ Pa^{-1}	**0.04**	12.9	13.4	14	12.9	13.2	14
	0.138	10.9	12	12.3	10.9	11.26	11.7
	0.16	10.5	10.9	11.3	10.5	10.8	11.1
	0.030	8.8	9.1	9.6	8.8	9	9.2
	0.37	8.2	8.5	8.8	8.2	8.3	8.6

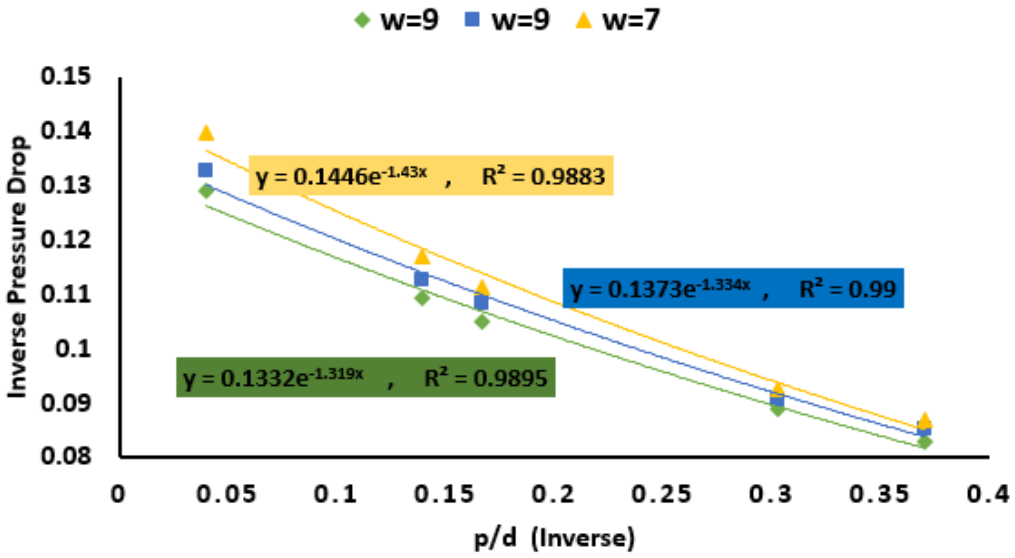

Figure 3.16. Inverse of twisted tapes ratios with inverse of pressure drop for different widths of the twisted tapes

4. EFFECT OF TWISTED TAPES ON FLOW WITHIN ROD BUNDLE SUBCHANNELS

4.1. OVERVIEW

Researchers are working to develop a new generation of nuclear reactors utilizing many different technologies to meet the criteria of enhanced safety [102]. Passive heat removal is an important aspect of keeping the reactor safe [113]. Typically, nuclear fuel assemblies for pressurized water reactors (PWR) are arranged in a square configuration consisting of rod bundles with coolant channels between them. To hold the fuel rods in an assembly, spacer grids are used. Spacer grids maintain a constant distance between the rods and support the rods along the length of the assembly. On the other hand, the coolant flows axially in the sub-channels, which is the area between the rods. Most spacer grids are designed to influence the thermal hydraulic performance of the fuel assembly by means of enhanced coolant mixing. The coolant mixing in turn (1) increases heat transfer, but at the cost of (2) increased pressure drop due to flow area constriction [116]. Due to this important hydrodynamic feature, research is often focused on enhancing coolant mixing. It is often an optimization problem when one is required to increase heat transfer while keeping pressure drop at an acceptable level.

Twisted tapes are commonly employed as heat transfer enhancers. Moreover, twisted tapes are one of the passive methods that does not require external power. Twisted tapes are preferred due to their simplicity and economic advantage during maintenance, installation, and operation [117]. Insertion of twisted tapes results in a longer flow path and longer time for fluid to pass through the core. Consequently, heat transfer is enhanced and pressure drop is increased.

The main objective of the present work is to numerically evaluate the impact of twisted tapes for the water flow through a 2X2 pressurized water reactors (PWR) rod bundle by using the commercial code fluent 18.1. In this study, the presence of twisted tapes inside the spacer grid and the presence of twisted tapes along the entire sub-channel will be investigated at the normal NuScale SMR reactor operating conditions.

4.2. PHYSICAL MODEL

In general, twisted tapes are metallic tapes that are simple to manufacture and used in many applications. Turbulence and swirl are generated by twisted tapes, and are useful features for heat transfer enhancement, which come at the expense of increased pressure drop. Enhancement characteristics of twisted tapes depend on "twist ratio" (y=p/d), that is the ratio of pitch (p) to the diameter (d). Pitch is the distance between two points on the tape that are on the same plane (a full 360^{o} twist) [118]. The geometries that are simulated for twisted tapes are depicted in Figure. 4.1.

In fact, twisted tapes lead to flow field modifications. Rather than a sub-channel, now the sub-channel is divided into two half circles. Each half will be subjected to rotation motion in addition to the axial motion. By rotating with a frequency and exerting a centrifugal force on the sub-channel wall hence changing the flow and producing a pronounced change occurs in heat transfer and pressure drop.

For the simulations, the length of rod bundle is 510 mm, which is the proposed fuel rod length for NuScale design. The spacer grid height is 44.45 mm wide square housing. On the other hand, the outside diameter for the fuel rod and fuel rod pitch are 9.5 mm and 12.6 mm respectively. The rod bundle has hydraulic diameter (D_h) 11.77

mm. The twisted tapes thickness is 0.5 mm. These dimensions are consistent with NuScale design. The twist pitch (p) values used in this study are 50, 30, 20, and 10, hence the twist ratios (p/d) are 4.2, 2.5, 1.7, and 0.85 respectively. Water is selected as the fluid for this simulations. The specific heat, thermal conductivity (k), density, and dynamic viscosity (μ) for H_2O are given as 4182 J/kg-K, 0.6 W/m-K, 998 kg/m3 and 1.003E-3 Kg/m-s respectively. This study is performed using the $k - \varepsilon$ turbulence model.

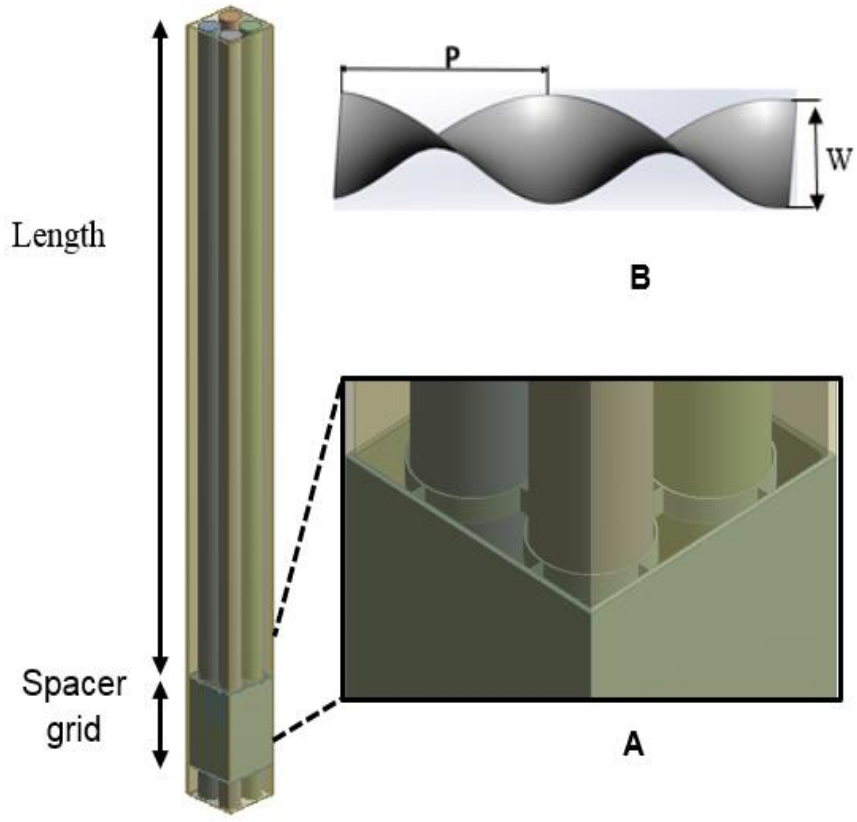

Figure 4.1. (A) Rod bundle. (B) Classic twisted tape

4.3. NUMERICAL MODEL

ANSYS/FLUENT 18.1 is used to perform CFD simulations of the geometry described in this study. Fluent uses the finite-volume method to solve the following

equations: (1) mass conservation; (2) momentum conservation in X, Y and Z; energy conservation. Moreover, turbulent flow used the $k-\varepsilon$ standard turbulence model. Thus, the k and ε Equations are showing in Equation 4.1 and 4.2 [119]:

$$\frac{\partial}{\partial t}(\rho k)+\frac{\partial}{\partial x_i}(\rho k u_i)=\frac{\partial}{\partial x_j}\left\{a_k \mu_{eff}\frac{\partial k}{\partial x_j}\right\}+G_k+G_b-\rho\varepsilon-Y_M+S_k \tag{4.1}$$

and

$$\frac{\partial}{\partial t}(\rho \varepsilon)+\frac{\partial}{\partial x_i}(\rho \varepsilon u_i)=\frac{\partial}{\partial x_j}\left\{a_k \mu_{eff}\frac{\partial \varepsilon}{\partial x_j}\right\}+C_{1\varepsilon}\frac{\varepsilon}{k}(G_k+C_{3\varepsilon}C_b)-C_{2\varepsilon}\rho\frac{\varepsilon^2}{k}-R_\varepsilon+S_\varepsilon \tag{4.2}$$

4.3.1. Boundary Conditions. The boundary conditions that were selected in this study correspond to the average values of a NuScale reactor under normal operation. The temperature was set to 531 K and the velocity of 0.832 m/s was defined at the entrance of the rod bundle, while an average pressure of zero was defined at the outlet of each rod bundle simulated in this study. The heat flux on the rod's surface constant was defined at 268.28 KW/m^2, which is the expected condition for NuScale SMR. Moreover, the surfaces of the rods and spacer grid were assumed to have no slip conditions.

4.3.2. Data Reduction. There are two flow fields a primary flow that is parallel to the main direction of fluid motion, and a secondary flow that is dependent on the magnitude of the resultant vector from velocities (Ux, Uz) divided by bulk velocity (Uy bulk) as showing in Equation 4.3:

$$SF=\frac{\bar{U}_{cross}}{\bar{U}_{bulk}}=\frac{1}{A}\sum_i\frac{(\sqrt{U^2_{xi}+U^2_{zi}})A_i}{U_{ybulk}} \tag{4.3}$$

where *A* is the total cross flow area and *Uxi* and *Uzi* are the velocities perpendicular to the main direction of fluid motion. The dimensionless Nusselt number (Nu) is used to

estimate the convective heat transfer that occurs at the surface of the rods. The Nusselt number is defined by Equation 4.4:

$$Nu = \frac{\bar{h} D_h}{\bar{K}} \tag{4.4}$$

where *K* is the average thermal conductivity of the fluid that is used in this study, and D_h is the hydraulic diameter that is defined by Equation 4.5:

$$D_h = \frac{4A}{P_w} \tag{4.5}$$

where *Pw* is a wetted perimeter of the channel [2] and *h* is the average heat transfer coefficient defined by Equation 4.6:

$$\bar{h} = \frac{q''}{(\bar{T}_r - \bar{T}_f)} \tag{4.6}$$

where q" is the average heat flux on the surface of the fuel rods, T_r is the average temperatures at the fuel rods surface and T_f is the average temperature of fluid in this study. Reynold's number is defined by Equation 4.7:

$$Re = \frac{\rho v l}{\mu} \tag{4.7}$$

where ρ is the density of the fluid that was using in this study, v is the velocity, l is the characteristic length, and μ is the dynamic viscosity.

4.3.3. The Mesh Parameters. Proper meshing for such simulations is critical for capturing the thermal hydraulic behavior. Therefore, Ansys Meshing is used in this simulation to mesh the geometry. To make sure that the results acquired do not vary with the cell size, four meshes were generated with different mesh sizes. The meshes were 3.5 M, 5.1 M, 6.2 M, and 7.1 M for the pressure profiles for a twisted ratio of 1.7 as shown in Figure 4.2. A small grid dependence is observed for 1.32 M nodes, but all results were

identical for 5.1 M nodes and higher. For this reason, grids with 5.1 M nodes are used for the rest of the simulations.

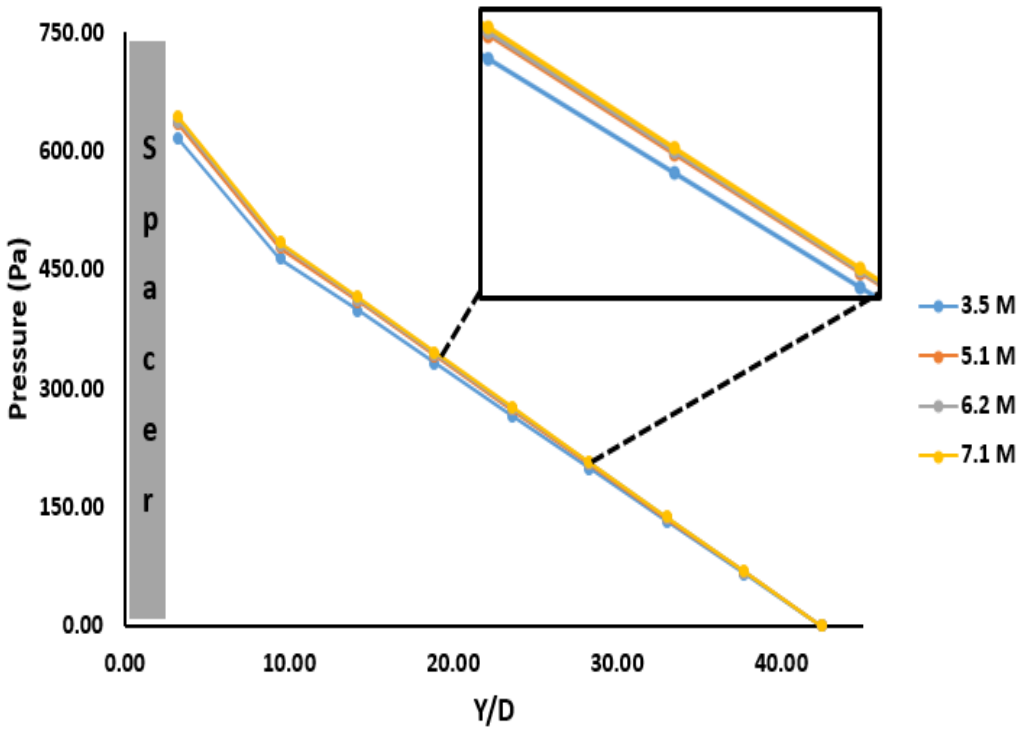

Figure 4.2. Different of meshes for pressure profiles

In fact, meshing for a geometry with twisted tape is significantly more complicated compared to sub-channels without twisted tapes. The fine mesh that was defined for all meshes had uniform size and a slow transition. Moreover, near the walls of the rods, four layers of inflated (prismatic) elements with a transition ratio of 0.1 and growth rate of 1.2 were used. The min size, max face size, and max Tet size were 7.31e-2 mm, (0.2 mm-0.76 mm), and (0.2 mm- 0.76 mm) respectively, depending on mesh complexity for segments. Inflated 4-layer (prismatic) elements were used next to the twisted tape as shown in Figure 4.3.

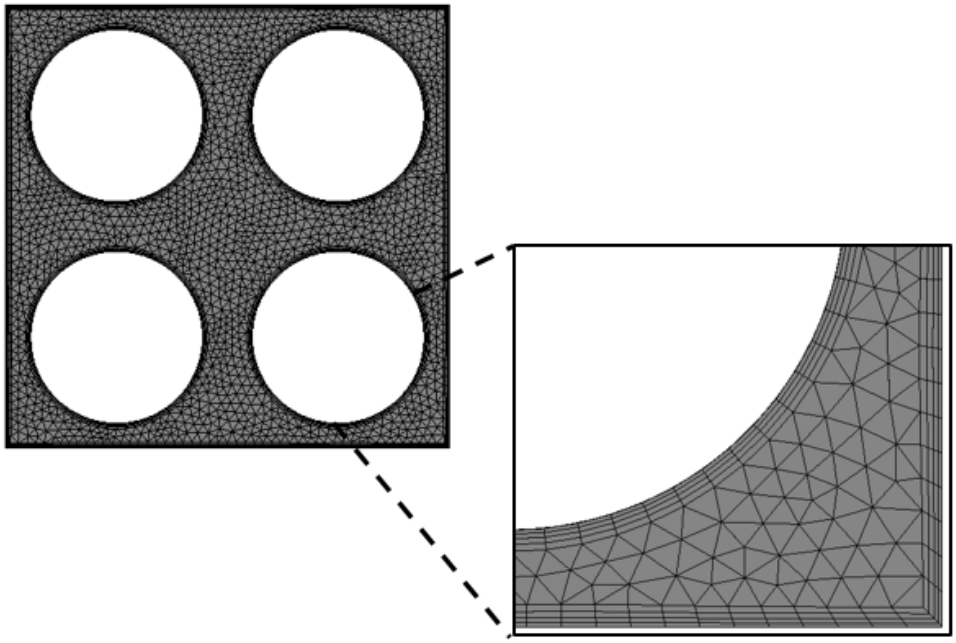

Figure 4.3. Mesh cross section of sub-channel

4.3.4. Numerical Solution. Initial conditions were defined at the channel inlet and were used to test the numerical convergence. The number of iterations ranged between 450 and 1300 depending on each case. For plain sub-channels, cases with high twisted ratios that were under normal operation converged between 470 and 1170 iterations, respectively. With lower twist ratios, the convergence took longer and had a higher number of iterations. Convergence criteria was set to 1E-5 for velocity, continuity, *k*, and epsilon. A tighter criterion of 1E-6 was used for energy. In this work, more than 93 simulations were performed using an Intel core (TM) i7-7700 CPU@ 3.6 GHz and a memory of 16.00 GB. Most simulations were completed within 8-14 hours; however, computation speed can be significantly increased with high power computers. Table 4.1 is showing setup and solver setting for this section.

Table 4.1. Setup and solver settings

Model	Energy, K-epsilon (2 eqn)
Outlet	Pressure Boundary
Density Model	Constant
Pressure-Velocity Coupling	SIMPLE
Pressure Solver	Body Force Weighted
Momentum	2nd Order Upwind
Turbulent Kinetic Energy	2nd Order Upwind
Turbulent Dissipation Rate	2nd Order Upwind
Energy	2nd Order Upwind
Gradient	Least Squares Cell-Based

4.4. RESULTS AND DISCUSSION

Results of this study are divided into two sections. In the first section, the presence of twisted tapes on a 2 x 2 rod bundle inside only spacer grid was investigated. In the second section, the presence of twisted tapes on a 2 x 2 rod bundle along the entire sub-channel was investigated. The spacer grid and the gap between spaces were evaluated through the comparison of the results for no twist tapes and for twist tapes with various twist ratios. Three average thermo-fluid dynamic parameters are used to estimate the impact of twisted tape, pressure drop, Nusselt number with Re number and secondary flow (SF).

4.4.1. Twisted Tapes Inside Spacer Grid. Figure 4.4 shows the effect of twisted tape on pressure drop along the axial length of the rod bundle. As one can see, there is a sharp pressure drop from the exit of the spacer (where the twisted tape is situated) to a short distance down the flow, approximately 4.1-9.4 Y/D. Afterwards, the

pressure drops for all twist ratios are almost identical. The highest observed pressure drop is from 720 Pa to 475 Pa for a twist ratio of 0.85, which is much more than the linear drop of the no twisted tape case (495 to 432 Pa). All data sets containing pressure drops from 720 Pa to 475 Pa for several of twisted tapes ratios fit well to linear with R^2 =98.9% as shown in Figure 4.5. After the initial steep pressure drop, all twist ratios show an almost linear behavior not much different from the case of no twisted tape. The slope of the initial pressure drop is dependent on the twist ratio.

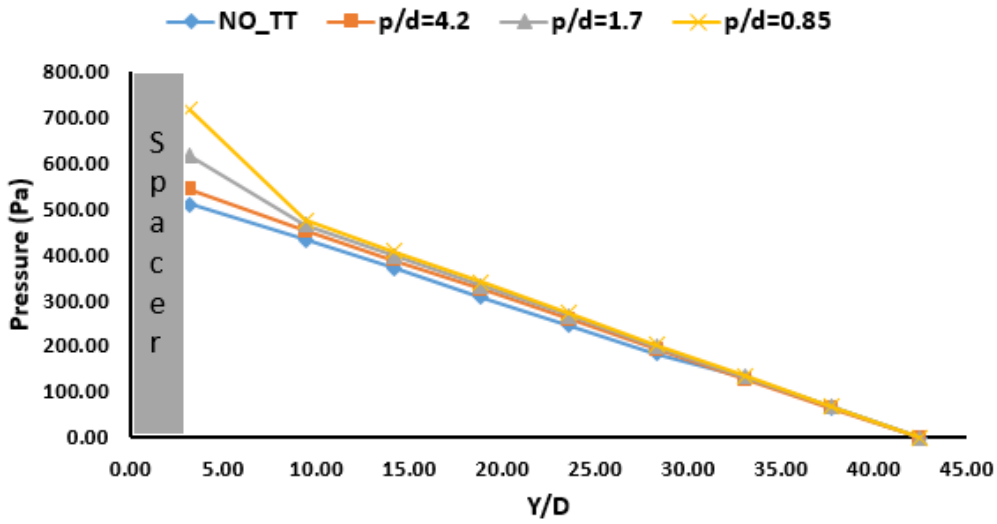

Figure 4.4. Effect of twisted tape ratios on pressure loss along the flow direction

The effect of the Reynolds number on the Nusselt number with variation of twisted tape ratios is presented in Figure. 4.6. Five velocities were simulated giving rise to five Reynolds numbers. Two Reynolds number values were above the average value in a NuScale reactor under normal operation, while two values were below the normal operation conditions. The results obtained from this study show that the average Nusselt number for a twist ratio of 4.2 is enhanced by 9% as compared to the case of no tape.

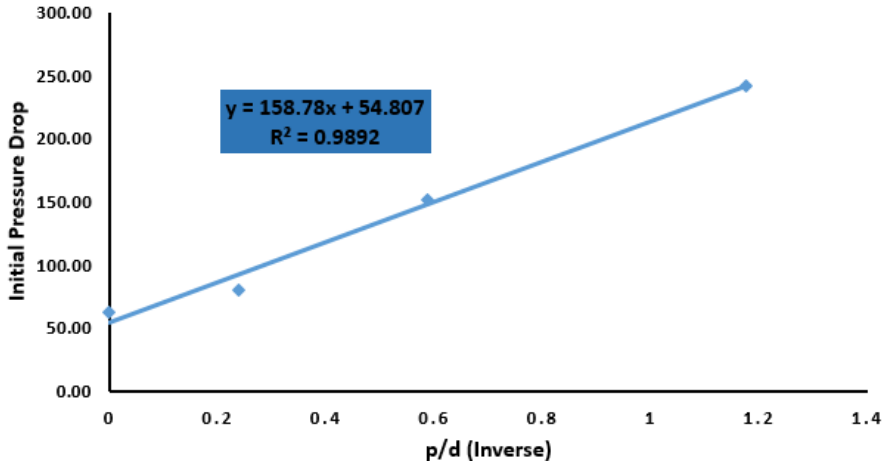

Figure 4.5. Inverse of twisted tapes ratios with inverse of initial pressure drop

The average enhancement is 18% and 25% for twisted ratios of 1.7 and 0.85, respectively. There appears to be a linear correlation between the Re and the Nu for any given case of twist ratio of no twist tape.

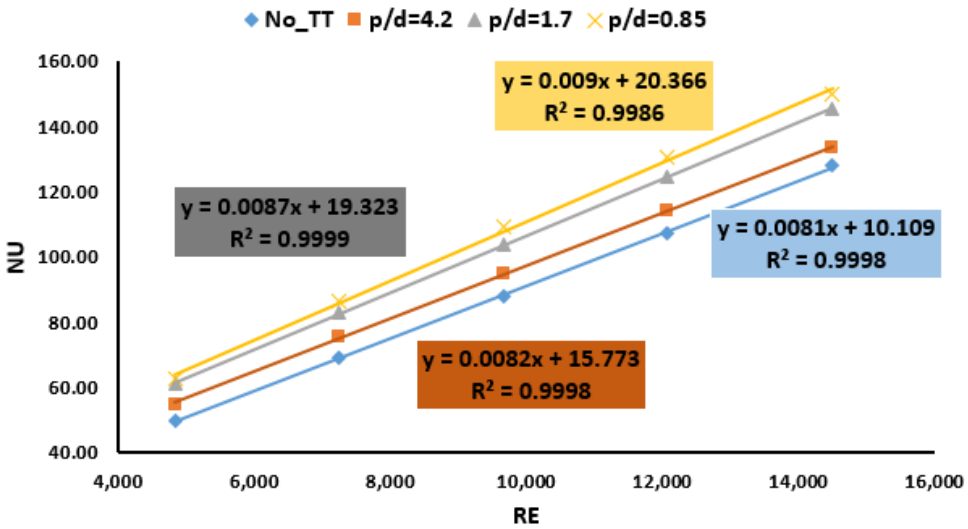

Figure 4.6. Effect of Reynolds number on the Nusselt number with variation of twisted tape ratios

Figure 4.7 shows the effect of twist ratios on secondary flow along the flow direction for Re = 9.6 k. The secondary flow is observed to be much more pronounced in the length with the twisted tape peaking at the exit point of the spacer grid where the twisted tape ends. From this point on, a sharp drop in secondary flow occurs followed by a slower drop before approaching zero. As expected, the SF increases with the decrease of the twisted ratio. Interestingly, increase of SF occurs significantly with changing twisted ratio. The highest secondary flow is achieved for the twisted ratio (p/d =0.85) which is the lowest twist ratio in this study by SF ~0.16. Secondary flow for the twisted ratios of p/d =1.7, 2.5, 4.2, and plain sub channel (without twisted tape) were SF~ 0.08, 0.035, 0.014 and 1.40e-5 respectively. These results are for Re=9.6 k which is approximately the normal operating conditions for the NuScale reactor. Secondary flow dependence is shown in Figure 4.8. There is a strong correlation between twist ratio and the secondary flow with R^2=0.97.

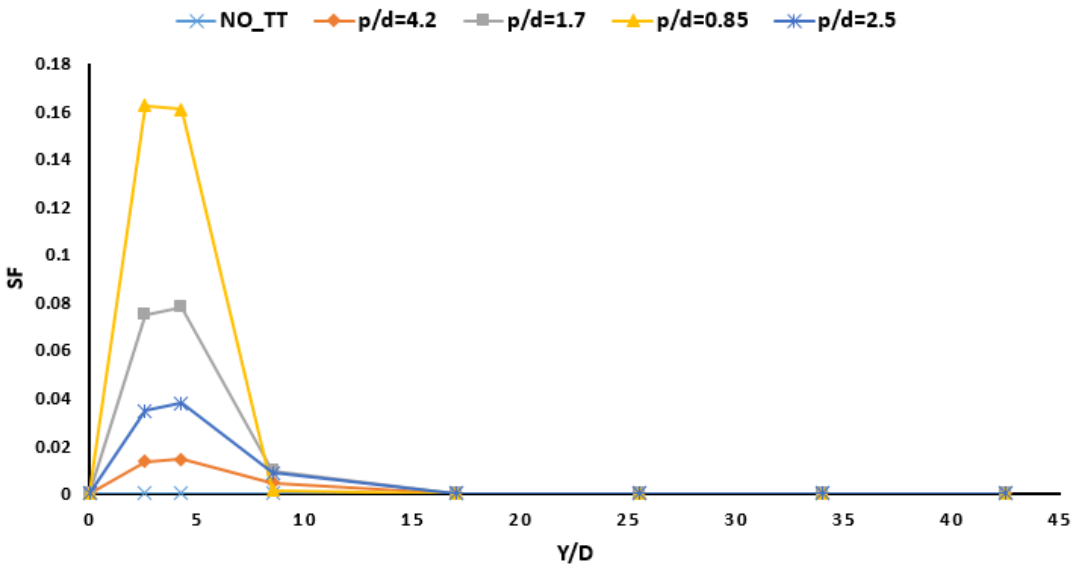

Figure 4.7. Effect of twisted tape ratios on secondary flow along the flow direction

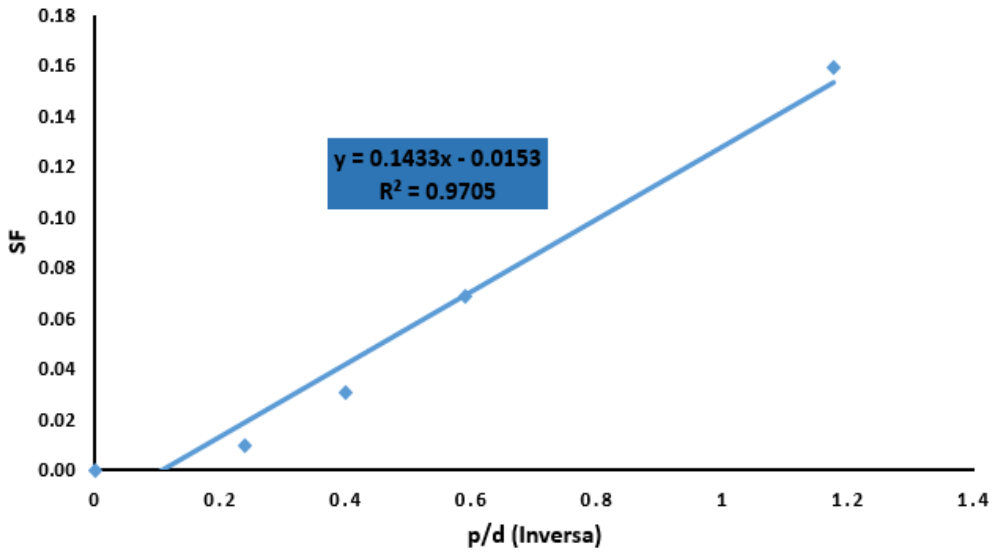

Figure 4.8. Inverse of twisted tapes ratios with secondary flow

In Figure 4.9, secondary flow at Y/D= 4.2 and 8.5 are highlighted, showing the velocity vectors in a cross sectional plane for the twisted ratio (p/d =0.85).

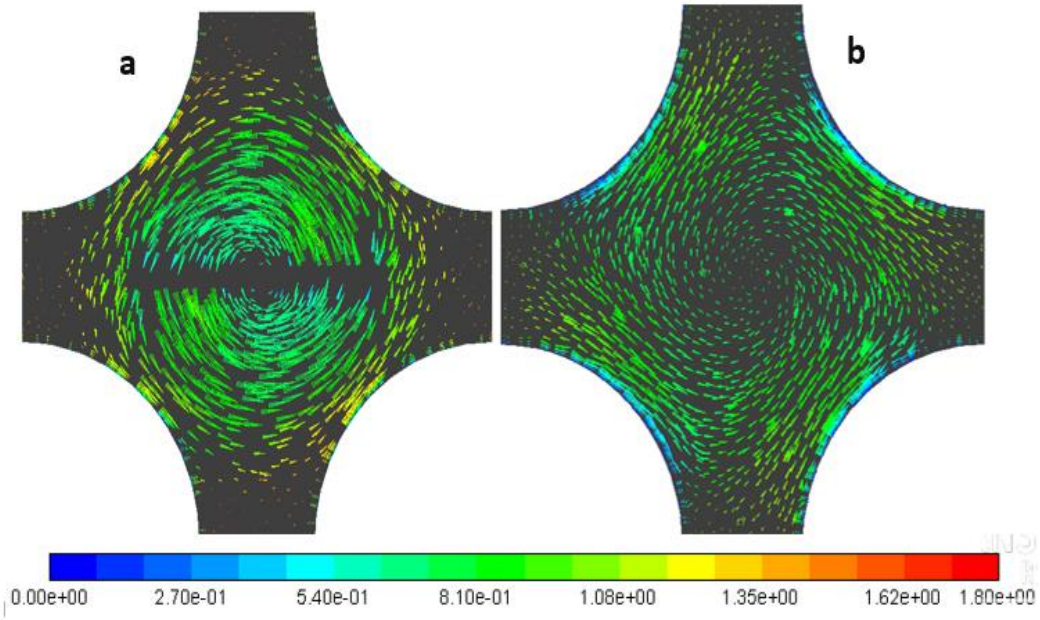

Figure 4.9. (A) Secondary flow at Y/D= 4.2. (B) Secondary flow at Y/D= 8.5 for the lowest twist ratio

4.4.2. Twisted Tapes Along Sub-channel. Figure 4.10 shows the effect of twisted tape on pressure drop along the sub-channel. As one can see, a linear pressure drop past the spacer occurs for all cases of twist ratios and the case of no twisted tape. Moreover, the slope of the initial pressure drop is dependent on the twist ratio. All data sets for various twist ratios fit well with R^2 = ~99% as shown in Figure 4.11. As expected, the highest observed pressure drop is for twist ratio of 0.85.

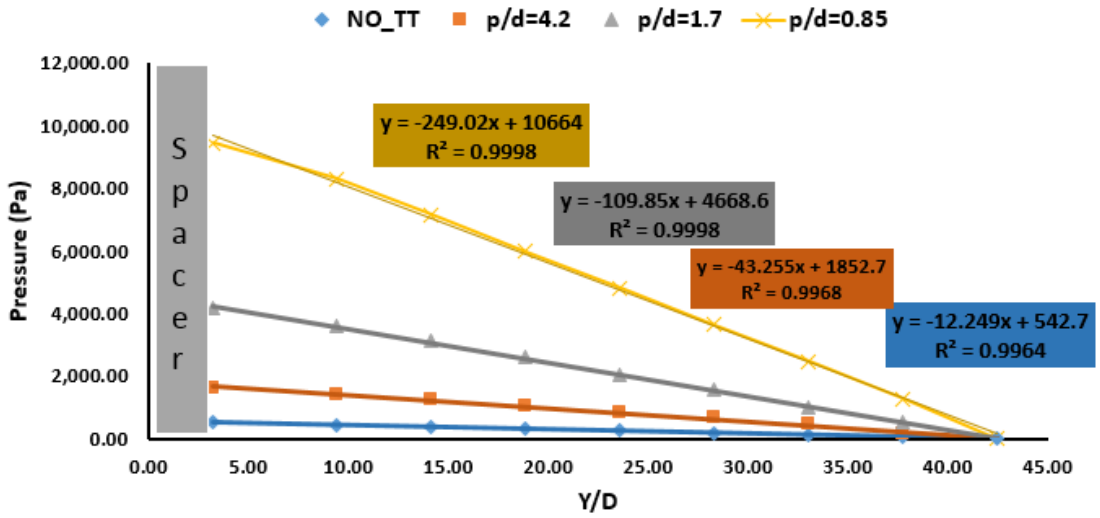

Figure 4.10. Effect of twisted tape ratios on pressure loss with the twisted tape along the sub-channel

The effect of the Reynolds number on the Nusselt number with variation of twisted tape ratios is presented in Figure 4.12. The results obtained from this study show that the average Nusselt number for the twist ratio of 4.2 is enhanced by 29% as compared to the case of no twisted tape. The average enhancement is 70.3% and 101% for twisted ratios of 1.7 and 0.85, respectively.

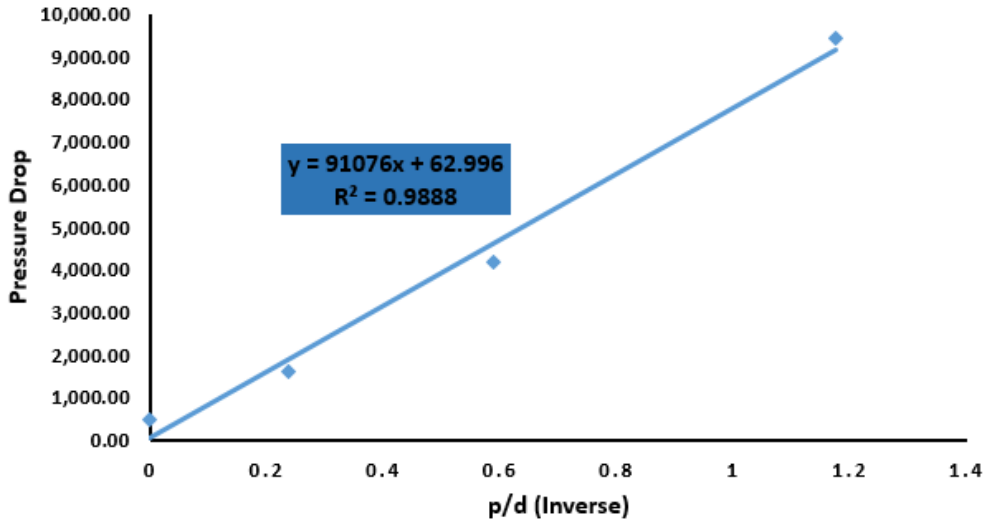

Figure 4.11. Inverse of twisted tapes ratios with pressure drop along the sub-channel

There appears to be a linear relationship between the Re and the Nu for any given case of twist ratio with no twist tape. All data fit well a linear with R^2 in the range of 98% to 99% for several of twisted tapes ratio.

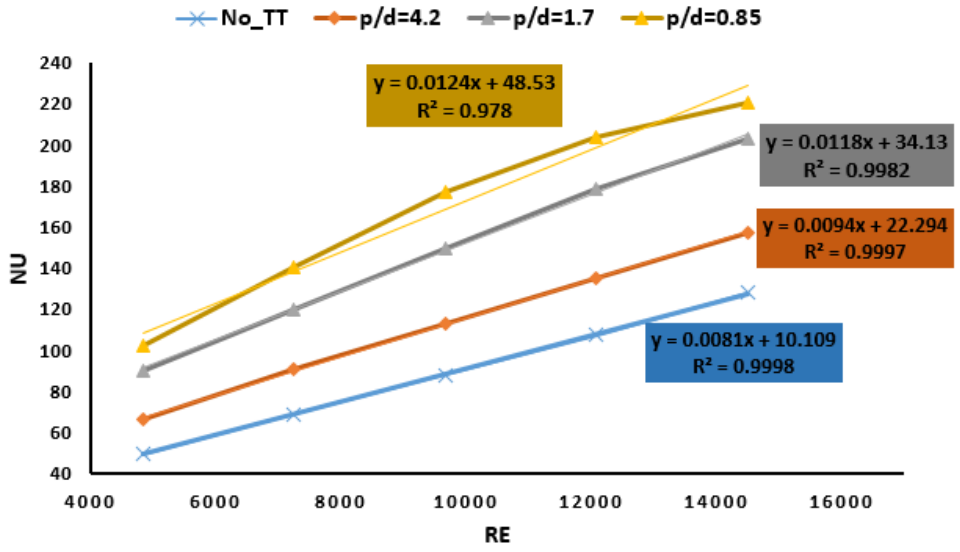

Figure 4.12. Effect of Reynolds number on the Nusselt number with variation of twisted tape ratios when the twisted tape along the subchannel

Figure 4.13 shows the effect of twisted tape ratios on secondary flow along the flow direction with twisted tapes along entire sub-channel for Re = 9.6 k. The secondary flow is observed to be much more pronounced in the length with the twisted tape. It seems to peak at Y/D=2.5 and then remains unchanged until Y/D=38. Interestingly, the decrease of SF occurs at the outlet of the sub-channel, which was more pronounced by a decreasing twisted ratio as shown in Figure 4.13. The highest secondary flow is achieved at the twisted ratio (p/d =0.85) which is the lowest twist ratio in this study by an average SF ~0.160 along the sub-channel, the secondary flow with the twisted ratio p/d =1.7 and 4.2 averaged SF~ 0.08 and 0.015, respectively.

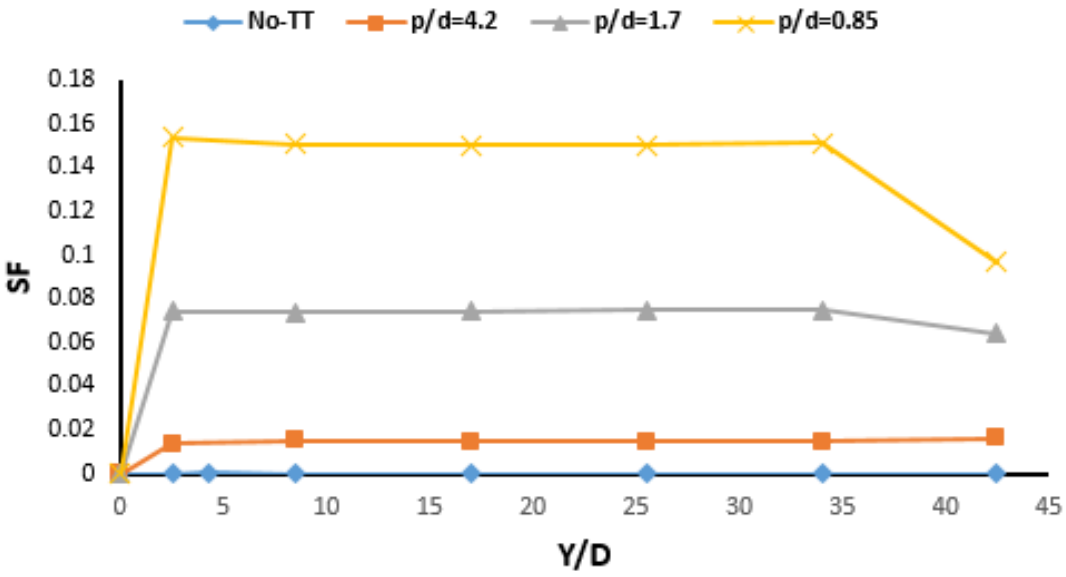

Figure 4.13. Effect of twisted tape ratios on secondary flow along the flow direction with TT along sub-channel

Figure 4.14 show the secondary flow at Y/D= 38 and 42.4 and shows the velocity vectors in a cross-sectional plane for the twisted ratio (p/d =0.85). This result gives very

good insight on how the secondary flow is generated by a swirling motion due to the twisted tape and the average flow. At the outlet (or close to the outlet), SF is observed to be much stronger than the inlet.

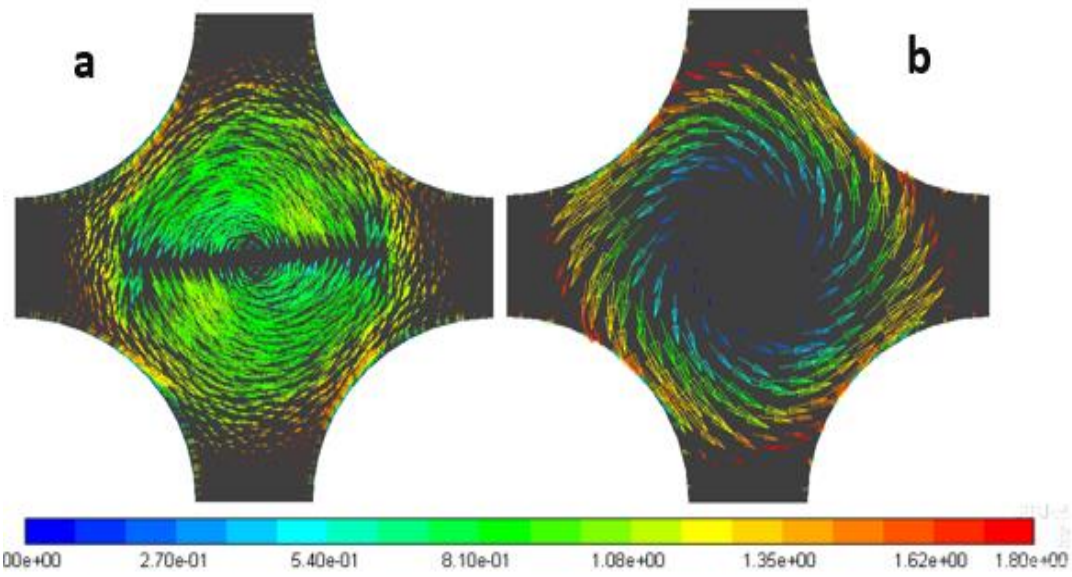

Figure 4.14. (A) Secondary flow at Y/D= 8.5. (B) Secondary flow at Y/D= 42.4 for the lowest twist ratio

The twisted tape geometry can be used to create a lateral swirling flow structure in the rod bundle sub-channels. Twisted tapes promote higher mixing rates in the rod bundle and create large lateral flow structures in the rod bundle sub-channels. To investigate the SF further, a 4x4 fuel rod was simulated. In this case, the Reynolds number for a nine sub-channel model is 9.6 K. Figures 4.15 and 4.16 show the development of the lateral velocity vectors and Y velocity, which is flow direction, at 42.4 Y/D. In the present study, the swirling flow structures that are in the center of each sub-channel are circular in shape.

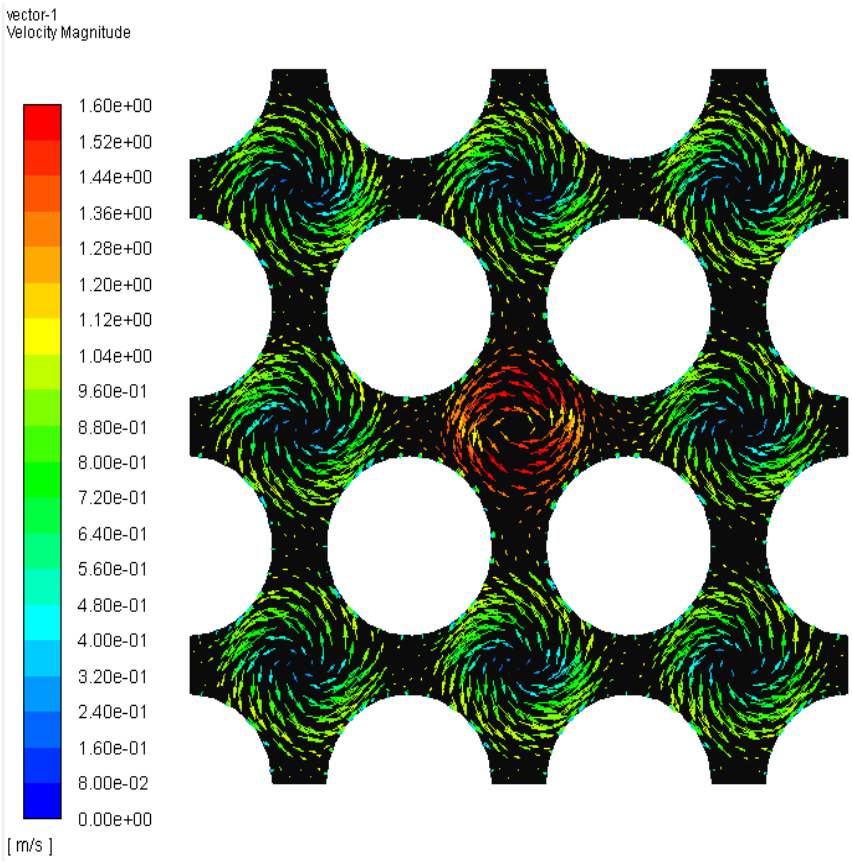

Figure 4.15. The lateral velocity vectors with Y velocity

Changing the twisted tape ratio in the same model creates strong lateral flows along the fuel rod surface. Furthermore, this change can be used to ensure uniform channel heating and to avoid hot spots as shown in Figure 4.15 and 4.16. The twisted tape ratio was 1.7 in all channels except for the center channel, which was 4.2, for a 4 × 4 rod bundle array. This design improved the velocity of center channel when compared to a center channel that used the same twisted ratio. Moreover, the secondary flow is observed to be higher in the center due to fluid movement generated by the swirling motion due to the change of twisted tapes ratios in the channels. Furthermore, improvement is observed in the gap between two channels, as shown in Figure 4.17

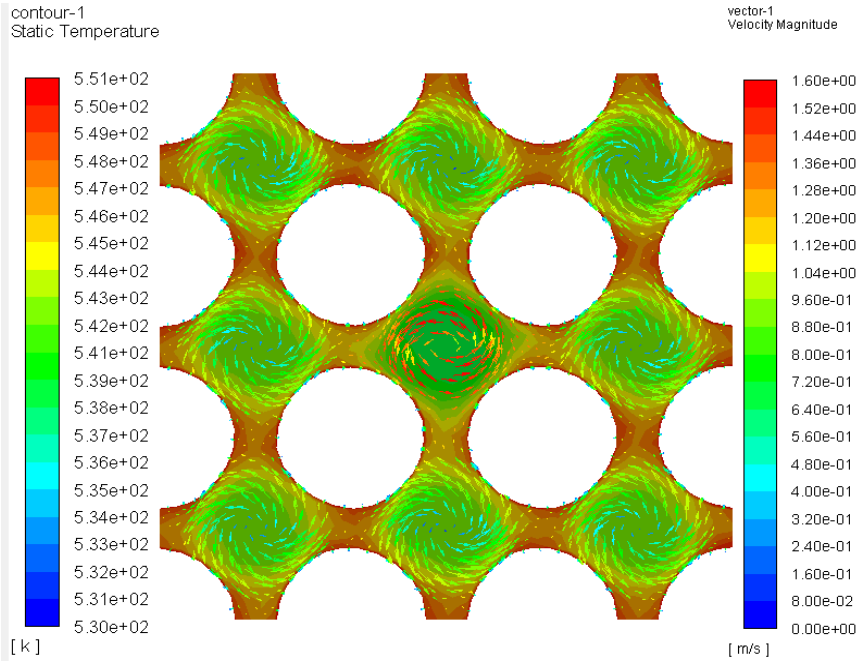

Figure 4.16. The lateral velocity vectors with temperature

At the exit (Y/D=42), the velocity perpendicular to the SF is shown in Figure 4.17. Thus, the design that used different twisted ratios achieved the highest velocity by about 1.26 m/s, while for the design that used the same twisted ratio achieved a higher velocity of 0.995 m/s.

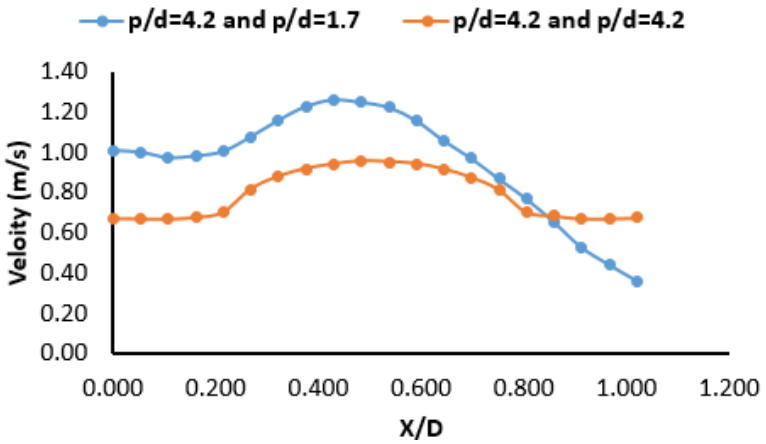

Figure 4.17. Comparison of the velocity in the gap of two central sub-channel

5. NUMERICAL INVESTIGATION OF FLOW IN ROD BUNDLE SUBCHANNELS ON NATURAL CONVECTION: EFFECT OF TWISTED

5.1. OVERVIEW

As nuclear energy is competitive with fossil fuels as a method of electricity generation, many nations look to add nuclear power to their national energy mix. However, the number of nuclear power reactors cannot be increased without increasing the level of nuclear reactor safety under all conditions [120].

In the modern nuclear reactor design, use of passive safety is becoming a standard feature. In the event of a reactor emergency, the passive safety approach relies on natural force and phenomena to keep the reactor under secure shutdown status, that is to say that the reactor can be safely cooled with no dependence on an active system or electricity. There are two main methods of convective heat transfer; forced convection, in which the motion of the fluid is affected by external means such as a pump or fan; and natural convection, in which the fluid flow is affected by natural forces, like buoyancy or change in a system's force field [121]. Passive safety rely on buoyancy for residual heat removal.

NuScale's Small Modulator Reactor (SMR), a new reactor design uses natural convection for cooling during an accident [8]. NuScale's reactor is arranged in a square configuration consist of rod bundles with coolant channels in between [122]. Spacer grids are used to hold the fuel rods, keep the constant distance between the rods, and support the rods along the length of the assembly. In this reactor, spacer grids are used to influence the thermal hydraulic performance by mixing the coolant that flows axially in sub-channels; that is, the area between the rods by vanes [123]. To mix coolant and

enhance heat transfer, devices such as twisted tape, ribs, baffles, plates, helicals, and wire coils can be utilized. The current open literature contains limited data on the effectiveness of these techniques for natural convection/circulation systems into reactors [124]. These applications are preferred for many reasons such as simplicity, economics, and advantages of maintenance, installation, and operation. In general, application of these devices results in the longer flow path and longer time for fluid to pass through the core. Consequently, heat transfer is enhanced and pressure drop is increased [125]. Heat transfer for natural convection is governed by Newton's law of cooling and driven by buoyancy force, which only changes the body force term in the momentum equations. The relative magnitudes of laminar and turbulent natural convection may be quantified by the Rayleigh number [126], shown in Equation 5.1:

$$Ra = \frac{g\beta\ \Delta T\ L^3}{\mu\alpha} \tag{5.1}$$

The main objective of this section is to evaluate the impact of the insertion of twisted tape on a 2x2 rod bundle of a pressurized water reactor (PWR), numerically, under natural convection for the NuScale SMR, with a variation of twisted tape ratios under heat flux boundary condition expected post shutdown. The study investigated the insertion of twisted tape along a spacer grid, as well as along an entire sub-channel at the abnormal operating conditions for the NuScale SMR. The simulation was performed using the commercial software ANSYS FLUENT 18.1.

5.2. PHYSICAL MODEL

Twisted tape generates swirl flow that is useful for heat transfer enhancement and hence is preferred for many applications. When utilizing twisted tape, the sub-channel is

divided into two half sub-channel. Each half is subjected to rotation motion in addition to the axial motion. This motion leads to flow field modifications. By rotating with a frequency and exerting a centrifugal force on the sub-channel is changed in thermo-fluid dynamic [36].

Table 5.1 shows general information about the fuel rods used in this study. Twist ratio (y=p/d), one of the enhancement characteristics, is the ratio of 360^0 pitch (p) to the diameter (d), as shown in Figure 5.1. Fuel geometry selected for this study is consistent with NuScale proposed fuel design. The twist pitch (p) values used in this study are 29.4 mm, 58.8 mm, 88.2 mm, 101.8 mm, 110.6 mm, and 148 mm; thus, the twist ratios (p/d) are 2.5, 5, 7.5, 8.6, 9.4, and 12.6 respectively.

Table 5.1. General information for fuel rods

Fuel rod diameter (mm)	9.5
Fuel rod length (mm)	510
Fuel rod pitch (mm)	12.6
Number of fuel rods	4
Spacer grid height (mm)	44.45
Hydraulic diameter of sub-channel (mm)	11.77

The selected fluid for this simulation was water. The specific heat (Cp), thermal conductivity (k), viscosity (μ), and thermal expansion coefficient (1/k) for H_2O are given as 4182 J/kg-K, 0.6 W/m-K, 1.003e-3 kg/m-s and 0.001 respectively. The Boussinesq

approximation was applied to simulate the natural convection phenomenon with a density equal to 998 kg/m^3 for water.

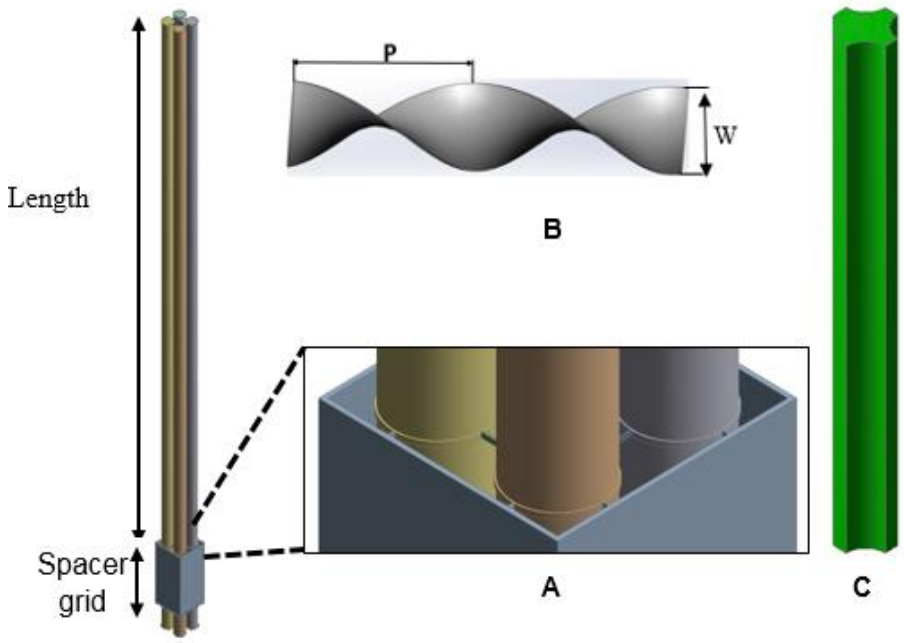

Figure 5.1. (A) Rod bundle. (B) Twisted tape. (C) Sub-channel

5.3. NUMERICAL MODEL

In this study, FLUENT 18.1 was employed to perform computational fluid dynamics (CFD) simulations of the geometry to investigate the natural convective flow characteristic. FLUENT uses the finite-volume method and solves three-dimensional continuity equations, momentum equations, and energy equations in the unsteady laminar.

5.3.1. Boundary Conditions. The boundary conditions selected for this investigation correspond to the values of the NuScale reactor. The water temperature was set to 531 K at the entrance of the rod bundle, while the average pressure of zero

was defined at the outlet of each simulation to mimic natural convection. The heat flux on the surface of the rods was constant and defined at 2682 kW/m2, 5364 kW/m2, 8048 kW/m2, and 10728 kW/m^2 - 1%, 2%, 3%, and 4% respectively - of the full power normal operation condition expected for the NuScale SMR. Additionally, the surfaces of the rods and spacer grid were assumed to have no-slip conditions.

5.3.2. Data Reduction. The dimensionless Nusselt number (Nu) is used to estimate the convective heat transfer at the surface of the rods. The Nusselt number is calculated by Equation 5.2:

$$Nu = \frac{\bar{h} D_h}{\bar{K}} \tag{5.2}$$

Convective heat transfer coefficient is shown in Equation 5.3:

$$\bar{h} = \frac{q''}{(\overline{T_w} - \overline{T_b})} \tag{5.3}$$

Bulk mean fluid temperature is shown in Equation 5.4:

$$\overline{T_b} = \frac{T_o - T_i}{2} \tag{5.4}$$

Hydraulic diameter is shown in Equation 5.5:

$$D_h = d\left[\frac{4}{\pi}\left(\frac{P}{d}\right)^2 - 1\right] \tag{5.5}$$

Rayleigh number is shown in Equation 5.6:

$$Ra = Gr * Pr \tag{5.6}$$

The Grashof number, interpreted physically as a dimensionless group, is the ratio of buoyancy forces to viscous forces in free-convection flow. The Grashof number's role is similar to that of the Reynolds number in a forced convection scenario [127]. The Grashof number is shown in Equation 5.7:

$$Gr = \frac{g\beta\ \Delta T\ D^3}{\mu^2} \tag{5.7}$$

The Prandtl number is shown in Equation 5.8:

$$Pr = \frac{\mu\ Cp}{k} \tag{5.8}$$

5.3.3. The Mesh Parameters. Proper meshing is critical to capture the thermal hydraulic behavior. This study utilized ANSYS Mesh model to mesh the geometry. The small size prismatic cell was utilized to ensure more accurate results and to reduce the number of high-skewed cells generated near the fuel rods. Inflated four layers were used next to the twisted tape with growth rate of 1.2 and transition ratio of 0.1 as shown in Figure 5.2.

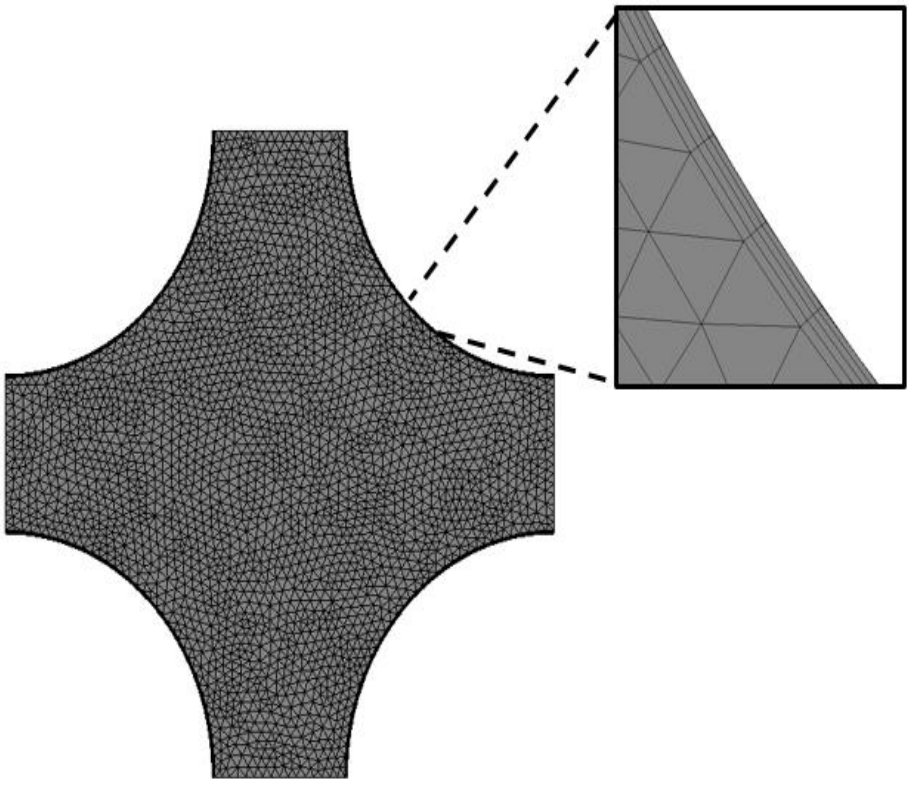

Figure 5.2. Mesh cross section of sub-channel

To check the influence of the mesh resolution on the results, a comprehensive mesh sensitivity study was performed. To ensure that results acquired did not vary with the cell size, five meshes were generated with different mesh sizes for twisted ratio 2.5. The meshes were 1.2 M, 2.2 M 3.8 M, 5.5 M, and 7.1 M for the pressure profiles as shown in Figure 5.3.

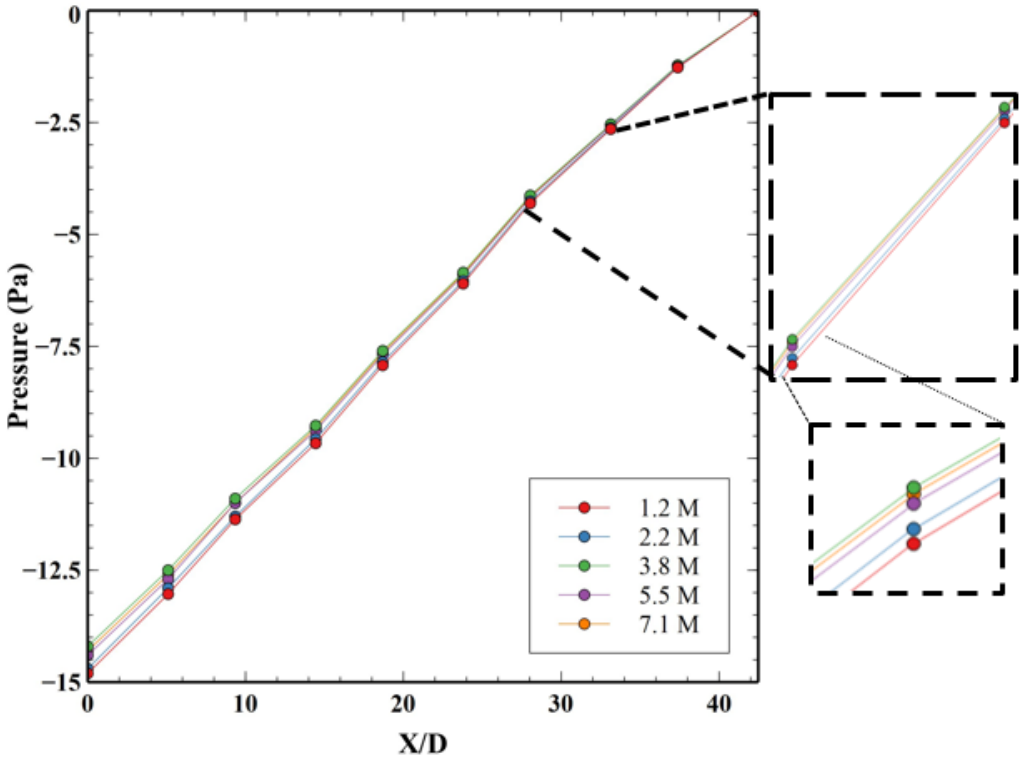

Figure 5.3. Difference of meshes for pressure profiles

In this comprehensive mesh, all results were identical for node elements of 3.8 M and above. For this reason, a grid with elements of 3.8 M was used for the rest of the simulations. Meshing for a geometry with twisted tape was significantly more complicated compared to meshing for a sub-channel without twisted tapes. However, the fine mesh was defined for all meshes with uniform size and slow transition. The

minimum size, maximum face size, and maximum Tet size were dependent upon mesh complexity for segments. In this study, the minimum size and maximum face size were 1.511E-2 mm and 0.25 mm, respectively.

5.3.4. Numerical Solution. In this study, more than 42 simulations were performed using Intel Core (TM) i7-7700 CPU@ 3.6 GHz and memory 16.00 GB. The first solution converged after 811 iterations, while most simulations ranged between 417 and 1256 iterations, depending on each case (with twisted tape and without). Most simulations were completed within 6-12 hours. Convergence criteria were set to 1E-5 for velocity in (x, y, and z) and continuity, while a tighter criterion of 1E-6 for energy was used. Table 5.2 shows FLUENT solver settings used for all cases.

Table 5.2. FLUENT solver settings

Model	Energy, Laminar
Outlet	Pressure Boundary
Density Model	Boussinesq
Pressure-Velocity Coupling	SIMPLE
Pressure Solver	Body Force Weighted
Momentum	2nd Order Upwind
Energy	2nd Order Upwind
Gradient	Least Squares Cell-Based

5.4. RESULTS AND DISCUSSION

This study investigated the effects on the thermo-fluid dynamic parameters of the Nusselt number and pressure loss relating to the presence of twisted tape on a 2x2 rod bundle along a spacer grid, and the presence of twisted tape on 2x2 rod bundle along a

sub-channel. Results were then evaluated through comparison of data regarding the application of twisted tape versus no twisted tape, with various twist ratios and under natural convection.

5.4.1. Twisted Tapes Along Spacer Grid. The average Nusselt number is a measure of the heat transfer on the fuel rods. Figure 5.4 shows the variation of Nusselt number (Nu) with Rayleigh Number (Ra) for different heat flux that was 1%, 2%, 3% and 4% of heat flux under normal operation for NuScale SMR, while the twisted tape along the spacer grid had twisted ratios p/d = 7.5, 5, and 2.5. Results showed the average Nusselt number increased as the Rayleigh number increased. The Nusselt number increased sharply when heat flux was between 3% and 4% using twisted tapes ratios 2.5, 5, and 7.5. This enhancement in the Nusselt number could be attributed to the natural convection heat transfer and the buoyancy force enhancement when the Rayleigh number increases. Additionally, viscosity differences led to a higher heat transfer.

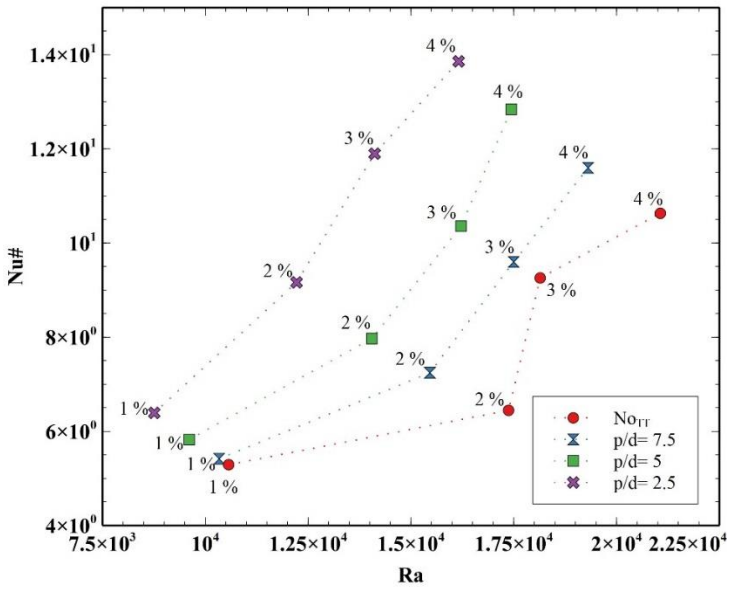

Figure 5.4. Nusselt Number (Nu) with Rayleigh Number (Ra)

Figure 5.5 shows the effect of twist ratios on Nu for q = 2682 W/m^2, which was 1% of heat flux under normal operation of the NuScale SMR. The highest Nu was achieved for the twist ratio p/d = 2.5, which was the lowest twist ratio in this study. Nu with the twist ratio p/d = 2.5 was higher than for p/d = 7.5 and p/d = 5 by about 18%, and ~ 10%, respectively. Nu with the twisted ratio p/d = 2.5 was better than Nu for the sub-channel with no twisted tape under similar operating conditions by ~19%. The swirling motion generated by reducing the twisted tape resulted in a longer flow path and longer time for fluid to pass through the sub-channel.

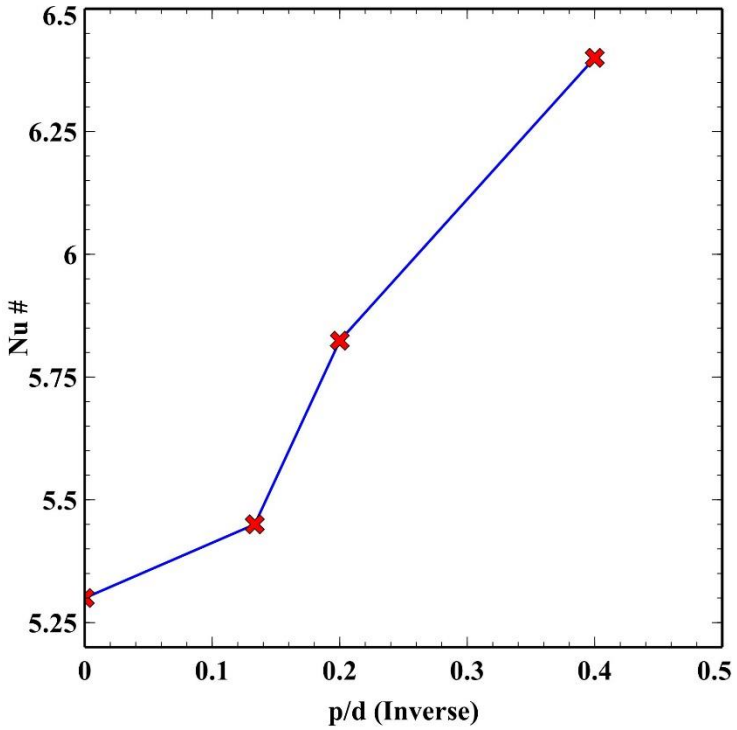

Figure 5.5. Effect of twisted tape ratios on the Nusselt number (Nu)

Figure 5.6 shows the effect of twisted tape on pressure drop along the axial length of the rod bundle where twisted tapes were inserted along the spacer grid. The pressure

drops are more pronounced at the inlet of sub-channel, where the twisted tape is situated. The pressure drop for all twist ratios was almost a linear behavior from Y/D = 0 to Y/D = 36. The smallest twist ratio, p/d = 2.5, resulted in the highest pressure drop. The increase in pressure drop for p/d = 2.5 was 20.3% and 8 % higher than those for larger twist ratios of p/d = 7.5 and 5, respectively. The increase in pressure drop was 41.4 % over the sub-channel with no twisted tape.

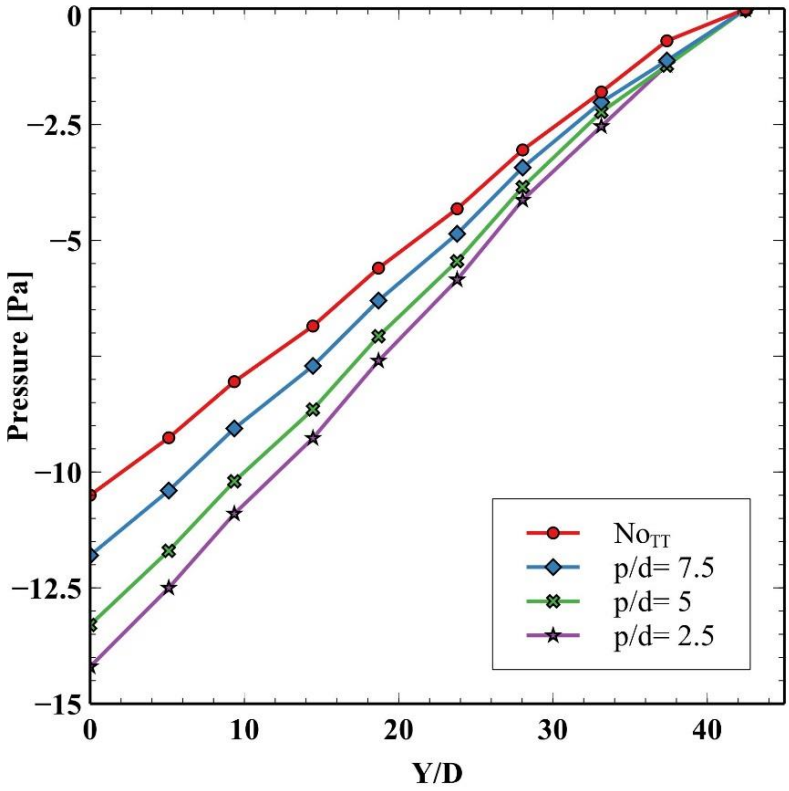

Figure 5.6. Effect on pressure drop when twisted tape inserted along spacer grid

5.4.2. Twisted Tapes Along the Entire Sub- channel. The same operating conditions surrounding fluid. Then, buoyancy forces will induce a free convection boundary layer; the heated fluid rises vertically, and the fluid in the quiescent region will

be entrain. In this case, the twisted tape ratio was changed to avoid increasing the temperature. The twisted tape ratios are 8.65, 9.4 and 12.6. Figure 5.7 shows the effect of twist ratios on Nu for q = 2682 W/m^2. The highest Nu was achieved for the twisted ratio p/d = 8.65, which is the lowest twist ratio in this case. The Nu with twisted ratio p/d =8.65 is better than Nu for the sub-channel with no twisted tape, under similar operating conditions, by 39.5%. The high enhancement in this case is due to tape length along the entire sub-channel. Nu with twist ratio p/d = 8.65 in this case is better than Nu of twisted ratio p/d = 2.5, (for twisted tape along the spacer grid) by about 15.6 %. This is significant result, in this case the smallest twist ratio is not producing the highest Nu number. Twisted tape length influence the heat transfer enhancement.

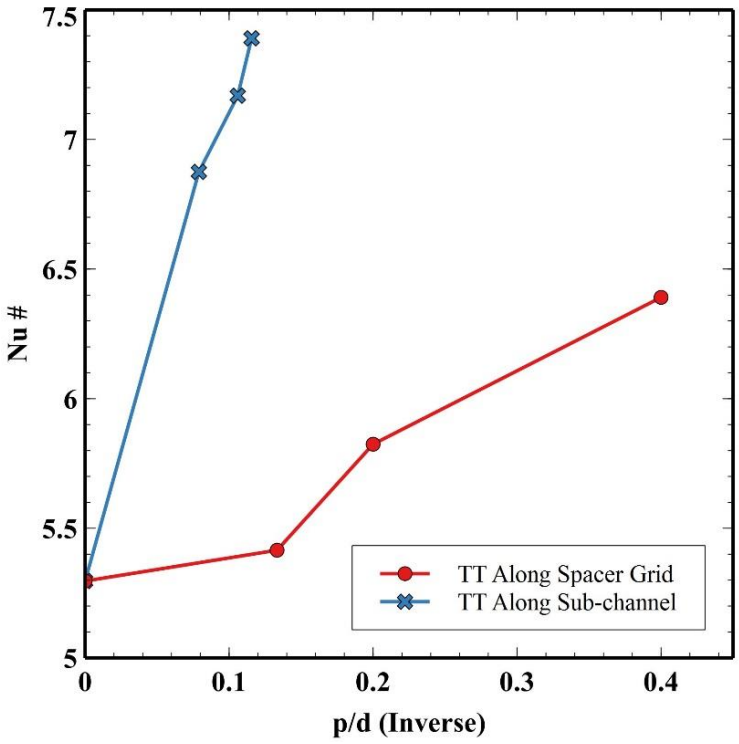

Figure 5.7. Effect of twisted tape ratios on the Nusselt number along the axial length of the rod bundle

Figure 5.8 shows the effect of twisted tape on pressure drop when inserted along the sub-channel. As shown, there is a linear pressure drop from Y/D = 0 to 30 for all cases of twist ratios and the case of no twisted tape. The pressure drop is dependent on the twist ratio and length of the twisted tape. In this study, the increasing pressure drop for twisted tape along the sub-channel is found to be 112.5% over the sub-channel with no twisted tape.

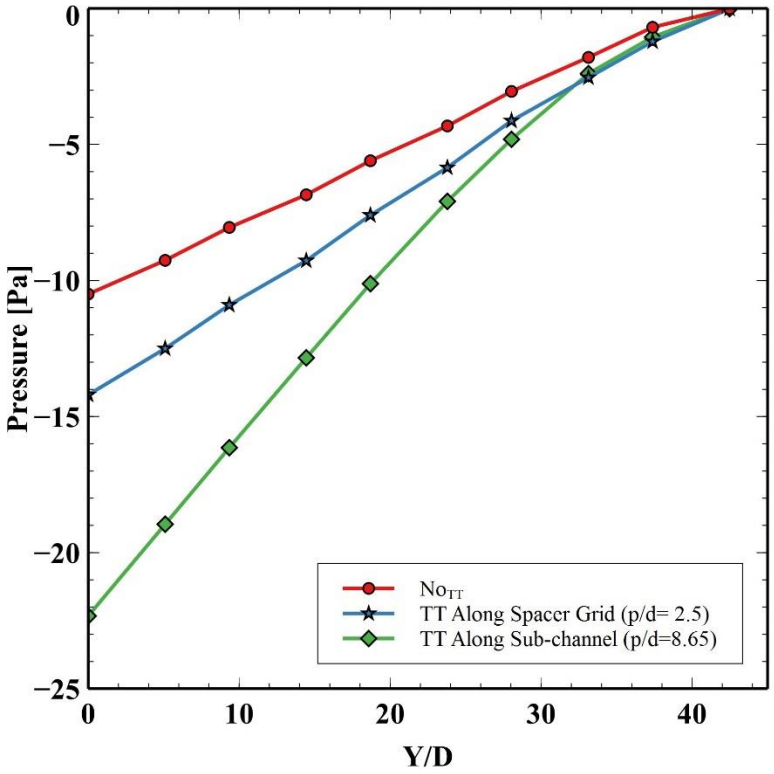

Figure 5.8. Effect of twisted tape ratios on pressure loss along the sub-channel

6. CONCLUSIONS

Computational fluid dynamics (CFD) simulations were performed for evaluation the impact of several different configurations of twisted tape on the enhancement of heat transfer and pressure drop under natural circulation. The research determined the ideal configuration for development of the lateral flow field in several subchannels by applying twisted tape in a rod bundle geometry representative of a NuScale SMR fuel assembly under natural and forced convection. To accomplish this, the research was divided into three parts - tubes containing twisted tapes of various geometries, a PWR rod bundle containing twisted tapes under forced convection, and a PWR rod bundle containing twisted tapes under neutral convection.

In the first part, simulations were performed for natural circulation in tubes containing twisted tapes of various geometries to investigate the effect of tape geometry on heat transfer rate and pressure drop. These tapes have been successful in enhancing heat transfer for forced convection but not much information is available in the open literature on their effectiveness under natural circulation conditions. From the results obtained in this study, one can conclude that twisted tapes will also be effective in enhancing heat transfer at the expense of pressure drop in natural circulation conditions. Twist ratio played an important role in the thermal hydraulic behavior of the system. The smallest twist ratio of 2.7 provided the highest heat transfer enhancement for all geometries; FLTT, RSTT, and different tape widths. But in all cases, the smallest twist ratio also resulted in the highest pressure drop. Since no external pump is involved for natural convection, higher pressure drop would have little design impact. Unfortunately,

open literature contains limited guidance for predicting heat transfer coefficient or Nusselt number under natural circulation with twisted tape not even empirical correlations are available. The other interesting observation was the shift of the highest wall temperature. As the twist ratio increases, the location of the highest wall temperature shifts away from the channel exit. In general, the following main conclusions for this section can be drawn by this CFD study:

- Twisted tapes enhance heat transfer.
- The pressure drop for tubes with twisted tape is always higher than simple tubes.
- Smaller twist ratios result in better heat transfer enhancement but higher pressure drop.
- RSTT has smaller pressure drop but also lower heat transfer enhancement.
- Width of the tape also impacts both heat transfer and pressure drop with highest impact from full width and reducing effect of heat transfer enhancement and pressure drop with reducing width.
- The most interesting observation was the shift of the location of highest temperature towards the channel inlet as the twist ratio was reduced.
- For any practical application the design effort will invariably involve optimization effort to compromise the heat transfer enhancement with an acceptable pressure drop. Therefore these results will be helpful in formulating a systematic approach for design optimization.

- There is no correlations for predicting heat transfer coefficient or Nusselt number under natural circulation with twisted tape, therefor no comparison with experimental data was possible.

In the second part, simulations were performed for forced convection in a 2X2 PWR rod bundle containing twisted tapes with different twisted ratios to evaluate the Nusselt number with Reynolds number, pressure drop, and the secondary flow. These tapes have been successful in enhancing heat transfer for forced convection in tubes and many applications. However, not much information is available in the open literature for a NuScale reactor's sub-channel under normal operation conditions. Twisted tapes are effective in enhancing the Nusselt number in a sub-channel under forced convection conditions. Moreover, results showed that the pressure drop and secondary flow are influenced by twisted tapes. The smallest twist ratio of 0.85 provided the highest Nusselt number enhancement and secondary flow rate in this study. Moreover, the smallest twist ratio also resulted in the highest pressure drop. In general, the following conclusions can be drawn from this section:

- Twisted tapes play an important role in enhancing heat transfer in sub-channels.
- The secondary flow is observed to be much pronounced in the length when using twisted tapes.
- The pressure drop for a sub-channel with twisted tape is always higher than a plain sub-channel.
- All results showed that the Nu, pressure drop, and secondary flow are influenced by changing the twisted ratio.

- The effect of twisted tapes for cases when the entire length of the channel contained a twisted tape was higher than when the twisted tape was only in the spacer grid.
- Presence of twisted tapes showed a combination of swirl and cross flow between subchannels, which increases with decreasing twisted ratio.
- Changing twisted tape ratio in the same model creates a good, strong lateral flow along the fuel rod surface that is used to control heat reduction in any hot spot.

In the final part of this research, simulations were performed for natural convection in a 2x2 PWR rod bundle containing twisted tape with different twisted ratios to evaluate the Nusselt number and pressure drop. The application of twisted tape has been successful in enhancing heat transfer for forced convection. However, limited information is available in the open literature on their effectiveness under natural convection, as well as for their use in the NuScale reactor's sub-channel. This section found that twisted tape was effective in enhancing the Nusselt number in the sub-channel under natural convection conditions. Results also showed that pressure drop is influenced by the insertion of twisted tape. The smallest twist ratio of 2.5 and 0.85 provided the highest Nusselt number enhancement in this study for all cases when the tape is limited to the spacer grid. Similarly, highest pressure drop for all cases was observed with the smallest twist ratio. The following conclusions can be drawn from this section:

- The results obtained show that twisted tape plays an important role in enhancing heat transfer in sub-channels under natural convection.
- The average Nusselt number increases as the Rayleigh number increases.

- The effect of twisted tape for cases when the entire length of the channel contained twisted tape was higher than when the twisted tape was along the spacer grid.
- The pressure drop for sub-channel with twisted tape is higher than the sub-channel with no twisted tape.
- All results showed that Nu and pressure drop are influenced by changing the twist ratio.

BIBLIOGRAPHY

[1] Outlook, E. (2010). International Energy Outlook. Outlook.

[2] Zohuri, B., & Fathi, N. (2015). Thermal-hydraulic analysis of nuclear reactors. New York: Springer.

[3] Todreas, N. E., & Kazimi, M. S. (2011). Nuclear systems volume I: Thermal hydraulic fundamentals. CRC press.

[4] Comsan, M. N. H. (2008). Status of nuclear power reactor development.

[5] WNA. (2009). "Power Reactors - characteristics." World Nuclear Association, London.

[6] Ingersoll, D. T., Houghton, Z. J., Bromm, R., & Desportes, C. (2014). NuScale small modular reactor for co-generation of electricity and water. Desalination, 340, 84-93.

[7] Power, N. (2016). NuScale Standard Plant Design Certification Application. Chapter One Introduction and General Description of the Plant.

[8] Power, N. (2016). NuScale Standard Plant Design Certification Application. Chapter Four Introduction and General Description of the Plant.

[9] AREVA Inc (2016). Fuel for the NuScale SMR. ANP:U-631-V1-16-ENG. (http://us.areva.com/home/liblocal/docs/Catalog/PWR/ANP-U-631-V1-16-ENG-NuScale.pdf)

[10] Bejan, A., & Kraus, A. D. (2003). Heat transfer handbook (Vol. 1). John Wiley & Sons.

[11] Ghogare, R. M., Gore, V. G., & Shaikh, A. S. (2018). A Review Of Passive Technique Used For Heat Transfer Enhancement In Heat Exchanger.

[12] Saha, A. K., Das, D., Srivastava, R., Panigrahi, P. K., & Muralidhar, K. (Eds.). (2016). Fluid Mechanics and Fluid Power–Contemporary Research: Proceedings of the 5th International and 41st National Conference on FMFP 2014. Springer.

[13] Mao, H., Yang, B. W., Han, B., & Liu, A. (2017). Modeling of spacer grid mixing effects through mixing vane crossflow model in subchannel analysis. Nuclear Engineering and Design, 320, 141-152.

[14] Hasanpour, A., Farhadi, M., & Sedighi, K. (2014). A review study on twisted tape inserts on turbulent flow heat exchangers: The overall enhancement ratio criteria. International communications in heat and mass transfer, 55, 53-62.

[15] Kanizawa, F. T., Hernandes, R. S., de Moraes, A. A., & Ribatski, G. (2011). A new correlation for single and two-phase flow pressure drop in round tubes with twisted-tape inserts. Journal of the Brazilian Society of Mechanical Sciences and Engineering, 33(SPE1), 243-250.

[16] E. Sanvicente, S. Giroux-Julein, C. Menezo, H. Bouia, Trnasitional natural convection flow and heat transfer in an open channel, Int J Therm Sci 63 (2013) 87–104.

[17] H.A. Mohammed, Y.K. Salman, Heat transfer by natural convection from a uniformly heated vertical circular pipe with different entry restriction configuration, Energy Convers Manag 48 (2007) 2244–2253.

[18] K. T. Lee, Fully developed laminar natural convection heat and mass transfer in partially heated vertical pipe, Int. Commun. Heat. Mass. Trans., 27(7) (2000), pp. 995–1001.

[19] T. Tsuji and Y. Nagano, (1988). Characteristics of a turbulent natural convection boundary layer along a vertical flat plate, Int. J. Heat Mass Transfer 31, 1723,4

[20] Shigeo K, Adrian B. Experimental study of natural convection in a horizontal cylinder with different end temperatures. Int J Heat Mass Transfer 1980;23(8):1117–26.

[21] Eiamsa-ard, S., Pethkool, S., Thianpong, C., & Promvonge, P. (2008). Turbulent flow heat transfer and pressure loss in a double pipe heat exchanger with louvered strip inserts. International Communications in Heat and Mass Transfer, 35(2), 120-129.

[22] Ibrahim, E. Z. (2011). Augmentation of laminar flow and heat transfer in flat tubes by means of helical screw-tape inserts. Energy Conversion and Management, 52(1), 250-257.

[23] Bhuiya, M. M. K., Chowdhury, M. S. U., Ahamed, J. U., Khan, M. J. H., Sarkar, M. A. R., Kalam, M. A., ... & Shahabuddin, M. (2012). Heat transfer performance for turbulent flow through a tube using double helical tape inserts. International Communications in Heat and Mass Transfer, 39(6), 818-825.

[24] Gül, H., & Evin, D. (2007). Heat transfer enhancement in circular tubes using helical swirl generator insert at the entrance. International Journal of Thermal Sciences, 46(12), 1297-1303.

[25] Tijing, L. D., Pak, B. C., Baek, B. J., & Lee, D. H. (2006). A study on heat transfer enhancement using straight and twisted internal fin inserts. International Communications in Heat and Mass Transfer, 33(6), 719-726.

[26] Chandrasekar, M., Suresh, S., & Bose, A. C. (2010). Experimental studies on heat transfer and friction factor characteristics of Al2O3/water nanofluid in a circular pipe under laminar flow with wire coil inserts. Experimental Thermal and Fluid Science, 34(2), 122-130.

[27] Wang, L., & Sunden, B. (2002). Performance comparison of some tube inserts. International Communications in Heat and Mass Transfer, 29(1), 45-56.

[28] Sideman, S., & Levin, A. (1979). Effect of the configuration on heat transfer to gravity driven films evaporating on grooved tubes. Desalination, 31(1-3), 7-18.

[29] Rainieri, S., Farina, A., & Pagliarini, G. (1996, May). Experimental investigation of heat transfer and pressure drop augmentation for laminar flow in spirally enhanced tubes. In Proceedings of the 2nd European Thermal-Sciences and 14th UIT Heat Transfer Conference (Vol. 1, p. 203).

[30] Barba, A., Rainieri, S., & Spiga, M. (2002). Heat transfer enhancement in a corrugated tube. International communications in heat and mass transfer, 29(3), 313-322.

[31] Kareem, Z. S., Jaafar, M. M., Lazim, T. M., Abdullah, S., & AbdulWahid, A. F. (2015). Heat transfer enhancement in two-start spirally corrugated tube. Alexandria Engineering Journal, 54(3), 415-422.

[32] Saha, S. K. (2010). Thermal and friction characteristics of laminar flow through rectangular and square ducts with transverse ribs and wire coil inserts. Experimental Thermal and Fluid Science, 34(1), 63-72.

[33] Bilen, K., Cetin, M., Gul, H., & Balta, T. (2009). The investigation of groove geometry effect on heat transfer for internally grooved tubes. Applied Thermal Engineering, 29(4), 753-761.

[34] Kathait, P. S., & Patil, A. K. (2014). Thermo-hydraulic performance of a heat exchanger tube with discrete corrugations. Applied Thermal Engineering, 66(1-2), 162-170.

[35] Garcia, A., Solano, J. P., Vicente, P. G., & Viedma, A. (2012). The influence of artificial roughness shape on heat transfer enhancement: Corrugated tubes, dimpled tubes and wire coils. Applied Thermal Engineering, 35, 196-201.

[36] Manglik, R. M., & Bergles, A. E. (1993). Heat transfer and pressure drop correlations for twisted-tape inserts in isothermal tubes: part I—laminar flows. Journal of heat transfer, 115(4), 881-889.

[37] P. Naphon. (2005). Heat transfer and pressure drop in the horizontal double pipes with and without twisted tape insert, International Communications in Heat and Mass Transfer, Vol. 33, pp. 166–175.

[38] W. Date, J. R. (2005). Singham, Numerical prediction of friction and heat transfer characteristics of fully developed laminar flow in tubes containing twisted tapes, Trans. ASME, Journal Heat Transfer, Vol. 17, 72.

[39] Hong, S. W., & Bergles, A. E. (1976). Augmentation of laminar flow heat transfer in tubes by means of twisted-tape inserts. Journal of Heat Transfer, 98(2), 251-256.

[40] Saha, S. K., & Dutta, A. (2001). Thermohydraulic study of laminar swirl flow through a circular tube fitted with twisted tapes. Journal of Heat Transfer, 123(3), 417-427.

[41] Agarwal, S. K., & Rao, M. R. (1996). Heat transfer augmentation for the flow of a viscous liquid in circular tubes using twisted tape inserts. International Journal of Heat and Mass Transfer, 39(17), 3547-3557.

[42] Lianshan, Z., Xianhe, D., Weitao, L., & Zhiping, Y. (2014). Investigation for Natural Convection Heat Transfer of Sucrose Solution Using a Converging and Diverging Tube with Regularly-spaced Twisted Tapes. China Petroleum Processing and Petro-chemical Technology, 16(1), 81-89.

[43] Du Plessis, J. P., & Kroger, D. G. (1984). Friction factor prediction for fully developed laminar twisted-tape flow. International journal of heat and mass transfer, 27(11), 2095-2100.

[44] Al-Fahed, S., & Chakroun, W. (1996). Effect of tube-tape clearance on heat transfer for fully developed turbulent flow in a horizontal isothermal tube. International journal of heat and fluid flow, 17(2), 173-178.

[45] Bhattacharyya, S., & Saha, S. K. (2012). Thermohydraulics of laminar flow through a circular tube having integral helical rib roughness and fitted with centre-cleared twisted-tape. Experimental Thermal and Fluid Science, 42, 154-162.

[46] Bhattacharyya, S., Saha, S., & Saha, S. K. (2013). Laminar flow heat transfer enhancement in a circular tube having integral transverse rib roughness and fitted with centre-cleared twisted-tape. Experimental Thermal and Fluid Science, 44, 727-735.

[47] Al-Fahed, S., Chamra, L. M., & Chakroun, W. (1998). Pressure drop and heat transfer comparison for both microfin tube and twisted-tape inserts in laminar flow. Experimental Thermal and Fluid Science, 18(4), 323-333.

[48] Liao, Q., & Xin, M. D. (2000). Augmentation of convective heat transfer inside tubes with three-dimensional internal extended surfaces and twisted-tape inserts. Chemical Engineering Journal, 78(2-3), 95-105.

[49] Promvonge, P. and Eiamsa-ard, S. "Heat transfer behaviors in a tube with combined conical-ring and twisted-tape insert", Int. Comm. Heat and Mass Transfer, Vol. 34, No. 7, pp. 849-859, 2007a.

[50] P. Ferroni, R.E. Block, N.E. Todreas, A.E. Bergles, (2011). Experimental evaluation of pressure drop in round tubes provided with physically separated, multiple, short-length twisted tapes, Experimental Thermal and Fluid Science, 35, pp. 1357–1369.

[51] Patil, A. G. (2000). Laminar flow heat transfer and pressure drop characteristics of power-law fluids inside tubes with varying width twisted tape inserts. Journal of heat transfer, 122(1), 143-149.

[52] Ray, S., & Date, A. W. (2001). Laminar flow and heat transfer through square duct with twisted tape insert. International journal of heat and fluid flow, 22(4), 460-472.

[53] Saha, S. K., Dutta, A., & Dhal, S. K. (2001). Friction and heat transfer characteristics of laminar swirl flow through a circular tube fitted with regularly spaced twisted-tape elements. International Journal of Heat and Mass Transfer, 44(22), 4211-4223.

[54] Sarada, S. N., Raju, A. S. R., Radha, K. K., & Sunder, L. S. (2010). Enhancement of heat transfer using varying width twisted tape inserts. International Journal of Engineering, Science and Technology, 2(6).

[55] Ujhidy, A., Nemeth, J., & Szépvölgyi, J. (2003). Fluid flow in tubes with helical elements. Chemical Engineering and Processing: Process Intensification, 42(1), 1-7.

[56] Saha, S. K. (2010). Thermohydraulics of turbulent flow through rectangular and square ducts with axial corrugation roughness and twisted-tapes with and without oblique teeth. Experimental Thermal and Fluid Science, 34(6), 744-752.

[57] Kreith, F., & Margolis, D. (1959). Heat transfer and friction in turbulent vortex flow. Applied Scientific Research, Section A, 8(1), 457-473.

[58] Smithberg, E., & Landis, F. (1964). Friction and forced convection heat-transfer characteristics in tubes with twisted tape swirl generators. Journal of Heat Transfer, 86(1), 39-48.

[59] Thorsen, R., & Landis, F. (1968). Friction and heat transfer characteristics in turbulent swirl flow subjected to large transverse temperature gradients. Journal of Heat Transfer, 90(1), 87-97.

[60] Lopina, R. F., & Bergles, A. E. (1969). Heat transfer and pressure drop in tape-generated swirl flow of single-phase water. Journal of Heat Transfer, 91(3), 434-441.

[61] Brevi, R., Cumo, M., Palmieri, A., & Pitimada, D. (1971). Measurement of the Effect of Twisted Tapes on the Forced-Convection Heat Transfer and Burnout in Heat Exchangers. Nuclear Science and Engineering, 46(1), 131-139.

[62] Date, A. W. (1974). Prediction of fully-developed flow in a tube containing a twisted-tape. International journal of heat and mass transfer, 17(8), 845-859.

[63] Muralidhara Rao, M., & Sastri, V. M. K. (1995). Experimental investigation for fluid flow and heat transfer in a rotating tube with twisted-tape inserts. Heat transfer engineering, 16(2), 19-28.

[64] Al-Fahed, S., & Chakroun, W. (1996). Effect of tube-tape clearance on heat transfer for fully developed turbulent flow in a horizontal isothermal tube. International journal of heat and fluid flow, 17(2), 173-178.

[65] Neshumayev, D., Ots, A., Laid, J., & Tiikma, T. (2004). Experimental investigation of various turbulator inserts in gas-heated channels. Experimental thermal and fluid science, 28(8), 877-886.

[66] Eiamsa-ard, S., Thianpong, C., & Promvonge, P. (2006). Experimental investigation of heat transfer and flow friction in a circular tube fitted with regularly spaced twisted tape elements. International Communications in Heat and Mass Transfer, 33(10), 1225-1233.

[67] Marner, W. J., & Bergles, A. E. (1989). Augmentation of highly viscous laminar heat transfer inside tubes with constant wall temperature. Experimental Thermal and Fluid Science, 2(3), 252-267.

[68] Krishna, S. R., Pathipaka, G., & Sivashanmugam, P. (2009). Heat transfer and pressure drop studies in a circular tube fitted with straight full twist. Experimental Thermal and Fluid Science, 33(3), 431-438.

[69] Thianpong, C., Eiamsa-Ard, P., Wongcharee, K., & Eiamsa-Ard, S. (2009). Compound heat transfer enhancement of a dimpled tube with a twisted tape swirl generator. International Communications in Heat and Mass Transfer, 36(7), 698-704.

[70] Eiamsa-Ard, S., Thianpong, C., Eiamsa-Ard, P., & Promvonge, P. (2009). Convective heat transfer in a circular tube with short-length twisted tape insert. International communications in heat and mass transfer, 36(4), 365-371.

[71] Bhuiya, M. M. K., Chowdhury, M. S. U., Saha, M., & Islam, M. T. (2013). Heat transfer and friction factor characteristics in turbulent flow through a tube fitted with perforated twisted tape inserts. International Communications in Heat and Mass Transfer, 46, 49-57.

[72] Eiamsa-Ard, S., & Promvonge, P. (2010). Performance assessment in a heat exchanger tube with alternate clockwise and counter-clockwise twisted-tape inserts. International Journal of Heat and Mass Transfer, 53(7-8), 1364-1372.

[73] Murugesan, P., Mayilsamy, K., & Suresh, S. (2010). Turbulent heat transfer and pressure drop in tube fitted with square-cut twisted tape. Chinese Journal of Chemical Engineering, 18(4), 609-617.

[74] Jaisankar, S., Radhakrishnan, T. K., Sheeba, K. N., & Suresh, S. (2009). Experimental investigation of heat transfer and friction factor characteristics of thermosyphon solar water heater system fitted with spacer at the trailing edge of Left–Right twisted tapes. Energy Conversion and Management, 50(10), 2638-2649.

[75] Seemawute, P., & Eiamsa-Ard, S. (2010). Thermohydraulics of turbulent flow through a round tube by a peripherally-cut twisted tape with an alternate axis. International Communications in Heat and Mass Transfer, 37(6), 652-659.

[76] Malen, J. A., Todreas, N. E., Hejzlar, P., Ferroni, P., & Bergles, A. (2009). “Thermal hydraulic design of a hydride-fueled inverted PWR core”. Nuclear Engineering and Design, 239 (8), 1471-1480.

[77] Weisman, J., Yang, J.Y., Usman, S., 1994. “A phenomenological model for boiling heat transfer and the critical heat flux in tubes containing twisted tapes”. International Journal of Heat and Mass Transfer, 37 (1), 69-80

[78] Lim, J.C., Weisman, J., 1988. “A phenomenologically based prediction of rod-bundle dryout”. Nuclear Engineering and Design, 105 (3), 363-371

[79] Todreas, N.E., Ferroni, P., 2009. “Enhancing reactor core thermal performance through inverted fuel design”, Paper N13P1445, Kanazawa City, Japan, NURETH 13.

[80] Todreas, N.E., Kazimi, M.S., 2012. “Nuclear Systems I: Thermal Hydraulic Fundamentals”, 2nd ed. CRC Press, Boca Raton, Florida.

[81] Akiba, M., Morooka, S., & Shirakawa, K. (2003). “Effect of twisted tape on liquid film flow rate in rod bundle”. In T. J. O Hern, & T. J. O Hern (Eds.), Proceedings of the ASME Fluids Engineering Division Summer Meeting (Vol. 2, pp. 437-441).

[82] Arment, T. W., Todreas, N. E., & Bergles, A. E. (2013). “Critical heat flux and pressure drop for tubes containing multiple short-length twisted-tape swirl promoters”. Nuclear Engineering and Design, 257, 1-11.

[83] Bieder, U., Falk, F., & Fauchet, G. (2015). CFD analysis of the flow in the near wake of a generic PWR mixing grid. Annals of Nuclear Energy, 82, 169-178.

[84] Liu, C. C., & Ferng, Y. M. (2010). Numerically simulating the thermal–hydraulic characteristics within the fuel rod bundle using CFD methodology. Nuclear engineering and design, 240(10), 3078-3086.

[85] In, W. K., Chun, T. H., Shin, C. H., & Oh, D. S. (2008). Numerical computation of heat transfer enhancement of a PWR rod bundle with mixing vane spacers. Nuclear Technology, 161(1), 69-79.

[86] Lee, C. M., & Choi, Y. D. (2007). Comparison of thermo-hydraulic performances of large scale vortex flow (LSVF) and small scale vortex flow (SSVF) mixing vanes in 17× 17 nuclear rod bundle. Nuclear engineering and design, 237(24), 2322-2331.

[87] Holloway, M. V., Conover, T. A., McClusky, H. L., Beasley, D. E., & Conner, M. E. (2005). The effect of support grid design on azimuthal variation in heat transfer coefficient for rod bundles. Journal of Heat Transfer, 127(6), 598-605.

[88] Hata, K., Fukuda, K., & Mizuuchi, T. (2017). Natural convection heat transfer from vertical 5× 5 rod bundles in liquid sodium. Journal of Heat Transfer, 139(3), 032502.

[89] Tandian, N. P., Alkharboushi, A. A. K., & Kamajaya, K. (2015). Natural convection heat transfer in vertical triangular subchannel in Zirconia-water nanofluid. In IOP Conference Series: Materials Science and Engineering (Vol. 88, No. 1, p. 012010). IOP Publishing.

[90] Choi, J. H., Cleveland, J., & Aksan, N. (2011). Improvement in understanding of natural circulation phenomena in water cooled nuclear power plants. Nuclear Engineering and Design, 241(11), 4504-4514.

[91] Navarro, M. A., & Santos, A. A. (2011). Evaluation of a numeric procedure for flow simulation of a 5× 5 PWR rod bundle with a mixing vane spacer. Progress in Nuclear Energy, 53(8), 1190-1196.

[92] Karouta, Z., Gu, C. Y., & Schölin, B. (1995). 3-D flow analyses for design of nuclear fuel spacer (No. NUREG/CP--0142-VOL. 4).

[93] Khan, M. O., Hussain, S., Rafique, M., Ahmad, A., & Akhtar, W. (2013, January). CFD study of single phase flow in a PWR spacer grid. In Applied Sciences and Technology (IBCAST), 2013 10th International Bhurban Conference on (pp. 243-248). IEEE.

[94] Podila, K., Rao, Y. F., Krause, M., & Bailey, J. (2014). A CFD simulation of 5× 5 rod bundles with split-type spacers. Progress in Nuclear Energy, 70, 167-175.

[95] Du Plessis, J. P., & Kroger, D. G. (1984). Friction factor prediction for fully developed laminar twisted-tape flow. International journal of heat and mass transfer, 27(11), 2095-2100.

[96] Peña-Monferrer, C., Muñoz-Cobo, J. L., & Chiva, S. (2014). CFD turbulence study of PWR spacer-grids in a rod bundle. Science and Technology of Nuclear Installations, 2014.

[97] Khan, M. O., Hussain, S., Rafique, M., Ahmad, A., & Akhtar, W. (2013, January). CFD study of single phase flow in a PWR spacer grid. In Applied Sciences and Technology (IBCAST), 2013 10th International Bhurban Conference on (pp. 243-248). IEEE.

[98] Navarro, M. A., & Santos, A. A. (2009). Numerical evaluation of flow through a 5x5 PWR rod bundle: effect of the vane arrangement in a spacer grid.

[99] Chen, D., Xiao, Y., Xie, S., Yuan, D., Lang, X., Yang, Z., ... & Lu, Q. (2016). Thermal–hydraulic performance of a 5× 5 rod bundle with spacer grid in a nuclear reactor. Applied Thermal Engineering, 103, 1416-1426.

[100] Lee, C. Y., In, W. K., & Lee, J. K. (2016). Augmentation of single-phase forced convection heat transfer in tightly arrayed rod bundle with twist-vane spacer grid. Experimental Thermal and Fluid Science, 76, 185-192.

[101] Podila, K., & Rao, Y. (2016). CFD modelling of turbulent flows through 5× 5 fuel rod bundles with spacer-grids. Annals of Nuclear Energy, 97, 86-95.

[102] INTERNATIONAL ATOMIC ENERGY AGENCY. (2015). Indicators for Nuclear Power Development, IAEA Nuclear Energy Series No. NG-T-4.5, IAEA, Vienna.

[103] INTERNATIONAL ATOMIC ENERGY AGENCY, (2017). Indicators for Nuclear Power Development, IAEA Nuclear Energy Series No. NG-T-4.5, IAEA, Vienna.

[104] Yuan X, Peng M, Xia G. (2013). Nuclear Power Plant Passive Residual Heat Removal System Design and Simulation. ASME. International Conference on Nuclear Engineering, Volume 6: Beyond Design Basis Events.

[105] Said, I. A., Taha, M. M., Usman, S., Woods, B. G., & Al-Dahhan, M. H. (2017). Investigation of natural convection heat transfer in a unique scaled-down dual-channel facility. AIChE Journal, 63(1), 387-396.4.

[106] Wolf, B., Kizerian, M., & Lucas, S. (2013). Analysis of Blowdown Event in Small Modular Natural Circulation Integral Test Facility. In Transactions of the ANS Winter Annual Meeting.

[107] Yousaf, M., Sipaun, S., Yigit, C., Usman, S. (2013, June), Velocity profile under natural convection between two parallel plates. In Transactions of the ANS Winter Annual Meeting.

[108] Ubale, Divyesh. (2017). Heat Transfer Enhancement in Heat Exchanger using Twisted-Tape Inserts: A Review. International Journal on Recent and Innovation Trends in Computing and Communication. 5. 425-428.

[109] ANSYS, 2017, FLUENT User Manual, ANSYS, Inc., Canonsburg, PA.

[110] K. Shivam, K. Prashant , P. Rohansingh, K Swapnil, (2017). Experimental analysis & simulation of double pipe heat exchanger, International journal of advance research and innovative ideas in education, vol-3 Issue-2 2017 IJARIIE-ISSN(O)-2395-4396.

[111] Ramakumar, B. V. N., Arsha, J. D., & Tayal, P. (2016). Tapered twisted tape Inserts for enhanced heat transfer. Journal of Heat Transfer, 138(1), 011901.

[112] I. A. Said, M. M. Taha, S. Usman, M. H. Al-Dahhan (2018). Experimental investigation of the helium natural circulation heat transfer in two channels facility using varying riser channel heat fluxes, Experimental Thermal and Fluid Science, 93 195–209.

[113] M. Al-Arabi, M. Khamis, M. Abdul-Aziz, (1991). Heat transfer by natural convection from the in side surface of a uniformly heated vertical tube, Int J Heat Mass Transf 34 1019–1025.

[114] H.A. Mohammed, Y.K. Salman, ((2007). Laminar air flow free convection heat transfer inside a vertical circular pipe with different inlet configuration, Therm Sci 11 (1) 43–63.

[115] M.M. Taha, I.A. Said, U. Shoaib, M.H. Al-Dahhan (2017). Missouri S&T scaled down facility (MSTF) preliminary tests and design developments, (Submitted, Nuclear Engineering and Design).

[116] McClusky, H. L., Holloway, M. V., Beasley, D. E., & Conner, M. E. (2002). "Development of swirling flow in a rod bundle subchannel", Journal of Fluids Engineering, 124 (3), 747-755.

[117] Yuan X, Peng M, Xia G. (2013). "Nuclear Power Plant Passive Residual Heat Removal System Design and Simulation". ASME. International Conference on Nuclear Engineering, Volume 6: Beyond Design Basis Events.

[118] E. Sanvicente, S. Giroux-Julein, C. Menezo, H. Bouia, "Transitional natural convection flow and heat transfer in an open channel", Int J Therm Sci 63 (2013) 87–104.

[119] ANSYS, 2018, "FLUENT User Manual", ANSYS, Inc., Canonsburg, PA.

[120] Sims, R. E., Rogner, H. H., & Gregory, K. (2003). Carbon emission and mitigation cost comparisons between fossil fuel, nuclear and renewable energy resources for electricity generation. Energy policy, 31(13), 1315-1326.

[121] Shah, R. K., & London, A. L. (2014). Laminar flow forced convection in ducts: a source book for compact heat exchanger analytical data. Academic press.

[122] Paparusso, L., Ricotti, M. E., & Sumini, M. (2011). World status of the SMR projects.

[123] Power, N. (2016). NuScale Standard Plant Design Certification Application. Chapter Nineteen Probabilistic Risk Assessment.

[124] Sriromreun, P., Thianpong, C., & Promvonge, P. (2012). Experimental and numerical study on heat transfer enhancement in a channel with Z-shaped baffles. International Communications in Heat and Mass Transfer, 39(7), 945-952.

[125] Ramakumar, B. V. N., Arsha, J. D., & Tayal, P. (2016). Tapered twisted tape inserts for enhanced heat transfer. Journal of Heat Transfer, 138(1), 011901.

[126] Jiji, L. M., & Jiji, L. M. (2006). Heat convection (p. 275). New York: Springer.

[127] Sachdeva, R. C. (2006). Fundamentals of Engineering Heat and Mass Transfer (SI Units). New Age International Publishers.

VITA

Salman Alzahrani was born in Alfaggar village, Saudi Arabia. He grew up in Taif city. He received his Bachelor's of Science in Computer Engineering from University of Umm Al-Qura, Makkah in May 2009. He joined as a research assistant in the National Center for Nuclear Technology, King Abdulaziz City for Science and Technology, Riyadh, Saudi Arabia in Jun 2009. In December 2014, he received his M.S. degree in Nuclear Engineering from Missouri S&T. He began his Ph.D. study in January 2015 in the same department of Nuclear Engineering. He attended several conferences related to his research interests and published two conference papers; additionally, one journal paper was submitted and placed under review. Moreover, one conference paper was submitted and placed under review. Salman received his Ph.D. degree in Nuclear Engineering from Missouri S&T in May 2019.